NATIONAL ADVISORY COMMITTEE FOR AERONAUTICS

TECHNICAL NOTE 4404

EFFECTS OF PROPELLER POSITION AND OVERLAP ON THE SLIPSTREAM DEFLECTION CHARACTERISTICS OF A WING-PROPELLER CONFIGURATION EQUIPPED WITH A SLIDING AND FOWLER FLAP

By William C. Hayes, Jr., Richard E. Kuhn, and Irving R. Sherman

Langley Aeronautical Laboratory
Langley Field, Va.

Washington
September 1958

NATIONAL ADVISORY COMMITTEE FOR AERONAUTICS

TECHNICAL NOTE 4404

EFFECTS OF PROPELLER POSITION AND OVERLAP ON THE SLIPSTREAM DEFLECTION CHARACTERISTICS OF A WING-PROPELLER CONFIGURATION EQUIPPED WITH A SLIDING AND FOWLER FLAP

By William C. Hayes, Jr., Richard E. Kuhn, and Irving R. Sherman

SUMMARY

An investigation has been made in a static-test facility at the Langley Aeronautical Laboratory to determine some of the effects of propeller position and overlap on the slipstream deflection characteristics of a configuration equipped with a sliding and Fowler flap. The effects of a leading-edge slat, nacelle size, flap segmentation, and number of propellers were also investigated.

The results indicate that lowering the thrust axis reduces the diving moments by virtue of the direct moment applied when the thrust vector passes below the moment reference point. Little or no change in the aerodynamics of the configuration arising from either vertical or chordwise changes in the position of the propeller was noted. Overlapping the propellers produced significant increases in thrust recovery at the highest flap deflection; however, these gains were greatly reduced by a corresponding loss in propeller static-thrust efficiency. The thrust-recovery factors obtained with only the inboard propeller operating were much lower than those obtained with both propellers. Segmenting the flaps to allow rearward extension of the nacelle greatly reduced both the thrust recovery and the turning angle. Increasing the nacelle size to that required for reciprocating engines reduced both the thrust recovery and the turning angle. Also, the addition of a leading-edge slat at deflections needed to appreciably reduce the diving moments reduced both the thrust recovery and the turning angle.

INTRODUCTION

The Langley 7- by 10-Foot Tunnels Branch is conducting a systematic program to investigate wing-propeller configurations intended to redirect propeller slipstream to the extent that capabilities for the airplane designed for vertical take-off and landing (VTOL) or short take-off and

landing (STOL) will be realized without excessive diving moments or power expenditure. Reference 1 demonstrated the strong influence of vertical displacement of the propeller on the pitching-moment characteristics of deflected slipstream configurations; however, this work on the effects of propeller position was limited primarily to a single propeller per semispan. The present investigation extends the work to a configuration having two propellers per semispan and covers the effects of changes in both vertical and longitudinal positions of the propellers.

In addition, previous work with two propellers, for the most part, has been with the propellers in an overlapped condition. The present investigation includes the effect of propeller overlap on the aerodynamic characteristics of the model and on the static-thrust efficiency of the propellers.

The data were obtained with a semispan wing employing a combination of sliding and Fowler flaps as well as a leading-edge slat immersed in the slipstream of two large-diameter propellers. The effect of flap segmentation, which was necessitated for some tests by the extension of the nacelles through the flaps, is also shown. Limited investigation of the effect of nacelle size and a comparison of results with one and two propellers is also included. Testing was done in a static-test facility at the Langley Aeronautical Laboratory.

SYMBOLS

The positive sense of forces, moments, and angles are indicated in figure 1. The symbols used in this paper are defined as follows:

b	propeller blade chord, ft
c_w	wing chord, ft
D	propeller diameter, ft
F	resultant force, lb
F_X	longitudinal force, Thrust minus Drag, lb
h	distance from ground board to trailing edge of wing, ft
h'	propeller blade thickness, ft
L	lift, lb

M_Y pitching moment, ft-lb

P propeller shaft power per propeller, ft-lb/sec

R radius of propeller, ft

r radius at any propeller blade section, ft

T measured propeller thrust (total, except as otherwise noted), lb

X chordwise position of propellers, positive ahead of wing leading edge, ft

x wing coordinate measured from leading edge

Y amount of propeller overlap, ft (see fig. 6)

y wing coordinate measured from chord plane

Z vertical position of propellers, positive above wing-chord plane, ft

α angle between thrust axis and ground plane, deg

δ_f flap deflection, deg

δ_{slat} slat deflection, deg

η static-thrust efficiency, $\frac{T^{3/2}}{2P\sqrt{\frac{\rho}{2}\frac{\pi}{4}D^2}}$ (where T is thrust for each propeller)

θ turning angle, inclination of resultant force vector from thrust axis, $\tan^{-1} L/F_X$

ρ mass density of air, slugs/cu ft

Subscripts:

F Fowler flap

I inner coordinate

L lower coordinate

s sliding flap

U upper coordinate

MODEL AND TESTS

Drawings of the semispan model and tables of geometric characteristics are presented in figures 2 and 3, and a photograph of the model is presented in figure 4. The wing was constructed on a steel spar which held the two motor nacelles, the wooden blocks which formed the wing contour, and the brackets which held the sliding flap in position. Several motor brackets were designed so that the nacelles could be located in several vertical and chordwise positions with respect to the wing (fig. 5). In addition, there were several attaching points along the spar so that the outboard nacelle could be moved in order to provide various amounts of propeller overlap. A drawing indicating these overlap positions is presented in figure 6.

The sliding flap rotated about a point 1.25 inches below the chord line at the 41-percent-chord station. The sliding ramp radius was 20 percent of the wing chord and was made tangent to the upper surface of the wing. The cavity which formed when the sliding flap was deflected was left unfilled. The rear flap, which was a Fowler flap, had a Clark Y airfoil section and a chord length equal to 40 percent of the wing chord, and when the flap was deflected, the flap leading edge was located so that a slot gap of $1\frac{1}{2}$ percent of the wing chord was maintained. The Fowler flap had a deflection range from 0° to 70° and was fully extended for all deflected conditions ($\delta_{f,F} = 0$ indicates that the Fowler flap was retracted). The sliding flap had a deflection range from 0° to 50°. Most of the tests were made with full-span flaps; however, both the sliding and Fowler flaps could be segmented as indicated in figure 3 to allow full deflection with the motor nacelles extended through them.

Two alternate wing leading edges were provided. For tests with the leading-edge slat, a leading edge was provided which gave the contour required to retract the slat as shown by the solid lines in figure 2. For all other tests the basic contour of the NACA 4415 airfoil was preserved as indicated by the dashed lines in figure 2.

The ground was simulated by a 5- by 8-foot sheet of plywood. The height above the ground board is defined as the distance from the wing trailing edge to the ground board. Thus, the position of the propeller with respect to the ground board changes with flap deflection.

The ground-board angle was determined from the turning angle which was measured for the test flap deflection out of the region of ground effect; that is, the turning angle θ plus the ground-board angle α add up to roughly 90°. This condition simulates the attitude of a VTOL airplane in hovering out of ground effect.

The propellers (geometric characteristics presented in fig. 7) were modified versions of the propellers of reference 2 (three blades instead of four blades) and were made of balsa covered with fiber glass and were driven by water-cooled variable-frequency electric motors operated in parallel from one variable-frequency power supply, which kept the motor speeds matched to 10 rpm. The speed of rotation of each propeller was determined by a stroboscopic-type indicator which received the output frequency of small alternators connected to each motor shaft. Both propellers rotated so as to oppose the direction of flow of the wing-tip vortex. During the tests the speed of rotation was maintained at approximately 5,800 rpm which corresponds to a propeller tip Mach number of 0.54.

The motors were mounted inside aluminum-alloy nacelles by means of strain-gage beams so that the propeller thrust and torque could be measured. The total lift, longitudinal force, and pitching moment were measured by a three-component strain-gage balance mounted below the end plate at the wing root.

The investigation was conducted in a static-test facility at the Langley Aeronautical Laboratory. All data presented were obtained at zero forward speed with a static thrust of approximately 25 pounds at each propeller. This gave a disk loading of 8 lb/sq ft which is probably somewhat below the level that would be used in most full-scale applications. Inasmuch as tests were conducted in a large room (ref. 3), none of the corrections which are applicable to wind-tunnel tests were applied.

RESULTS AND DISCUSSION

Effect of Number of Propellers

A comparison of the turning effectiveness obtained with one and with two propellers not overlapped is presented in figure 8. The chief effect of using only the inboard propeller is seen to be a large loss (up to 20 percent) in thrust-recovery factor (at a given turning angle) and a small loss in maximum turning angle. This result is in agreement with the data of reference 1 which also indicate a serious loss in thrust recovery for a double-slotted-flap configuration. Reference 4, on the other hand, exhibited primarily a loss in maximum turning angle

when only the inboard propeller was used on a model equipped with plain flaps and auxiliary turning vanes. The reasons for these losses and the different manners in which these losses present themselves are not clearly understood; however, tuft studies of the flow around these models indicate that spanwise flow develops at the edge of the slipstream when the slipstream impinges on the lower surface of the highly deflected flap system. The amount of this spanwise flow and the losses resulting therefrom increase with increasing flap deflection. When two slipstreams are parallel and tangent to each other, spanwise flow can develop only on their free sides. The losses in the turning processes would therefore be expected to be lower with two propellers per semispan.

Effect of Vertical Position of Propeller

Out of the region of ground effect, downward displacement of the propeller greatly reduced the diving moments inherent in this configuration but also generally produced slight losses in the turning angle (figs. 9 to 11). As has been noted on previous configurations, the reduction in the diving moments is almost entirely due to the direct moment of the thrust vector passing below the moment reference point. Little or no aerodynamic change is evident.

Reference 1 showed that lowering the thrust line generally reduced the losses in turning angle and thrust recovery usually encountered as the ground is approached. From figures 12 and 13 of the present report it is seen that lowering the thrust line from $\frac{Z}{D} = 0.021$ to $\frac{Z}{D} = -0.104$ resulted in some reduction in the losses experienced within the ground-effect region. However, further lowering of the thrust axis to $\frac{Z}{D} = -0.229$ resulted in sizeable increases in these losses in general. The lowest propeller position $\left(\frac{Z}{D} = -0.229\right)$ was found superior only when the wing was very close to the ground $\left(\frac{h}{D} = 0.20\right)$.

It should also be noted that the most serious ground effects are encountered with the highest flap deflections (fig. 13). This condition arises because the rear flap is more prone to flow separation when at the high deflection angles as has been noted previously in reference 1.

In general the present investigation did not show as large a beneficial effect of lowering the thrust line as might have been expected from reference 1. This difference may be due to a number of contributing factors including the difference in ground-board angles used and the fact that the flap system used in the present investigation is not as efficient as that of reference 1.

Effect of Extending Nacelles Through Flaps

Inasmuch as the motor length was fixed, it was necessary to segment the flaps to allow for flap deflections when the motor was mounted in the most rearward position. In order to demonstrate the effect of flap segmentation, tests were made with the propeller in chordwise position $\frac{X}{D} = 0.333$ utilizing segmented and full-span flaps. Figures 14 to 16 indicate that segmenting the flaps results in a very large loss in both thrust recovery and turning angle. This loss, of course, is to be expected inasmuch as the flaps are carrying practically all the load resulting from deflecting the slipstream. Any cutout in the flap system will therefore allow some of the slipstream to pass through without being deflected and also large turbulent mixing losses will be encountered at the ends of the flaps made by the cutout. The reductions in diving moment shown in figures 14 to 16 are a natural result of the reduced load carried by the flaps.

Effect of Chordwise Position of the Propellers

In general, changes in chordwise position had very little effect (figs. 17 to 26) on the slipstream deflection characteristics. Out of the region of ground effect, rearward displacement of the propellers from $\frac{X}{D} = 0.500$ to $\frac{X}{D} = 0.333$ produced an increase in turning angle and thrust recovery throughout most of the flap-deflection range (figs. 17 to 19), whereas a loss in turning angle and thrust recovery was noted at the larger flap-deflection angles when the propeller was moved farther rearward from $\frac{X}{D} = 0.333$ to $\frac{X}{D} = 0.167$ (fig. 22). Changes in diving moment were, for the most part, insignificant.

The effect of chordwise displacement of the propeller on the aerodynamic characteristics of the model in the region of ground effect was generally small and inconsistent. (See figs. 23 to 26.)

Effect of Propeller Overlap

Figures 27 to 29 present the effect of propeller overlap on the performance characteristics of the propellers and the aerodynamic characteristics of the model. Increasing the propeller overlap to 0.208D produced increases in turning effectiveness on the order of 10 percent in the highest range of flap deflections; however, this effect was not noticeable in the lower range of flap deflections. A further increase in overlap from 0.208D to 0.291D did not produce a corresponding increase

in turning effectiveness. The effect of overlap on pitching moment was negligible.

As the propellers are overlapped, however, the static-thrust efficiency of the propeller is reduced as shown in figure 30. Such a loss in efficiency is to be expected, of course, because as the propellers are overlapped they must each operate in the inflow or slipstream produced by the other propeller. If the overlapping were carried to the point that the propellers were coaxial, for instance (but the efficiency still based on the sum of the individual disk areas), it would be found that the efficiency of each would be reduced to 70.7 percent of their nonoverlapped value if the load were assumed to be equally divided between them.

Figure 30 indicates that almost all the loss was carried on the inboard propeller. This loss in efficiency of the inboard propeller was due primarily to a loss in thrust with overlap with only a small increase in torque (about 3 percent) appearing. Simultaneously the outboard propeller exhibited only a small increase in both thrust (about 4 percent) and torque (about 6 percent). During these tests the propeller rotational speed was maintained constant at 5,800 rpm.

The reason for these differences is not understood at present; however, there can be many contributing factors. For instance, reference 5 indicates that the inflow velocities produced by the outboard (rear) propeller on the inboard propeller can be appreciable even for the moderate amounts of overlap involved in these tests. The outboard (rear) propeller, on the other hand, is also subjected to an inflow which is the slipstream of the inboard propeller. Measurements of the slipstream velocities on a propeller similar to the present one, however, indicate that the slipstream diameter is appreciably smaller than the propeller diameter even 2 inches behind the propeller disk. The rear propeller (outboard) then would be subjected to the slipstream of the front propeller over only part of the overlapped area. These inflows probably account for the losses in efficiency shown, and differences in these inflows could account for some difference in the amount of loss carried on each propeller. Reference 6, on the other hand, indicated equal loss on each propeller. Reference 6, however, also used opposite rotation of the propellers, whereas in the present tests both propellers used right-hand rotation. This difference produces a change in the rotational component of velocity to which the rear propeller is subjected; thus, both the local blade angle and local velocity to which the blades are subjected over part of the overlapped area are altered.

The increase in thrust-recovery factor with overlap at the higher turning angles and flap deflections (fig. 29) and the loss in propeller efficiency with overlap (fig. 30) tend to be canceling effects.

The ability of the propeller to produce thrust varies as the two-thirds power of the efficiency; therefore, in order to compare the results on the basis of constant power it is necessary to multiply the ratios of lift to thrust L/T and longitudinal force to thrust $F_{X/T}$ by $\left(\frac{\eta_{Y/D}}{\eta_{Y/D=-.01}}\right)^{2/3}$ as shown in figure 31. The average of the inboard and outboard efficiencies was used in the calculation. From this comparison, based on constant power, it is seen that the effect of propeller overlap is to reduce the available resultant force at all but the very highest turning angles where some gain on thrust recovery is still evident.

This comparison is made on the basis of constant propeller diameter. If the design conditions fix the span of the wing, it is possible to increase the resultant force for a given power by overlapping larger propellers which will permit a gain in net disk area which will, in turn, produce a gain in thrust. However, to maintain the same turning angle the wing and flap chord would also have to be increased proportionally to the increase in propeller diameter.

Effect of Position and Deflection of a Leading-Edge Slat

Reference 7 indicated that a large-chord leading-edge slat could, to some extent, counteract the diving-moment characteristic of deflected slipstream configurations, and reference 8 showed that such a slat would delay wing stall in the transition speed range. Therefore, a 30-percent-chord slat mounted in several vertical positions was investigated in the region of ground effect and the results are presented in figures 32 to 37. The propellers were mounted at $\frac{X}{D} = 0.333$ and $\frac{Z}{D} = -0.104$ for all slat-position tests.

The immediate effect of the addition of the slat when deflected so as to reduce the diving moment, was a significant loss in thrust-recovery factor and turning angle. In general a slat deflection of 0° produced the best thrust recovery and highest turning angles although these values were seldom better than the slat-off values and this slat deflection only produced small reductions in the diving moments.

Propeller Static-Thrust Efficiency in Ground Effect

The variation of the static-thrust efficiency of the propellers with height above the ground and slat deflection is presented in figure 38 for two flap configurations. In general the outboard propeller showed little

change in efficiency with height above the ground; however, the inboard propeller showed a slight loss in efficiency at intermediate heights and a gain in the positions closest to the ground. This loss in efficiency at intermediate heights is unfortunately coincident with the loss in thrust recovery at these heights and for the case of constant power would tend to increase the loss in resultant force available to support the airplane in hovering at these intermediate heights.

Effect of Nacelle Size

The majority of the data of this and previous investigations were obtained with small nacelles which might represent a turboprop installation or a fairing over the power train from a remotely mounted engine. Use of reciprocating engines would require much larger nacelles. In order to investigate the effect of nacelle size, balsa-wood fairings (shown in fig. 39) were added to the model to simulate a reciprocating engine installation.

The results of the investigation of the effect of nacelle size (fig. 40) show approximately 5 to 10 percent loss in turning effectiveness when the larger nacelles are used. This loss appeared to be associated with flow separation at the juncture between the wing and nacelle on the lower surface, particularly on the rear tapered part of the nacelle. Attempts to regain some of these losses by the use of large fillets were only partially successful. These losses, in addition to the lower ratio of thrust to weight, place present reciprocating engines at a considerable disadvantage to turboprop engines for use on VTOL aircraft.

CONCLUSIONS

An investigation of the effect of propeller position and overlap on the slipstream deflection characteristics of a model equipped with a sliding and a Fowler flap indicates the following conclusions:

1. Large reductions in diving moments were obtained by lowering the thrust axis. However, these reductions were almost entirely due to the direct moment created by displacing the thrust vector below the moment reference point. Vertical and chordwise changes in propeller position produced little or no change in the aerodynamic characteristics out of the region of ground effect. In the region of ground effect, lowering the thrust axis about 10 percent of the diameter produced some reduction in the adverse effects of the ground.

2. In the highest range of flap deflections, propeller overlap produced a significant increase in thrust recovery while producing no change at low and intermediate deflections. However, as the amount of propeller overlap was increased, the static-thrust efficiency of the inboard propeller decreased while the efficiency of the outboard propeller remained nearly constant, the net result at constant power being a reduction in resultant force due to loss in propeller efficiency at low and intermediate flap deflections and only a small gain at high flap deflections.

3. The thrust recovery with inboard propeller alone was much lower than with two propellers.

4. Segmenting the flaps to permit rearward extension of the nacelle fairing greatly reduced both the thrust recovery and the turning angle.

5. The addition of a leading-edge slat caused a significant reduction in thrust recovery and turning angle at slat deflections needed to reduce the diving moments appreciably.

6. Increasing the nacelle size to simulate that required for reciprocating engines reduced both the turning angle and thrust recovery.

Langley Aeronautical Laboratory,
National Advisory Committee for Aeronautics,
Langley Field, Va., August 12, 1958.

REFERENCES

1. Kuhn, Richard E.: Investigation of the Effects of Ground Proximity and Propeller Position on the Effectiveness of a Wing With Large-Chord Slotted Flaps in Redirecting Propeller Slipstreams Downward for Vertical Take-Off. NACA TN 3629, 1956.

2. McLemore, H. Clyde, and Cannon, Michael D.: Aerodynamic Investigation of a Four-Blade Propeller Operating Through an Angle-of-Attack Range From 0° to 180°. NACA TN 3228, 1954.

3. Kuhn, Richard E.: Investigation of Effectiveness of a Wing Equipped With a 50-Percent-Chord Sliding Flap, a 30-Percent-Chord Slotted Flap, and a 30-Percent-Chord Slat in Deflecting Propeller Slipstreams Downward for Vertical Take-Off. NACA TN 3919, 1957.

4. Kuhn, Richard E., and Draper, John W.: An Investigation of a Wing-Propeller Configuration Employing Large-Chord Plain Flaps and Large-Diameter Propellers for Low-Speed Flight and Vertical Take-Off. NACA TN 3307, 1954.

5. Castles, Walter, Jr., and De Leeuw, Jacob Henri: The Normal Component of the Induced Velocity in the Vicinity of a Lifting Rotor and Some Examples of Its Application. NACA Rep. 1184, 1954. (Supersedes NACA TN 2912.)

6. Kuhn, Richard E., and Draper, John W.: Investigation of the Aerodynamic Characteristics of a Model Wing-Propeller Combination and of the Wing and Propeller Separately at Angles of Attack up to 90°. NACA Rep. 1263, 1956. (Supersedes NACA TN 3304 by Draper and Kuhn.)

7. Kuhn, Richard E.: Investigation at Zero Forward Speed of a Leading-Edge Slat as a Longitudinal Control Device for Vertically Rising Airplanes That Utilize the Redirected-Slipstream Principle. NACA TN 3692, 1956.

8. Kuhn, Richard E., and Hayes, William C., Jr.: Wind-Tunnel Investigation of Effect of Propeller Slipstreams on Aerodynamic Characteristics of a Wing Equipped With a 50-Percent-Chord Sliding Flap and a 30-Percent-Chord Slotted Flap. NACA TN 3918, 1957.

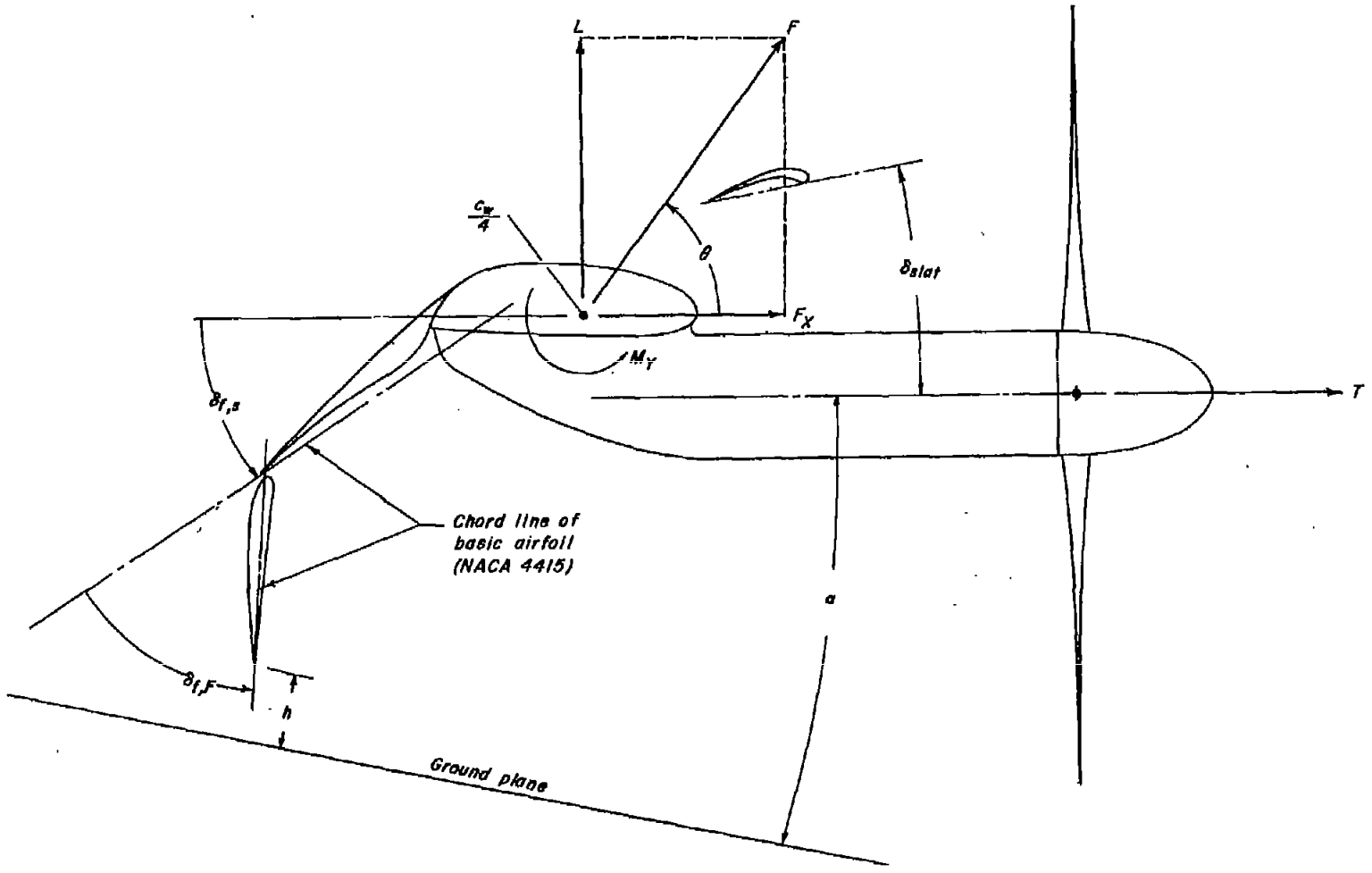

Figure 1.- Convention used to define positive sense of forces, moments, and angles.

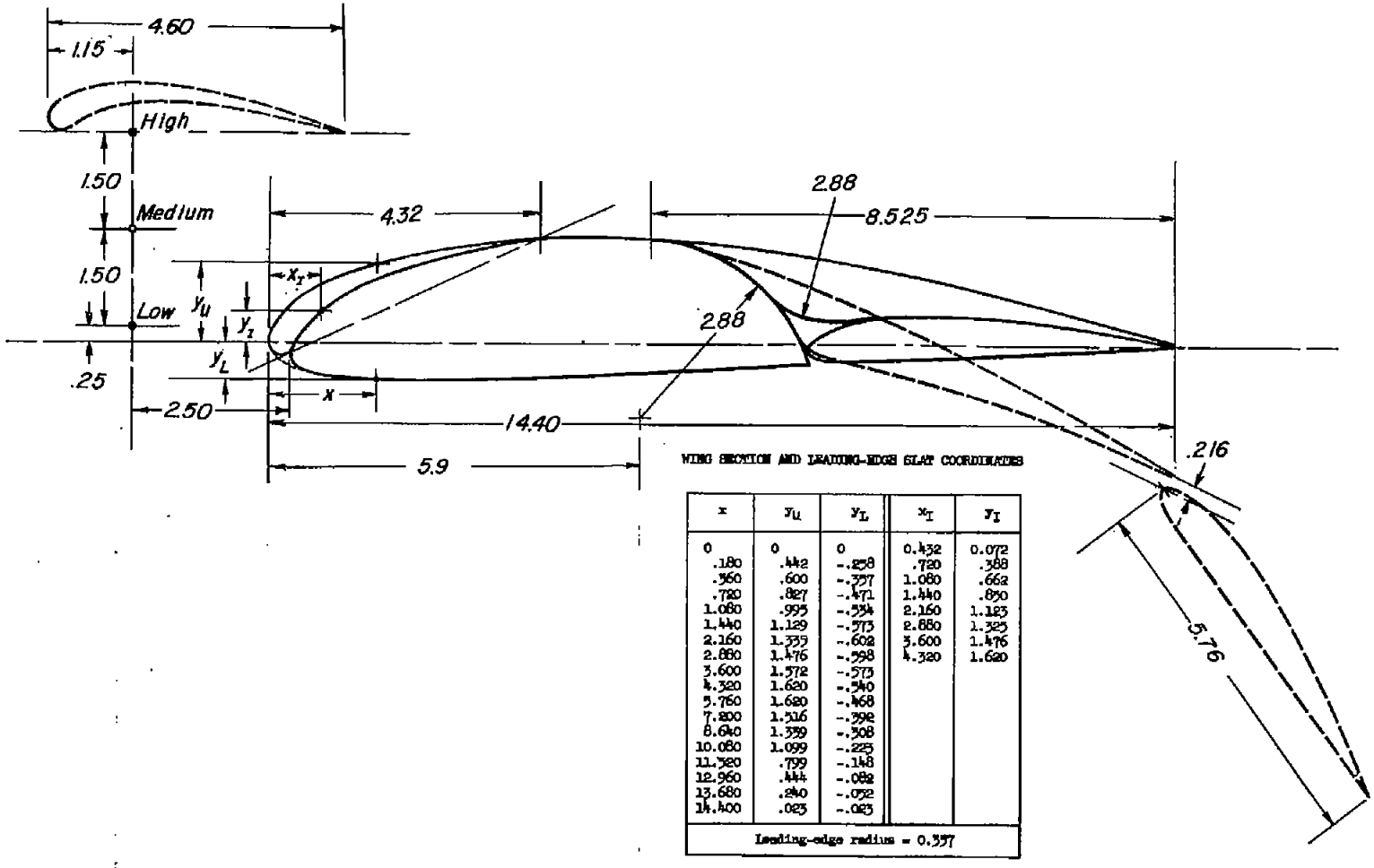

WING SECTION AND LEADING-EDGE SLAT COORDINATES

x	y_u	y_L	x_I	y_I
0	0	0	0.432	0.072
.180	.442	-.258	.720	.388
.360	.600	-.357	1.080	.662
.720	.827	-.471	1.440	.850
1.080	.995	-.554	2.160	1.123
1.440	1.129	-.573	2.880	1.325
2.160	1.339	-.602	3.600	1.476
2.880	1.476	-.598	4.320	1.620
3.600	1.572	-.573		
4.320	1.620	-.540		
5.760	1.620	-.468		
7.200	1.516	-.398		
8.640	1.359	-.308		
10.080	1.099	-.225		
11.520	.799	-.148		
12.960	.444	-.082		
13.680	.240	-.052		
14.400	.025	-.025		

Leading-edge radius = 0.337

Figure 2.- Geometric characteristics of wing section. All dimensions are in inches.

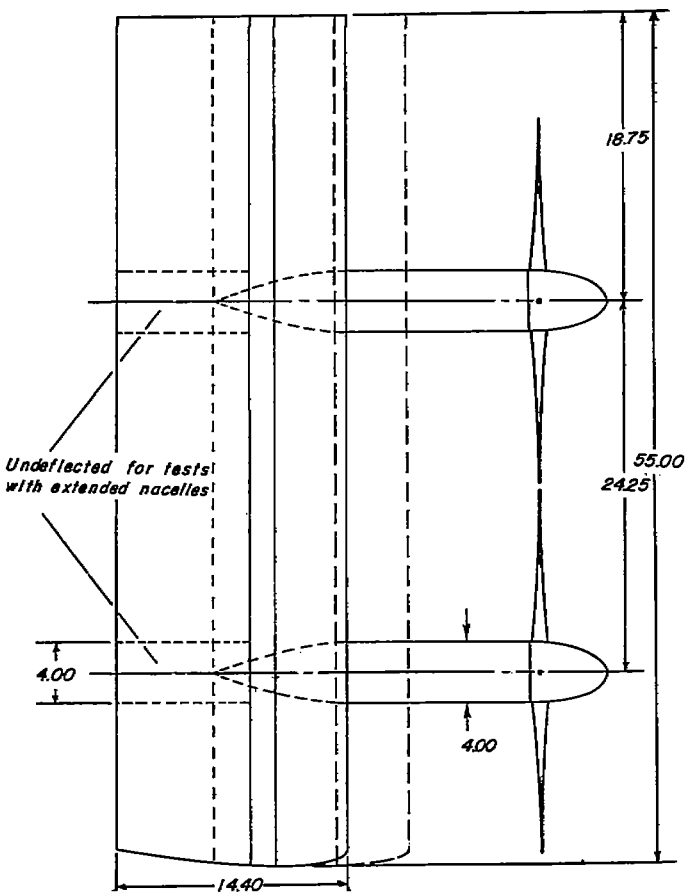

Geometric Characteristics

Wing:	
Area (semispan), sq ft	5.48
Semispan, ft	4.58
Chord, ft	1.20
Airfoil section	NACA 4415
Aspect ratio, full span	7.66
Propellers:	
Diameter, ft	2.00
Nacelle diameter, ft	.033
Number of blades (each)	3

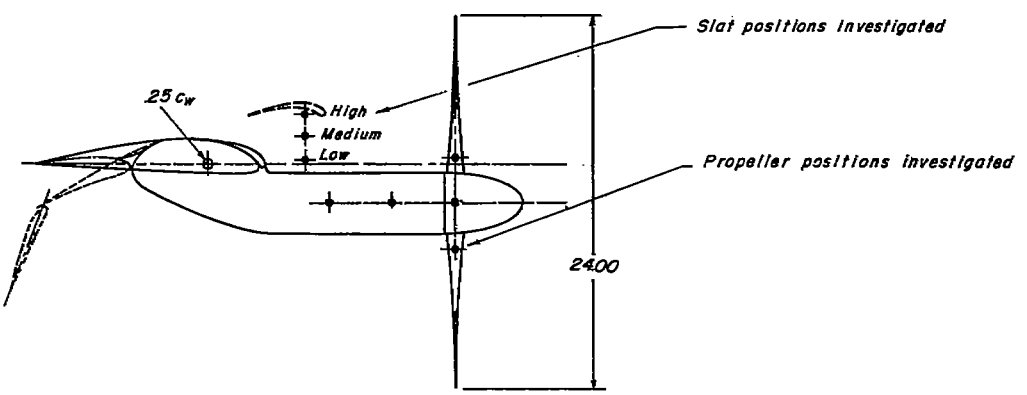

Figure 3.- Sketch of model with propellers in basic position $\left(\frac{X}{D} = 0.500;\ \frac{Z}{D} = -0.104\right)$. All dimensions are in inches.

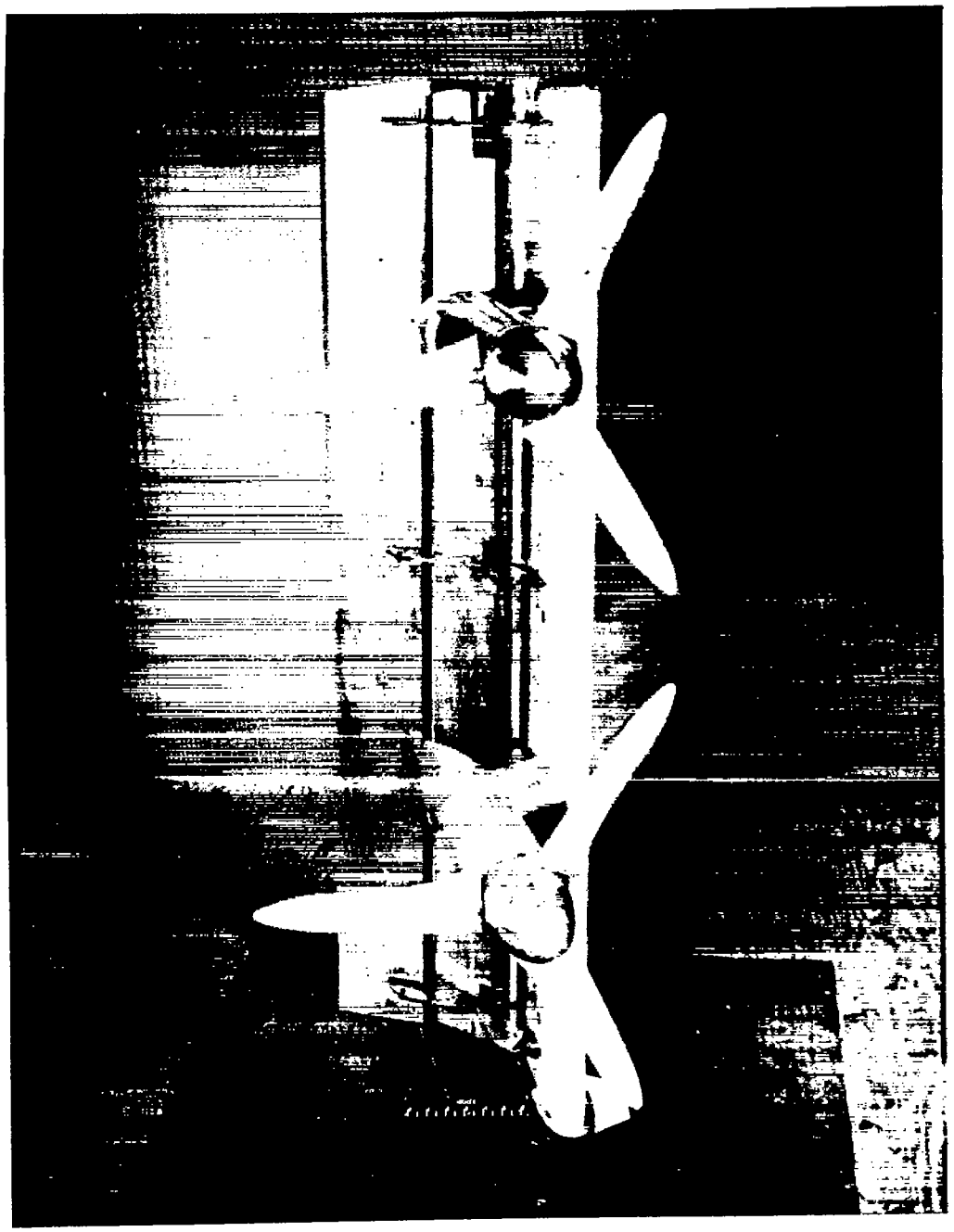

L-96515

Figure 4.- Model installed in a static-test facility at the Langley Laboratory. $\frac{X}{D} = 0.500$; $\frac{Y}{D} = -0.01$; $\frac{Z}{D} = -0.229$.

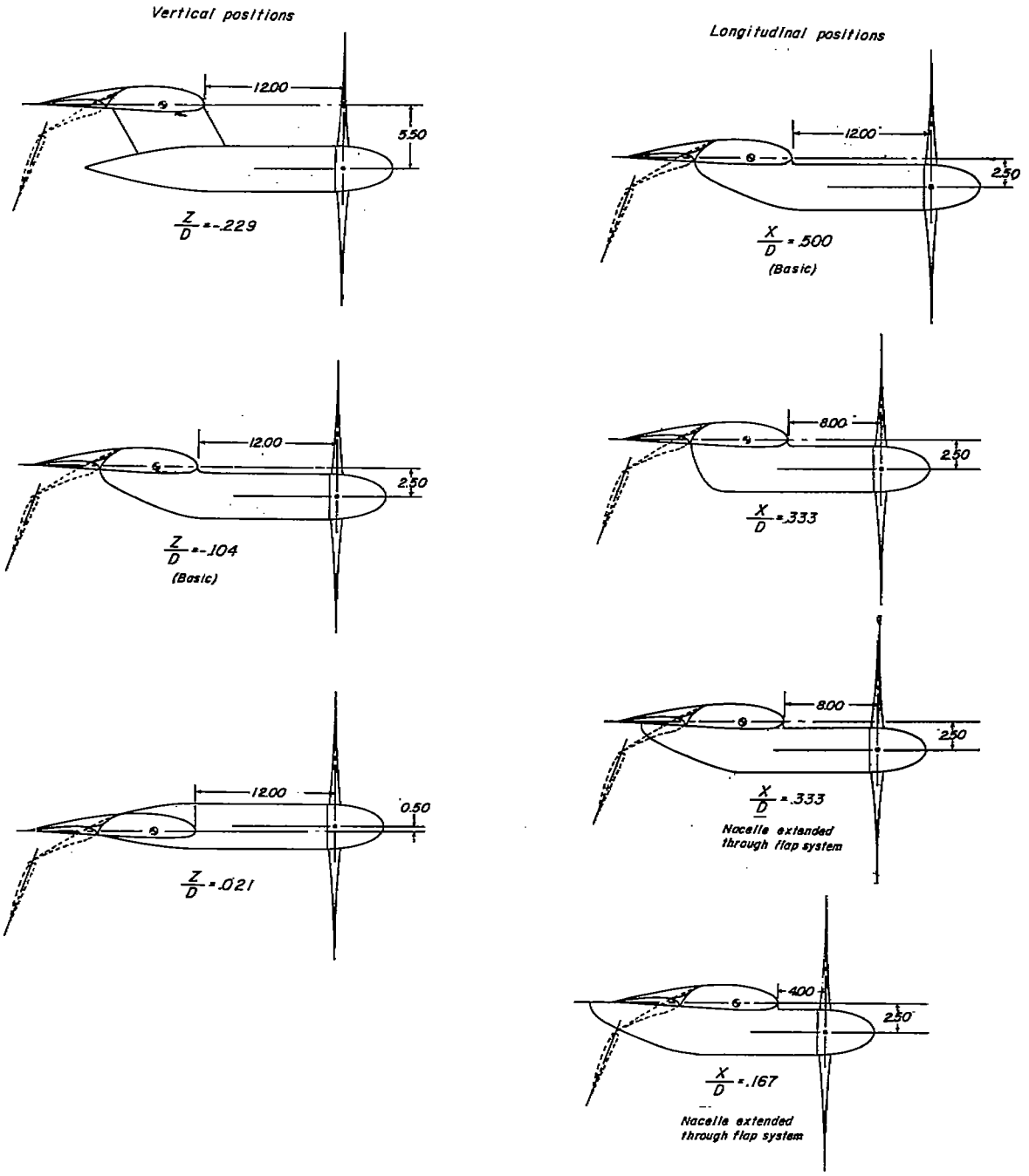

Figure 5.- Sketches of model showing vertical and chordwise positions of propellers. All dimensions are in inches.

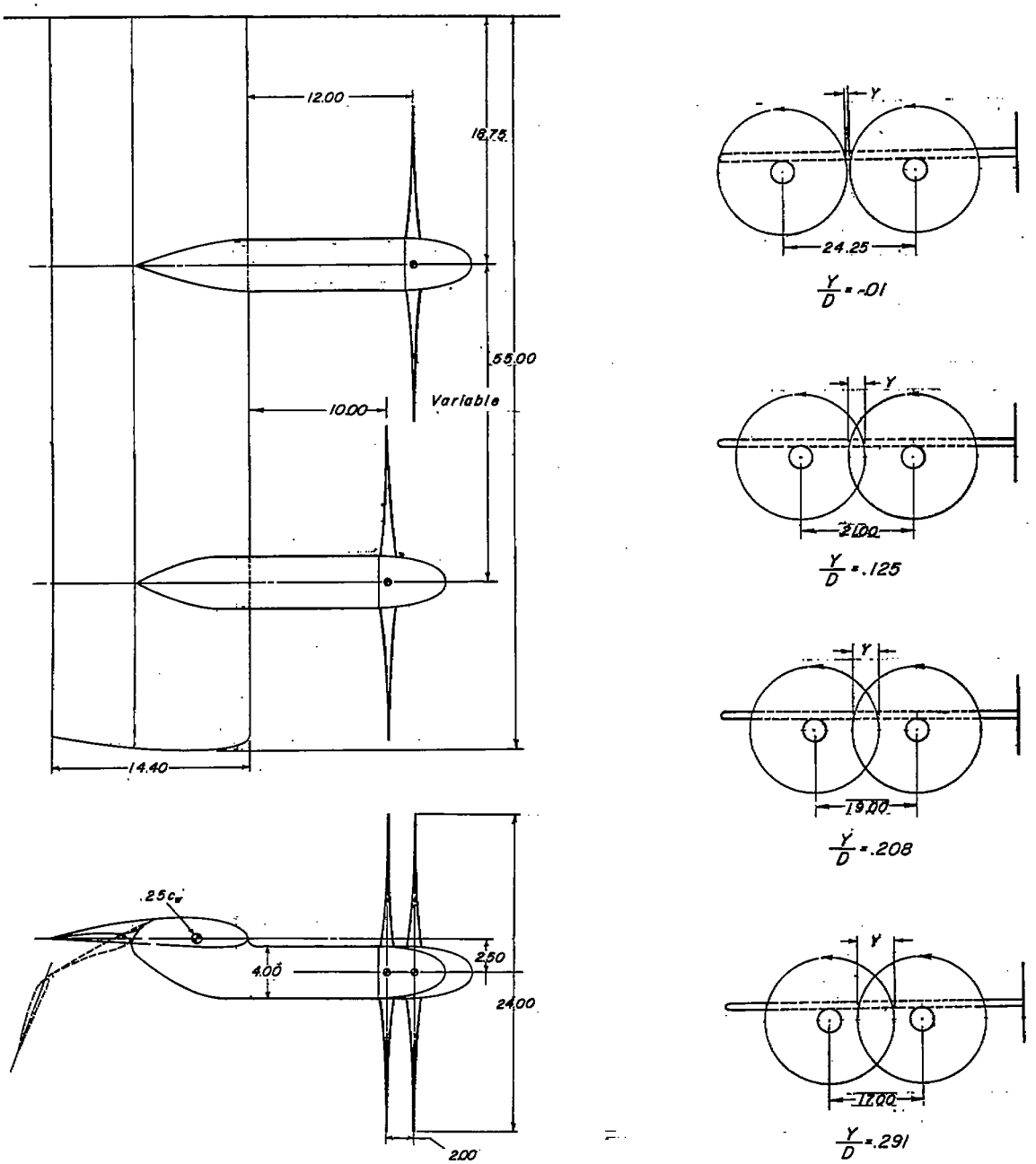

Figure 6.- Sketches of model showing propeller-overlap configuration. All dimensions are in inches.

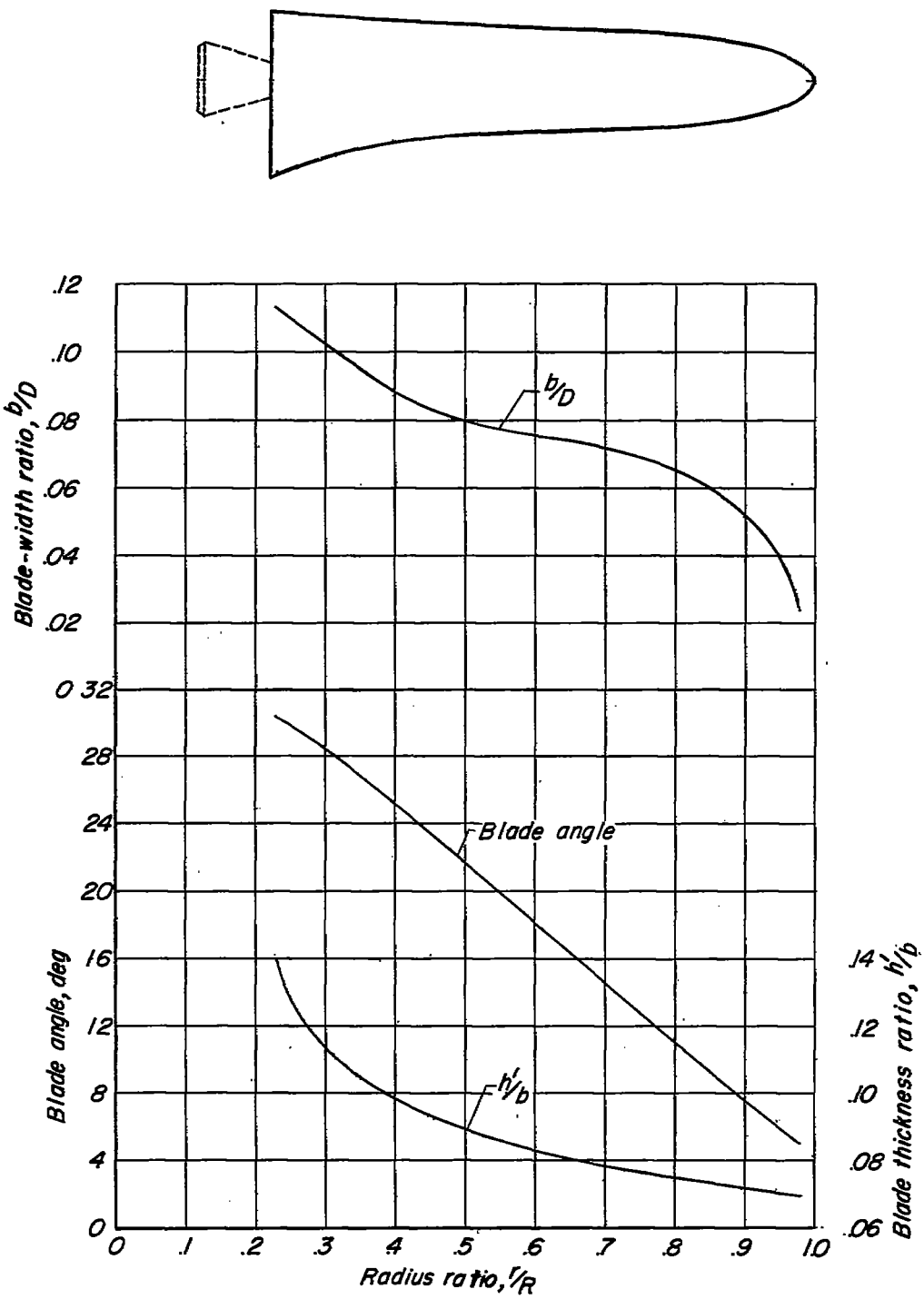

Figure 7.- Propeller blade-form curves. NACA 16-series section.

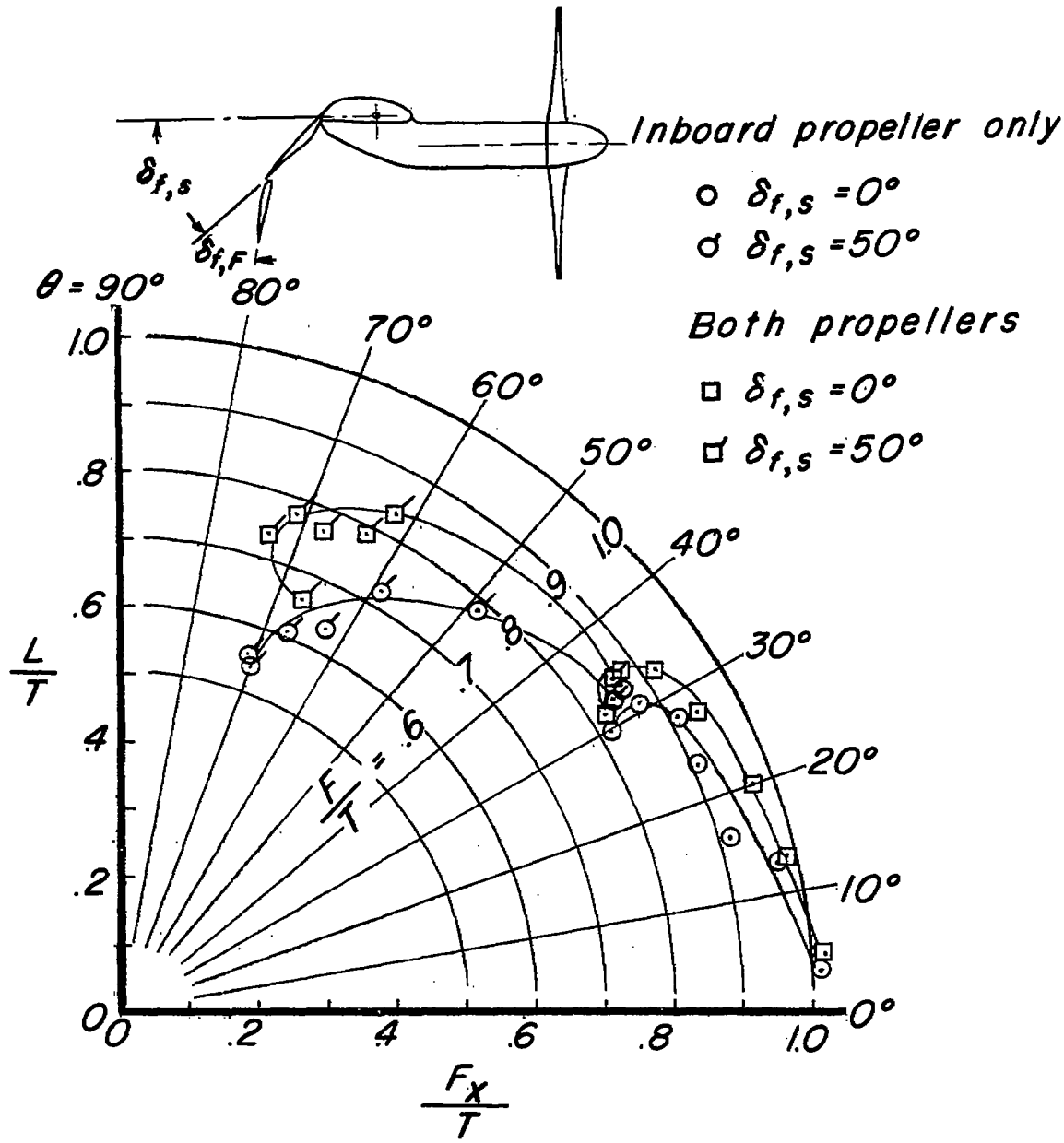

(a) Summary of turning effectiveness.

Figure 8.- Comparison of turning effectiveness obtained with one and two propellers. $\frac{X}{D}$ = 0.500; $\frac{Y}{D}$ = -0.01; $\frac{Z}{D}$ = -0.104; $\delta_{f,F}$, variable; full-span flaps.

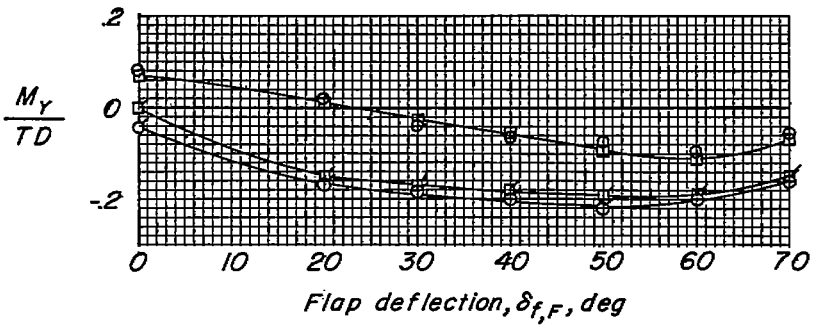

(b) Pitching moment.

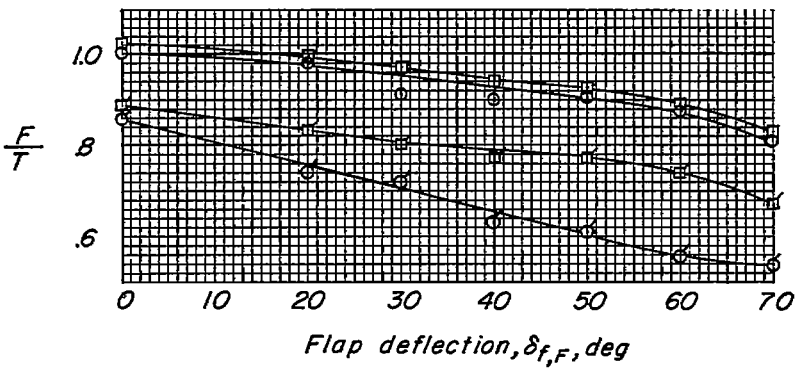

(c) Thrust-recovery factor.

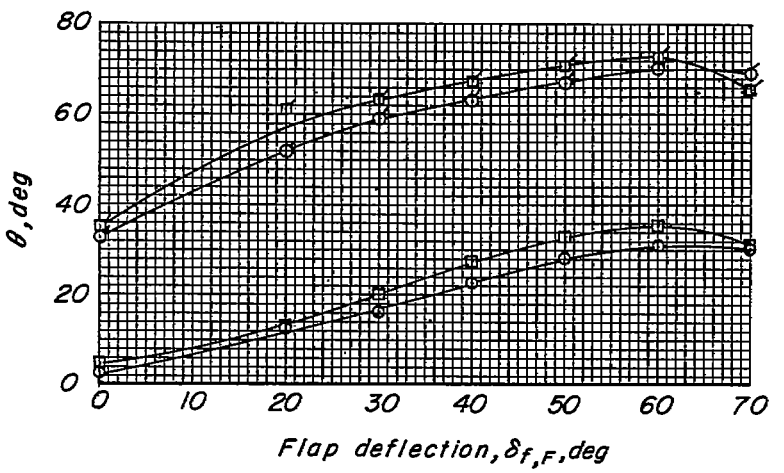

(d) Turning angle.

Figure 8.- Concluded.

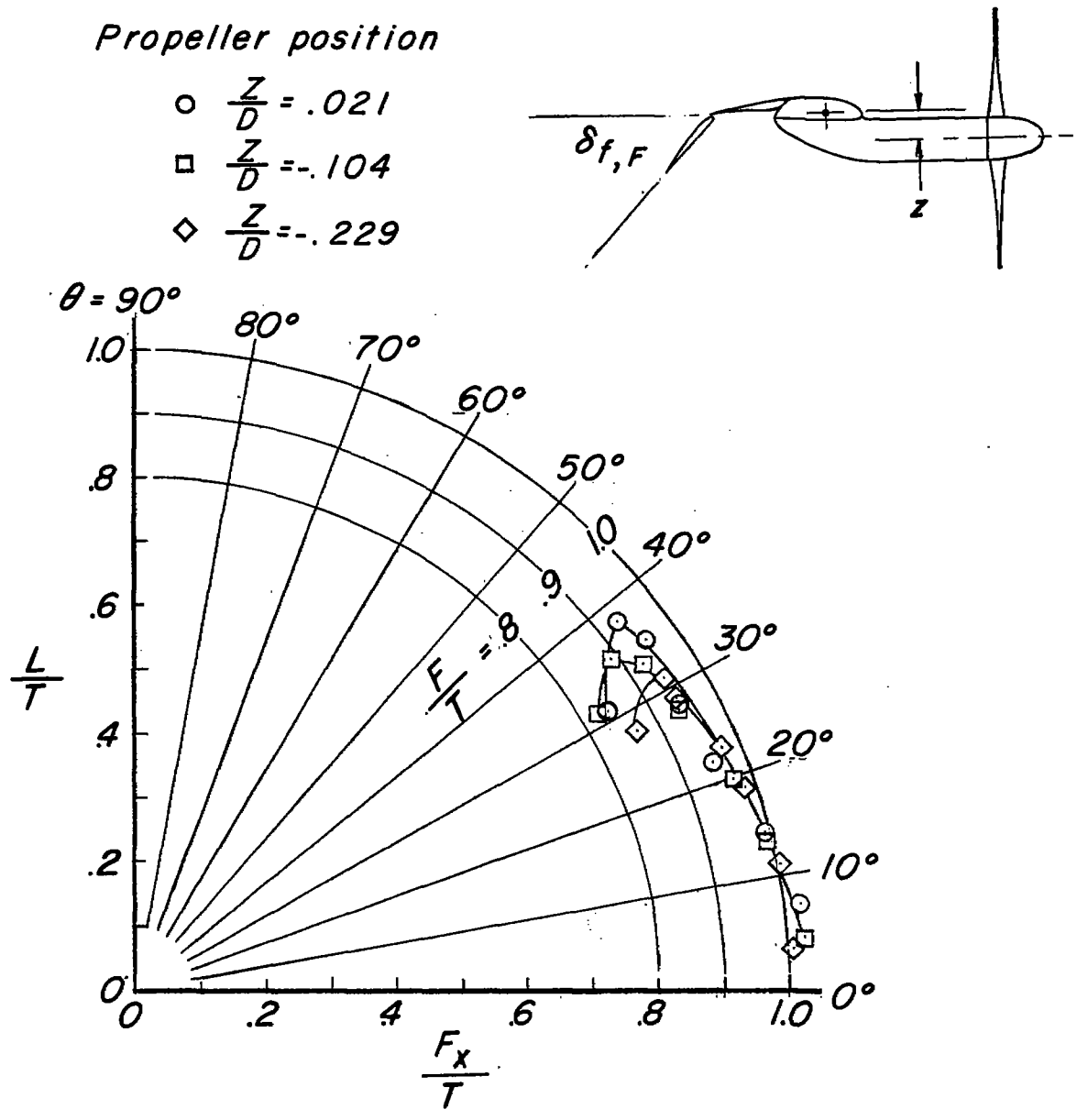

(a) Summary of turning effectiveness.

Figure 9.- Effect of vertical displacement of propellers. $\frac{X}{D} = 0.500$; $\frac{Y}{D} = -0.01$; $\delta_{f,s} = 0^{\circ}$; $\delta_{f,F}$, variable; full-span flaps.

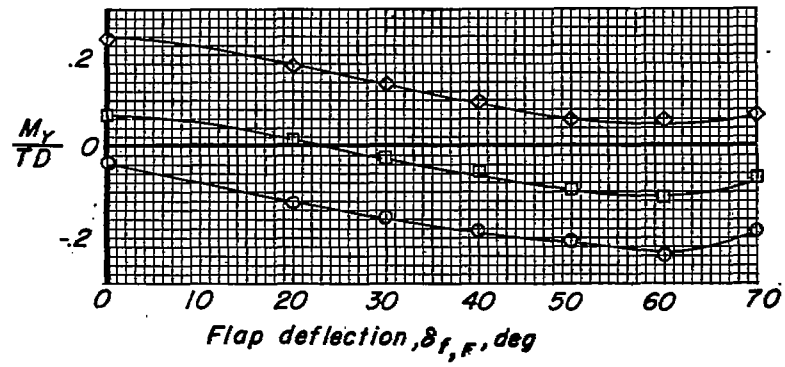

(b) Pitching moment.

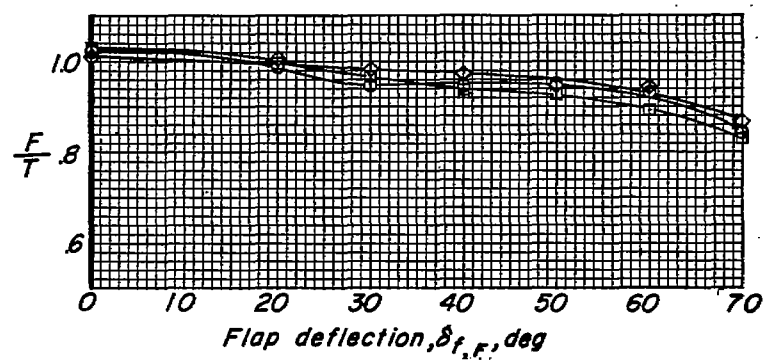

(c) Thrust-recovery factor.

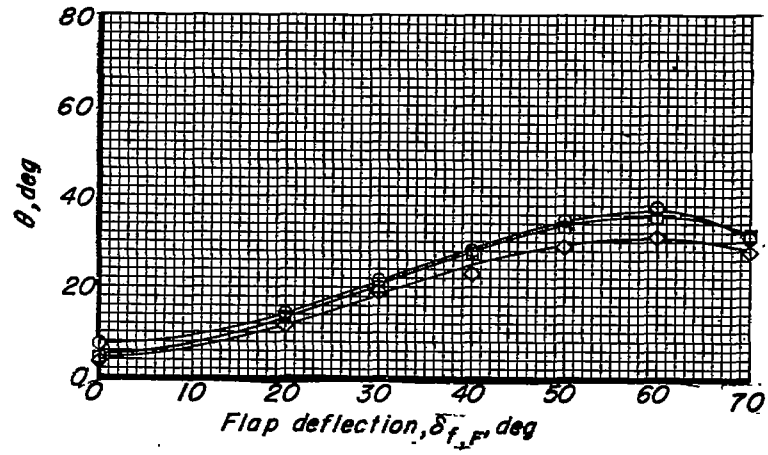

(d) Turning angle.

Figure 9.- Concluded.

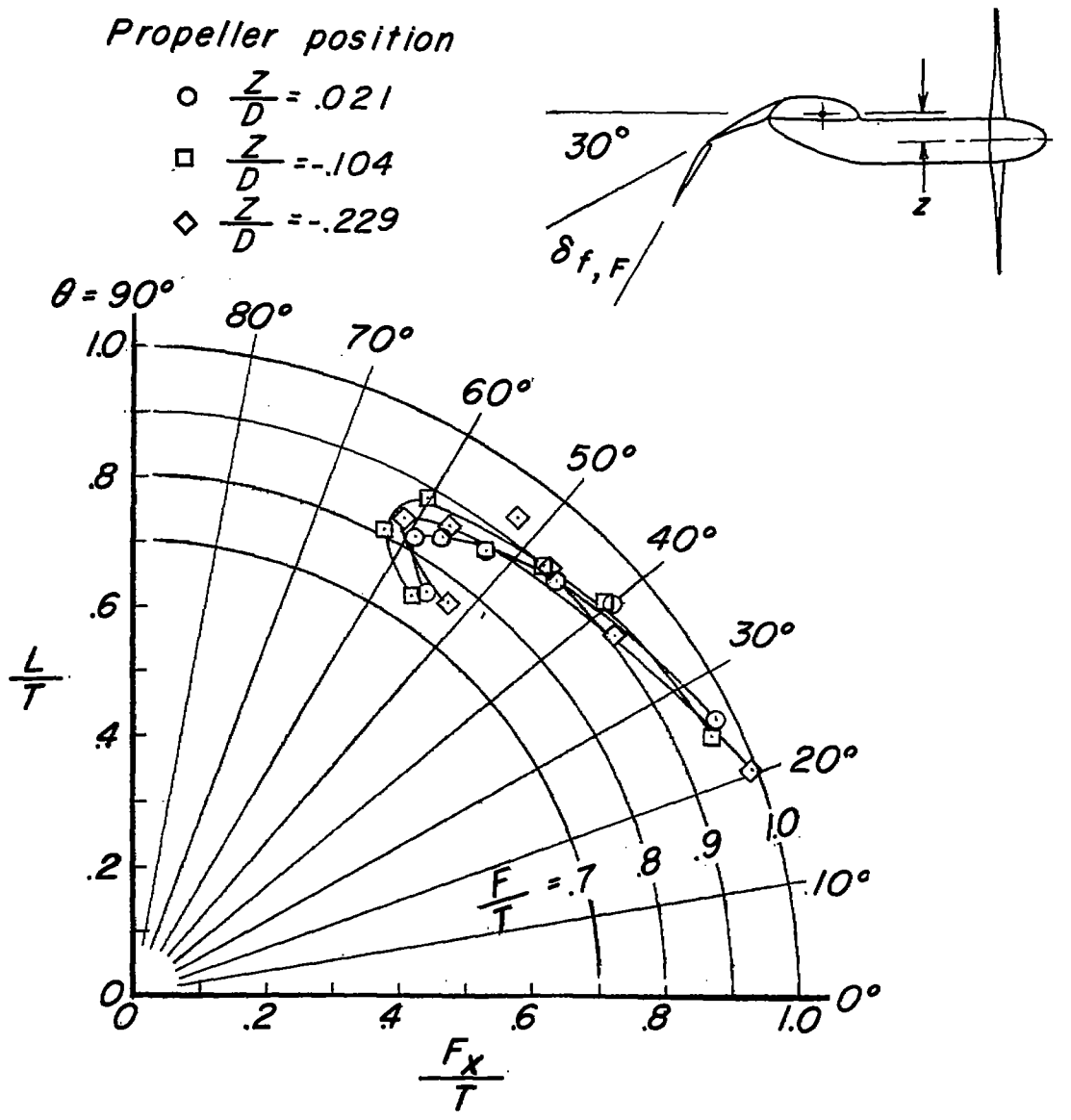

(a) Summary of turning effectiveness.

Figure 10.- Effect of vertical displacement of propellers. $\frac{X}{D} = 0.500$; $\frac{Y}{D} = -0.01$; $\delta_{f,s} = 30^{\circ}$; $\delta_{f,F}$, variable; full-span flaps.

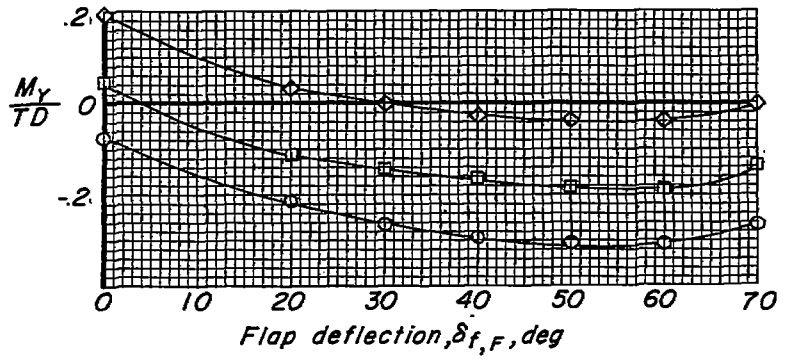

(b) Pitching moment.

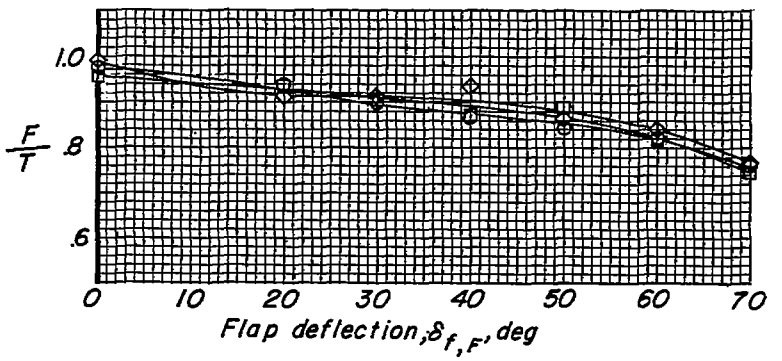

(c) Thrust-recovery factor.

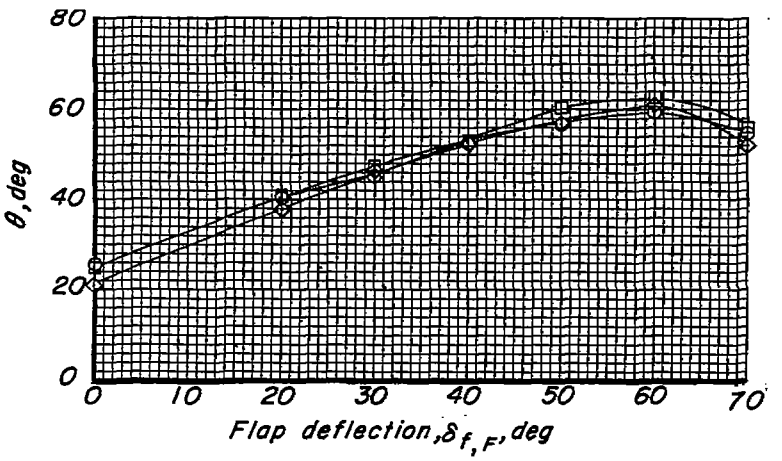

(d) Turning angle.

Figure 10.- Concluded.

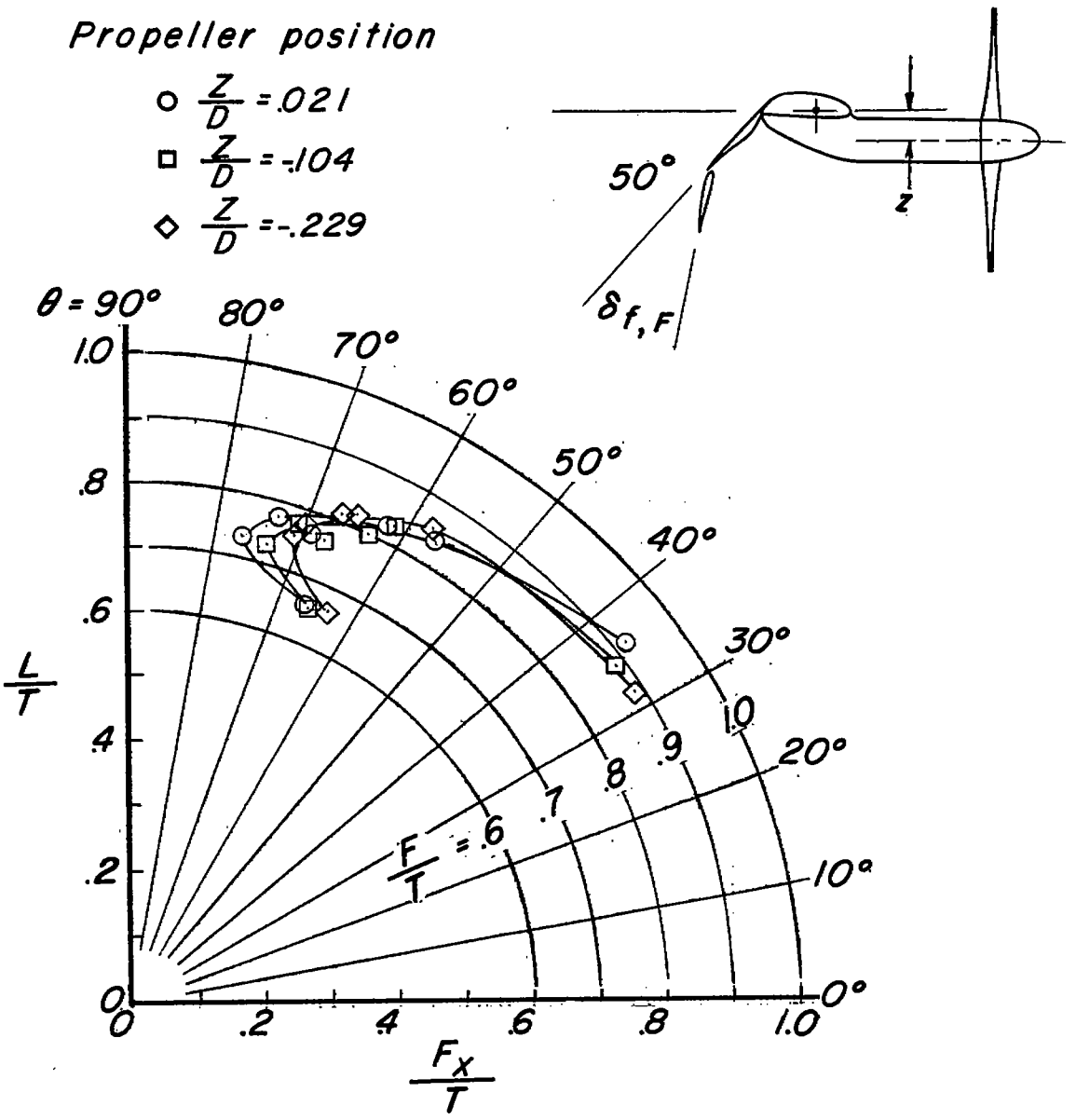

(a) Summary of turning effectiveness.

Figure 11.- Effect of vertical displacement of propellers. $\frac{X}{D} = 0.500$; $\frac{Y}{D} = -0.01$; $\delta_{f,s} = 50^{\circ}$; $\delta_{f,F}$, variable; full-span flaps.

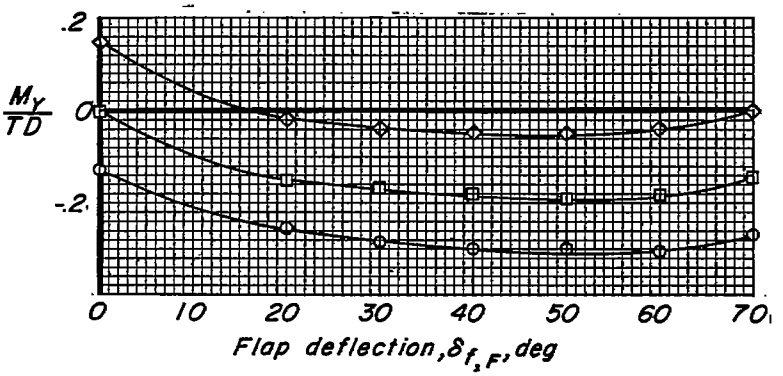

(b) Pitching moment.

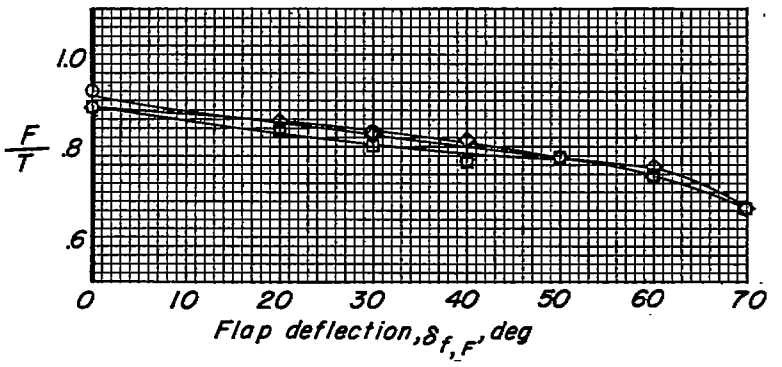

(c) Thrust-recovery factor.

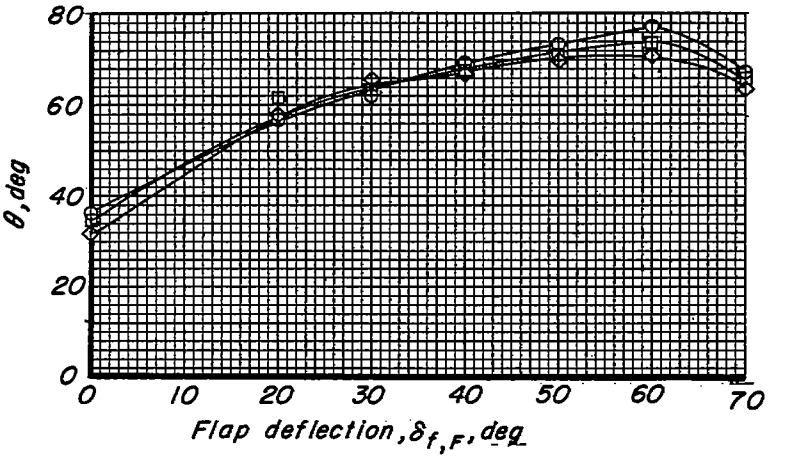

(d) Turning angle.

Figure 11.- Concluded.

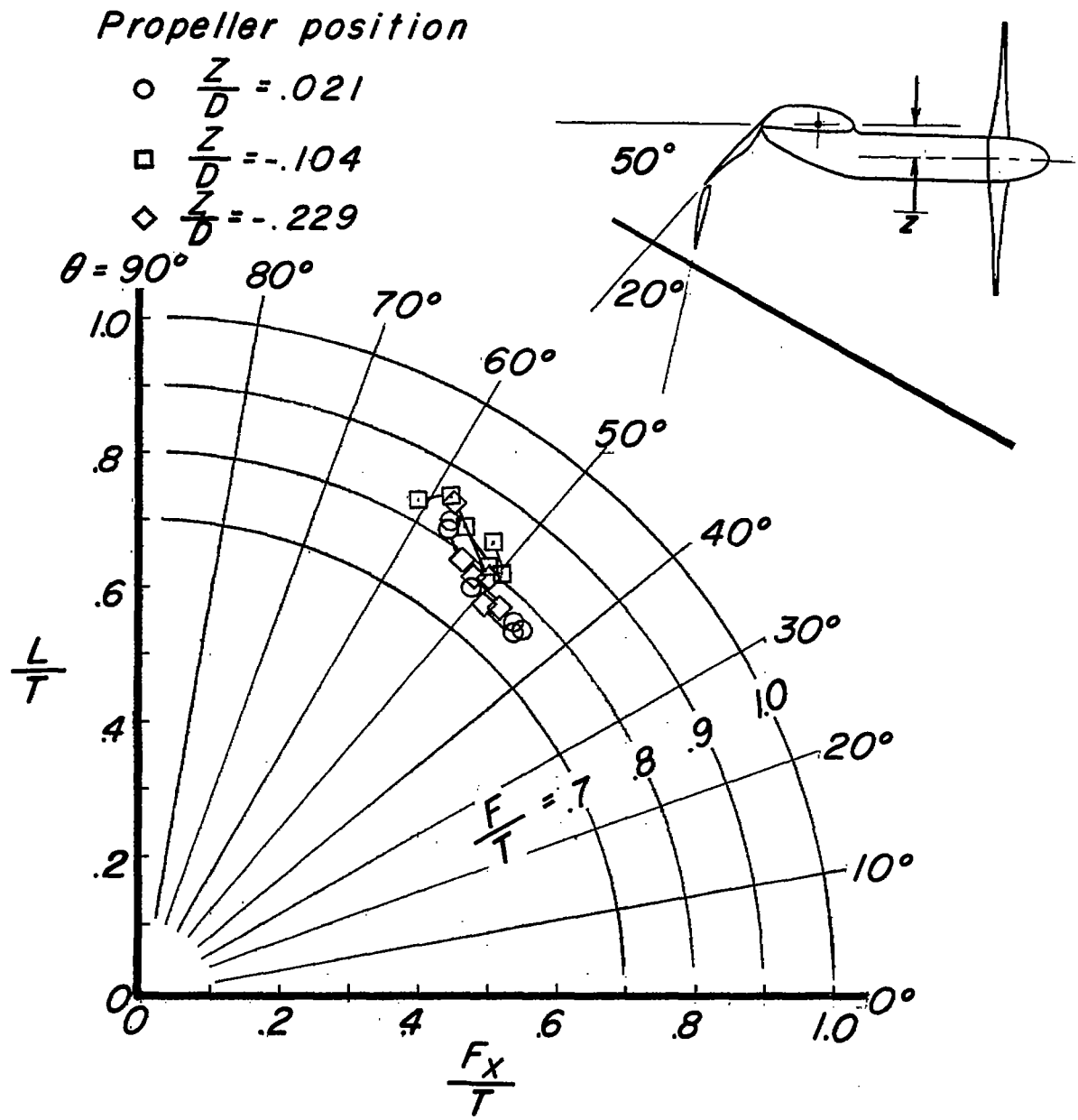

(a) Summary of turning effectiveness.

Figure 12.- Effect of vertical displacement of propellers in the region of ground effect. $\frac{X}{D}$ = 0.500; $\frac{Y}{D}$ = -0.01; $\delta_{f,s}$ = 50°; $\delta_{f,F}$ = 20°; ground-board angle, 32°; full-span flap; h/D, variable.

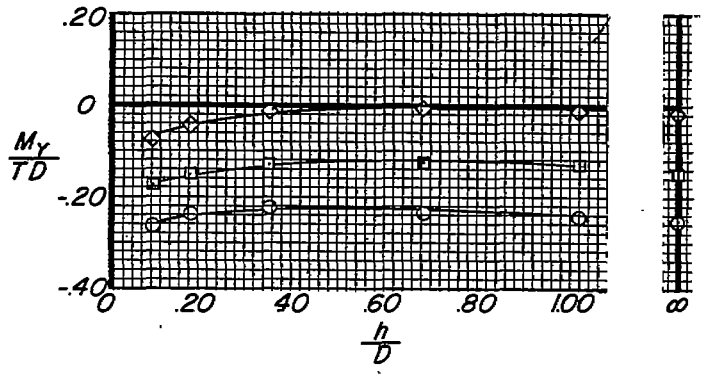

(b) Pitching moment.

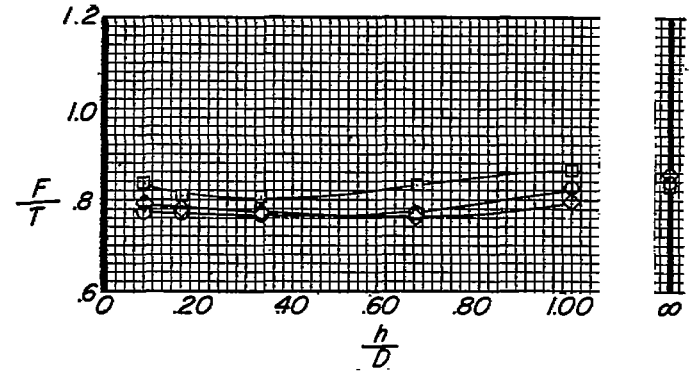

(c) Thrust-recovery factor.

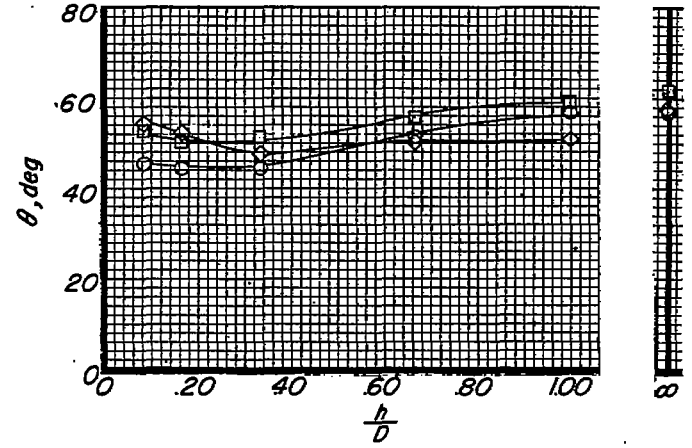

(d) Turning angle.

Figure 12.- Concluded.

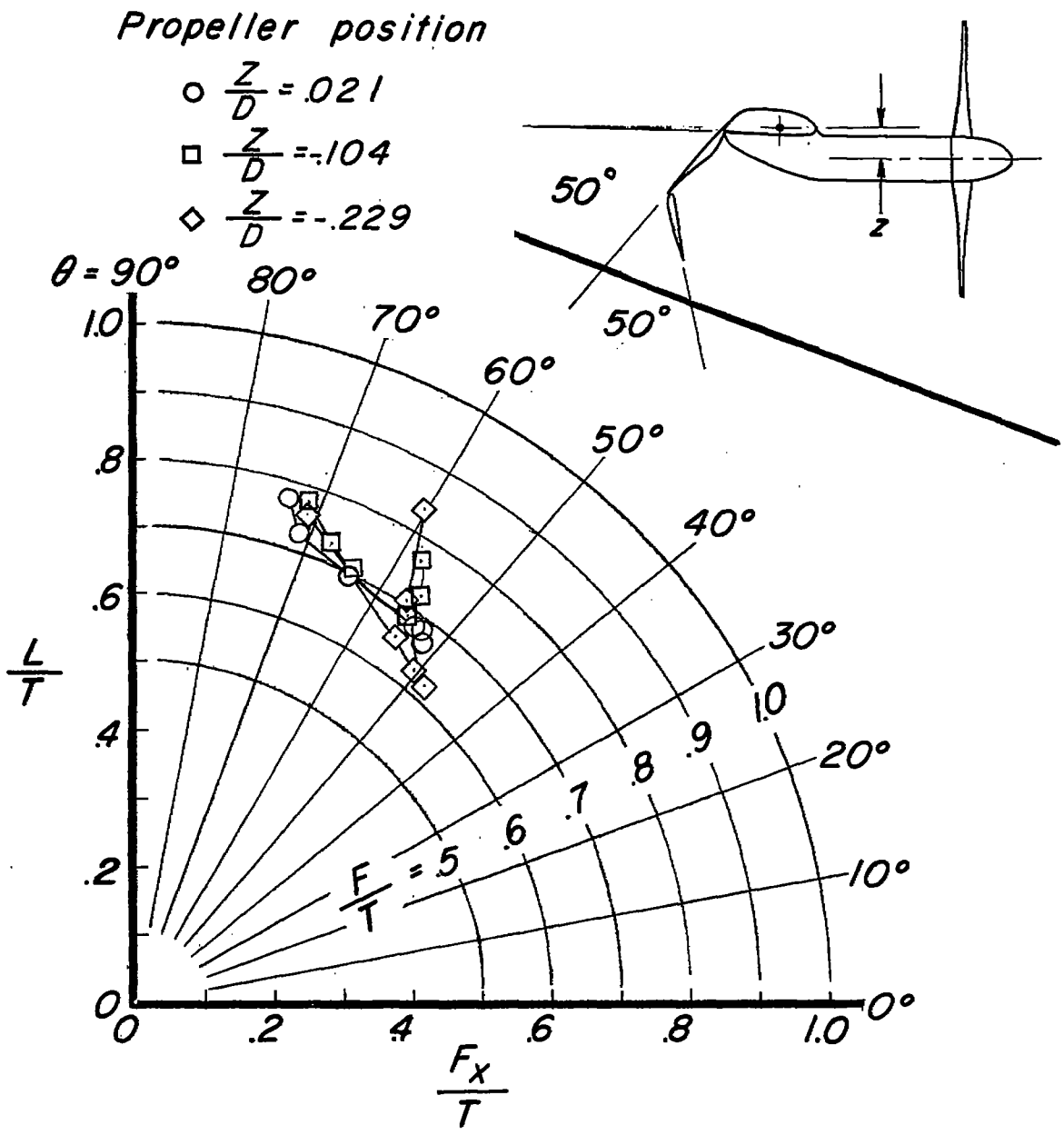

(a) Summary of turning effectiveness.

Figure 13.- Effect of vertical displacement of propellers in the region of ground effect. $\frac{X}{D}$ = 0.500; $\frac{Y}{D}$ = -0.01; $\delta_{f,s}$ = 50°; $\delta_{f,F}$ = 50°; ground-board angle, 20°; full-span flaps; h/D, variable.

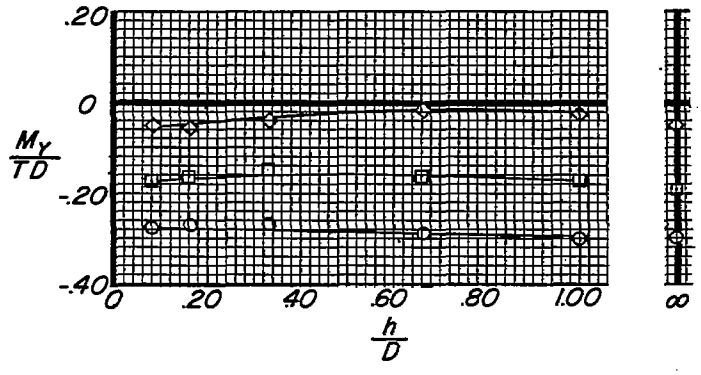

(b) Pitching moment.

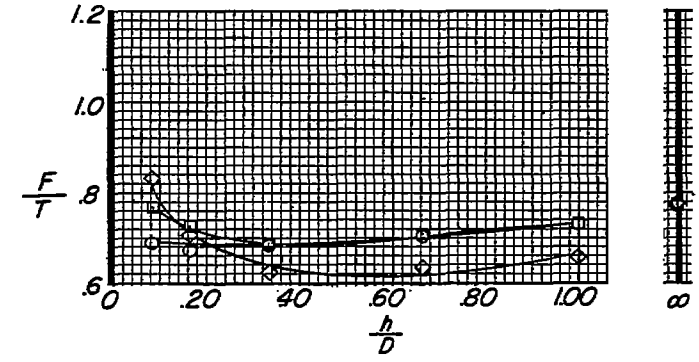

(c) Thrust-recovery factor.

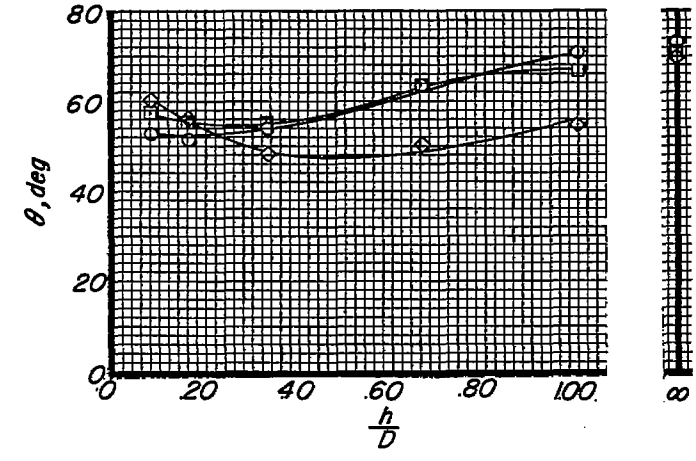

(d) Turning angle.

Figure 13.- Concluded.

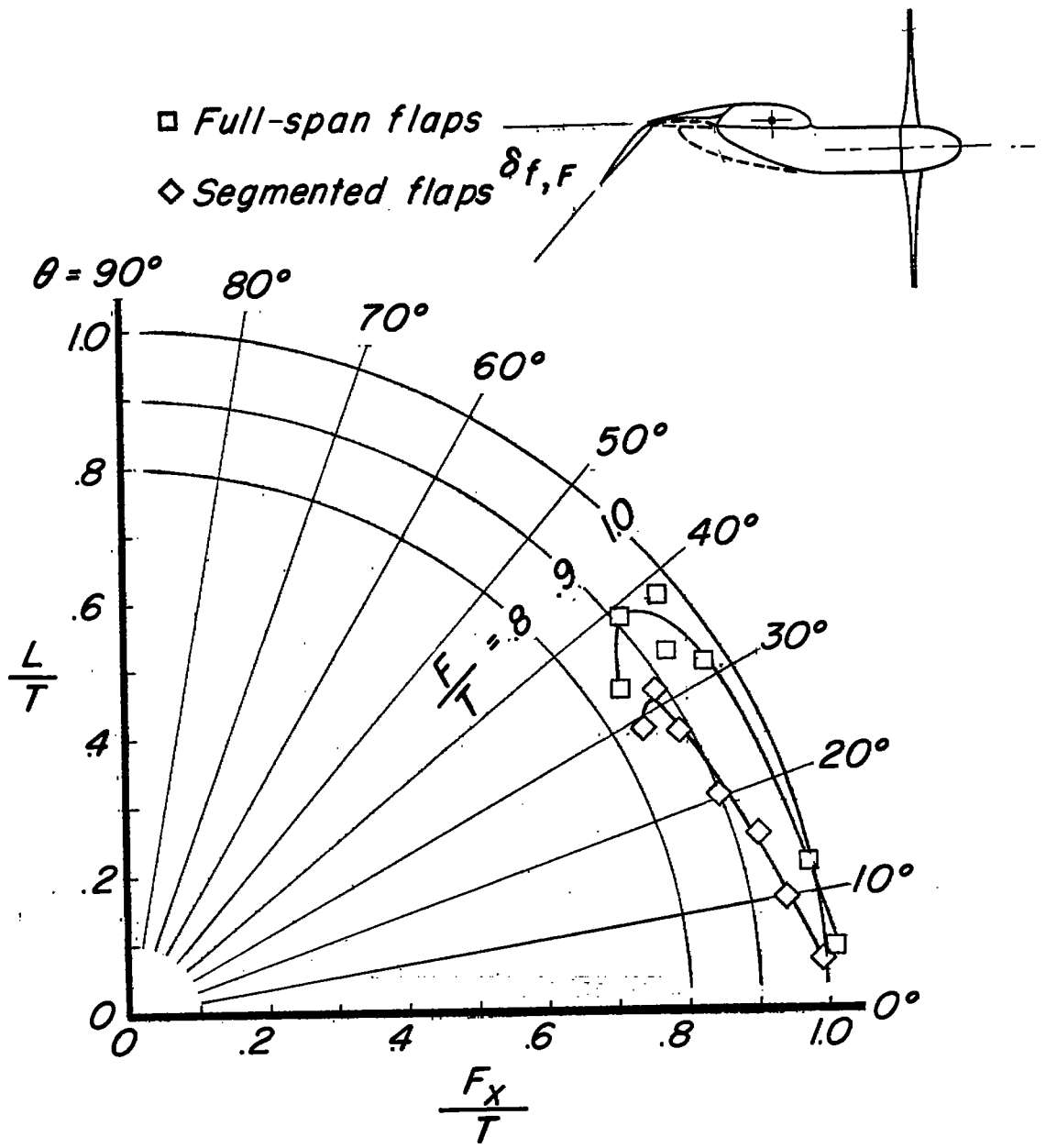

(a) Summary of turning effectiveness.

Figure 14.- Effect of segmenting flaps to permit extension of nacelle fairing. $\frac{X}{D} = 0.333$; $\frac{Y}{D} = -0.01$; $\frac{Z}{D} = -0.104$; $\delta_{f,s} = 0^\circ$; $\delta_{f,F}$, variable.

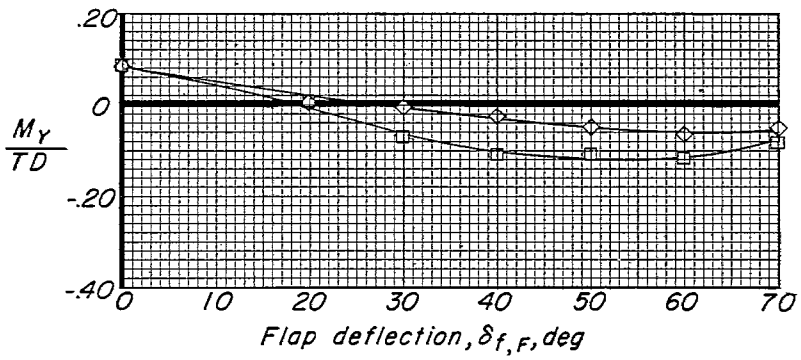

(b) Pitching moment.

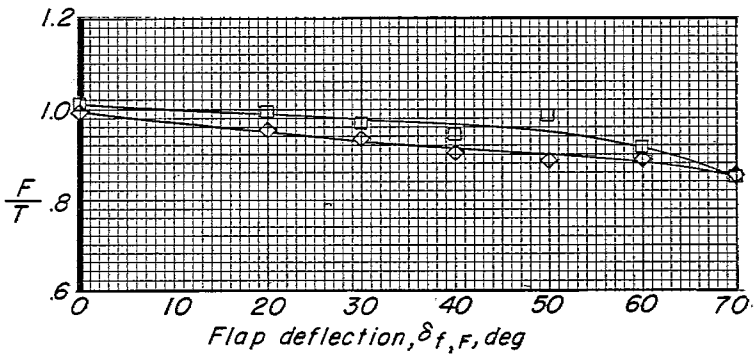

(c) Thrust-recovery factor.

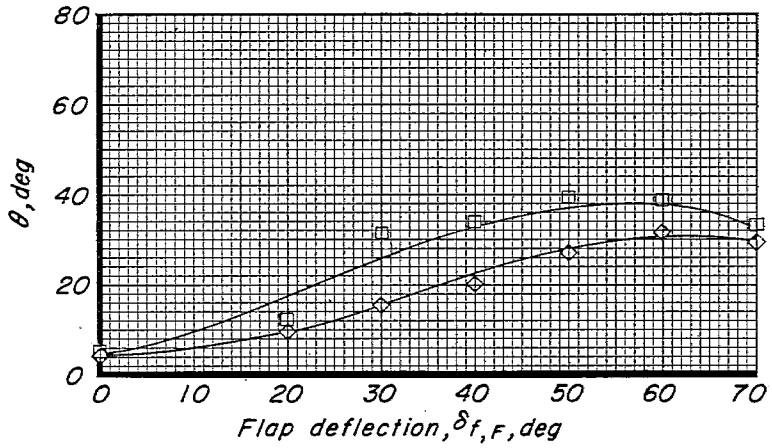

(d) Turning angle.

Figure 14.- Concluded.

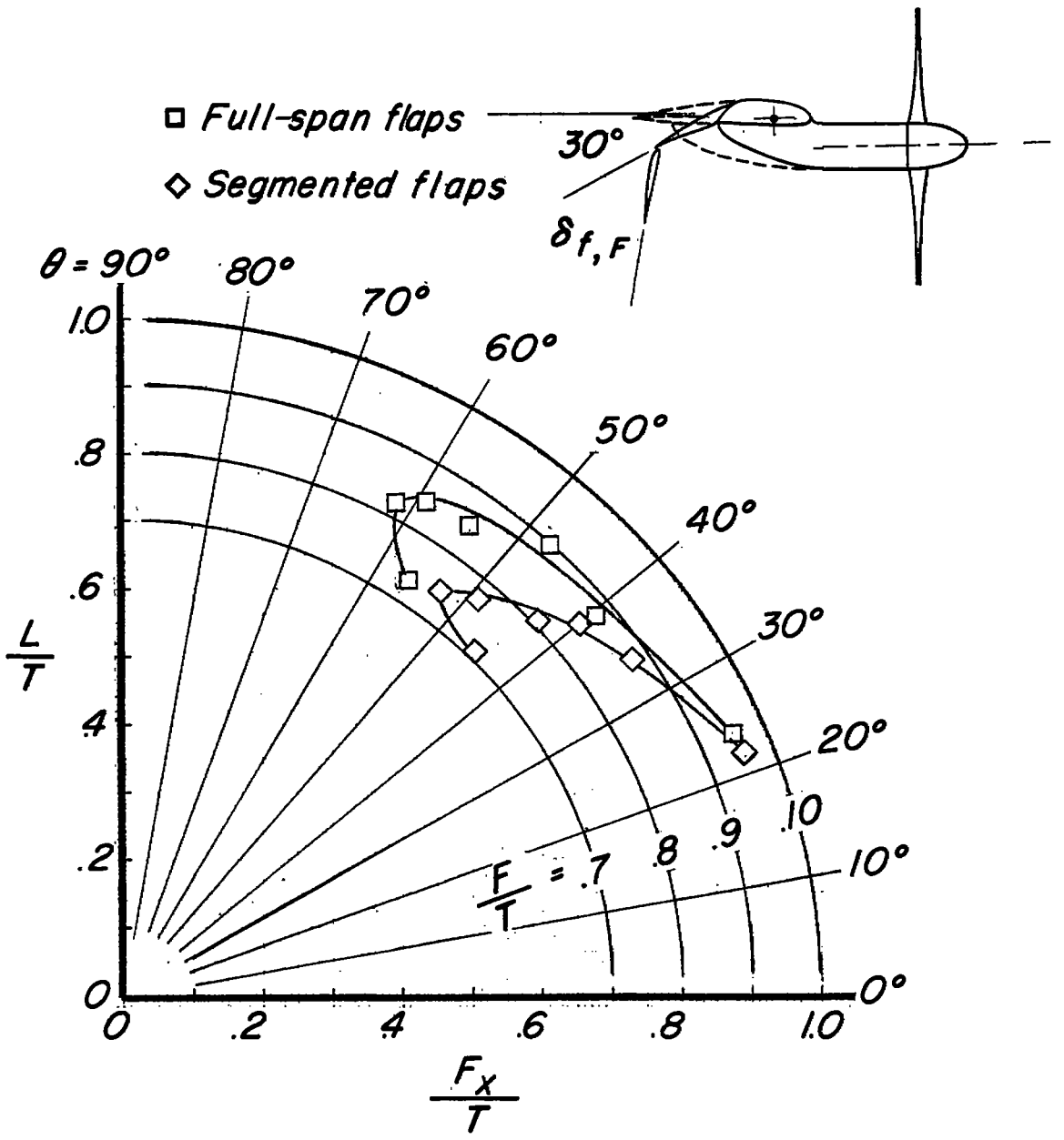

(a) Summary of turning effectiveness.

Figure 15.- Effect of segmenting flaps to permit extension of nacelle fairing. $\frac{X}{D} = 0.333$; $\frac{Y}{D} = -0.01$; $\frac{Z}{D} = -0.104$; $\delta_{f,s} = 30°$; $\delta_{f,F}$, variable.

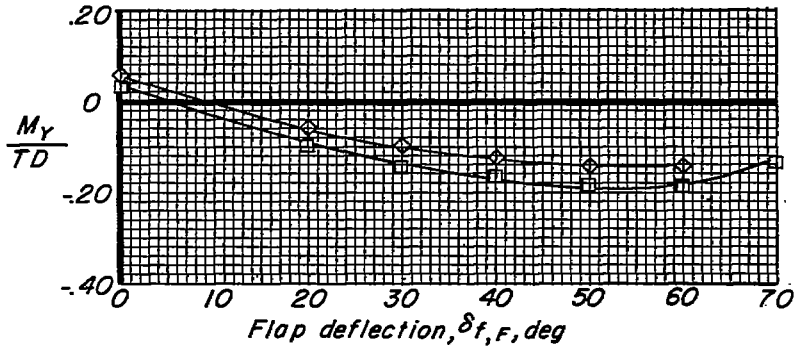

(b) Pitching moment.

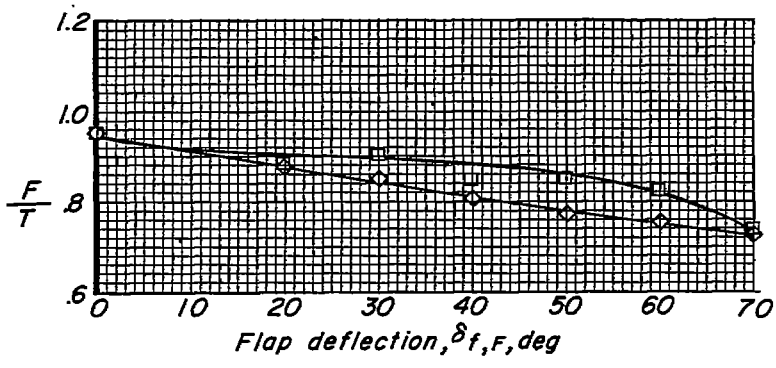

(c) Thrust-recovery factor.

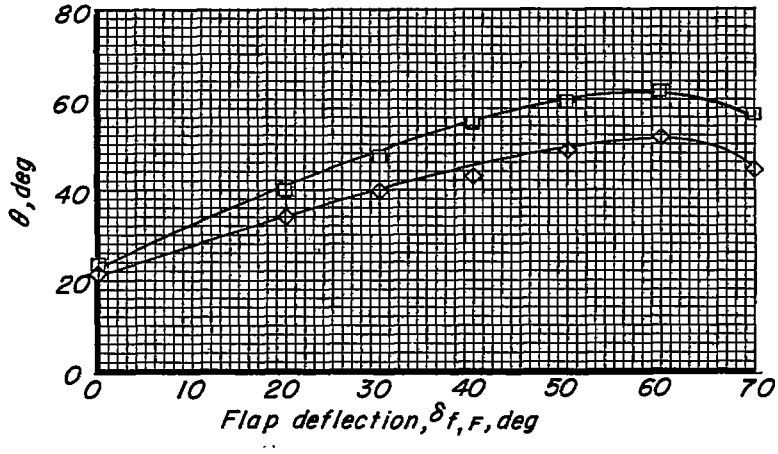

(d) Turning angle.

Figure 15.- Concluded.

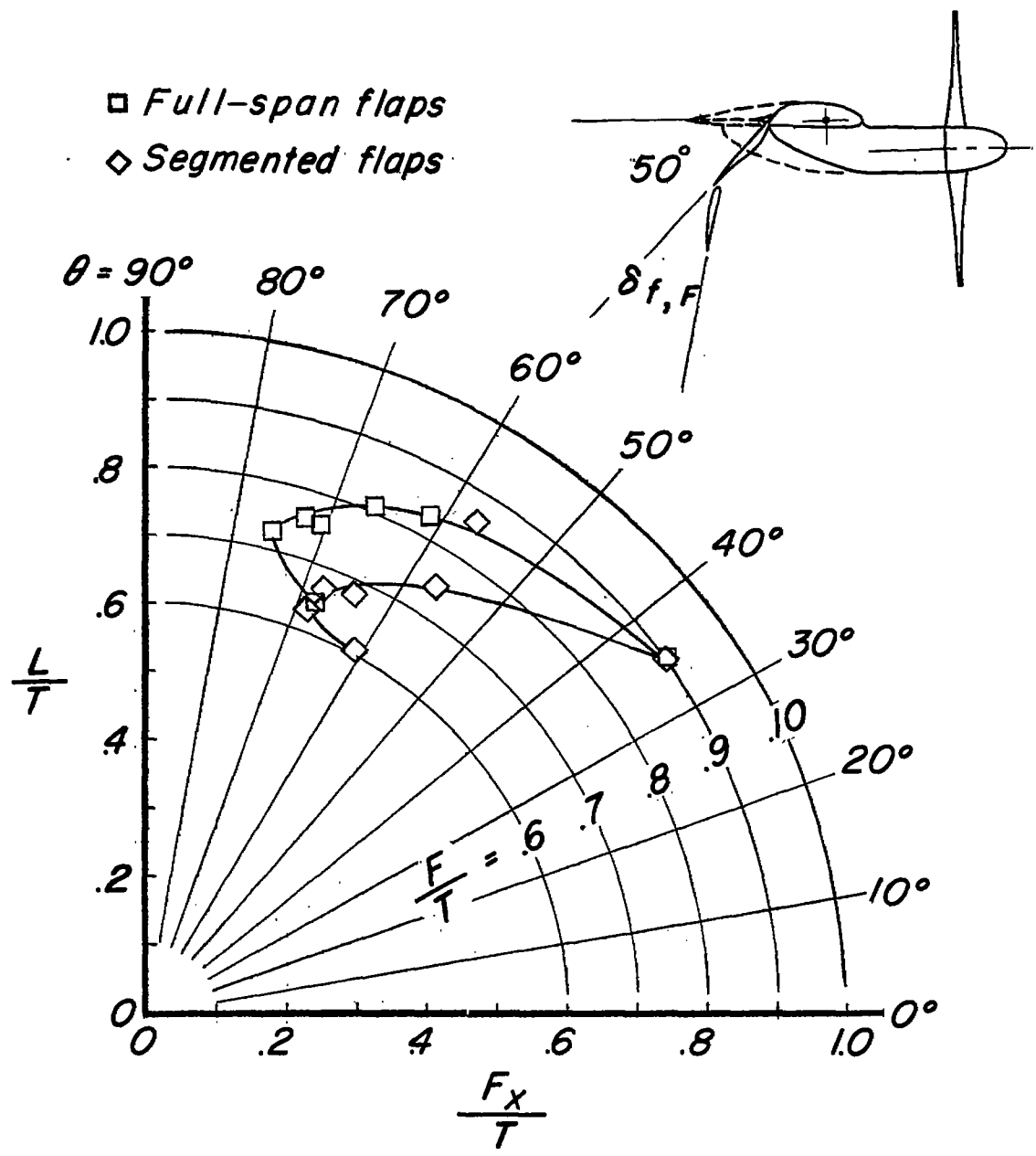

(a) Summary of turning effectiveness.

Figure 16.- Effect of segmenting flaps to permit extension of nacelle fairing. $\frac{X}{D} = 0.333$; $\frac{Y}{D} = -0.01$; $\frac{Z}{D} = -0.104$; $\delta_{f,s} = 50°$; $\delta_{f,F}$, variable.

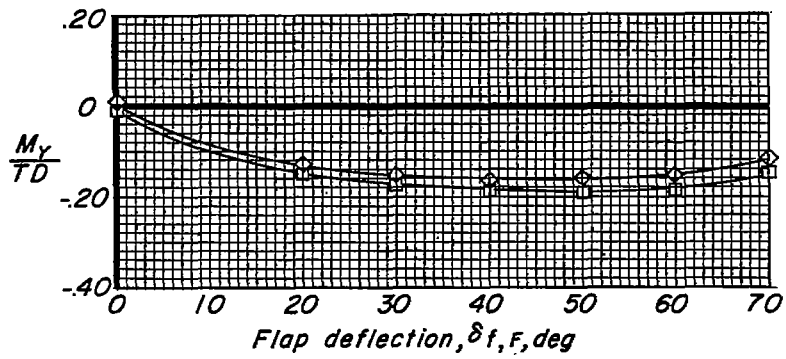

(b) Pitching moment.

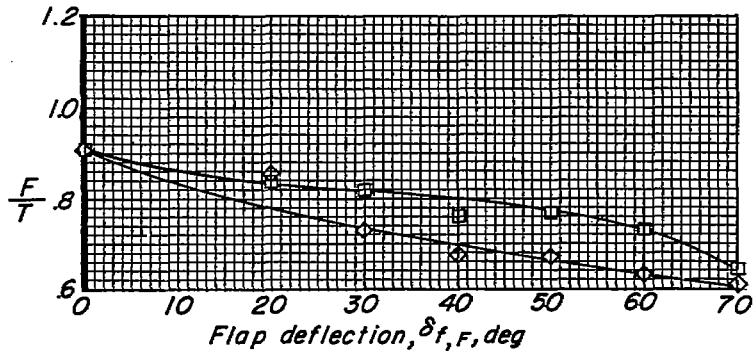

(c) Thrust-recovery factor.

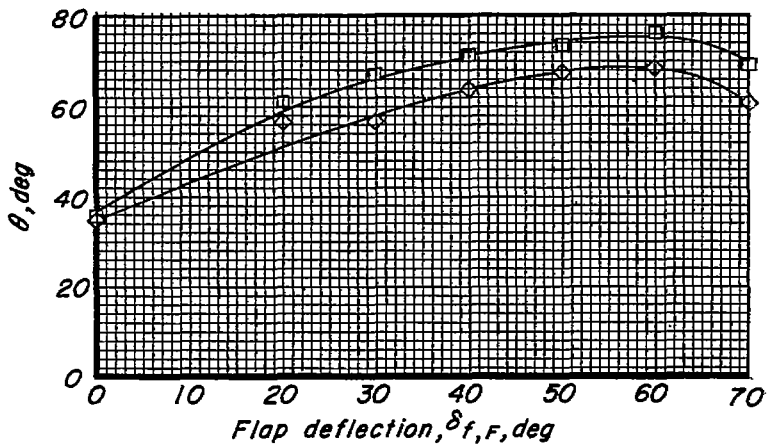

(d) Turning angle.

Figure 16.- Concluded.

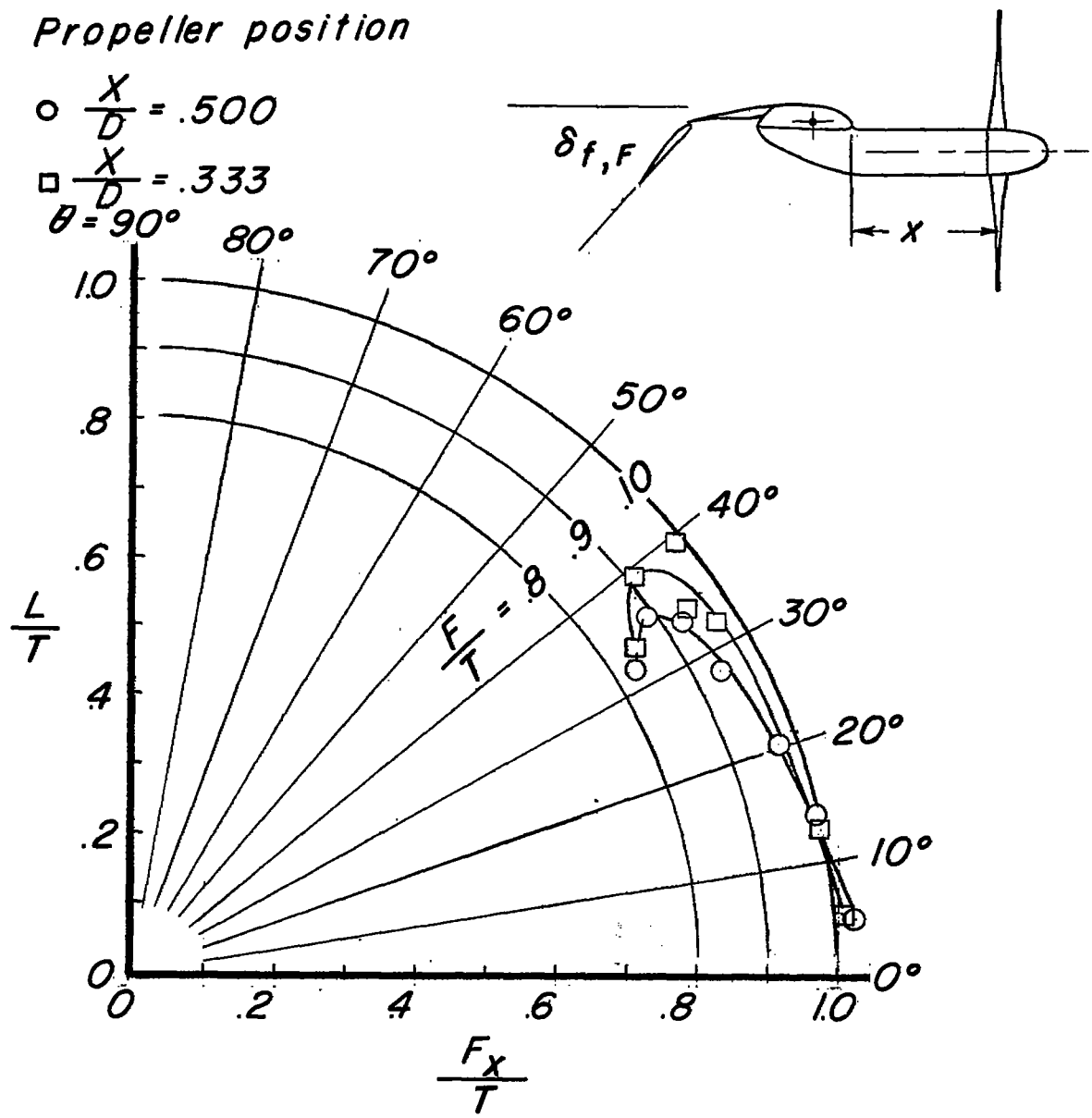

(a) Summary of turning effectiveness.

Figure 17.- Effect of chordwise displacement of propellers. $\frac{Y}{D}$ = -0.01; $\frac{Z}{D}$ = -0.104; $\delta_{f,s} = 0^{\circ}$; $\delta_{f,F}$, variable; full-span flaps.

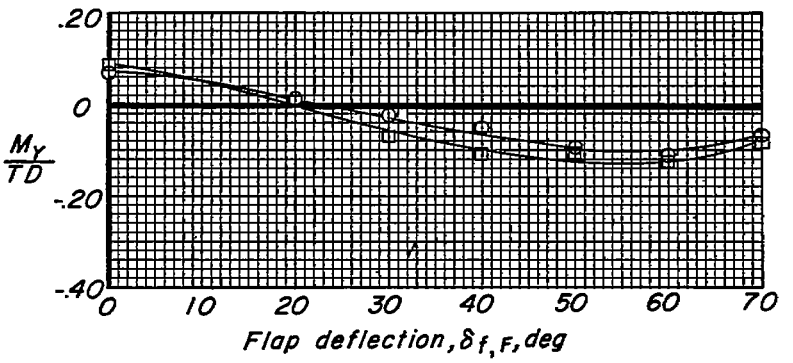

(b) Pitching moment.

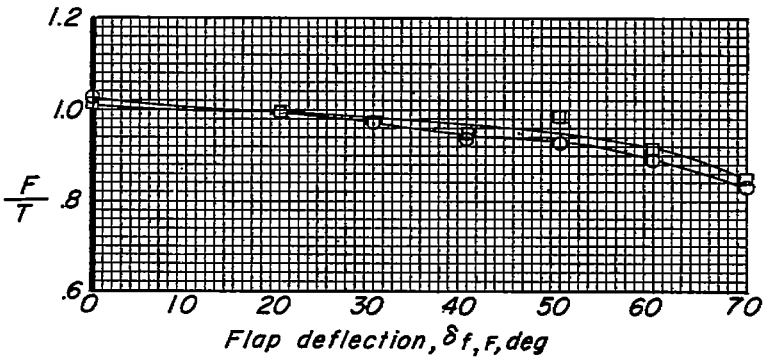

(c) Thrust-recovery factor.

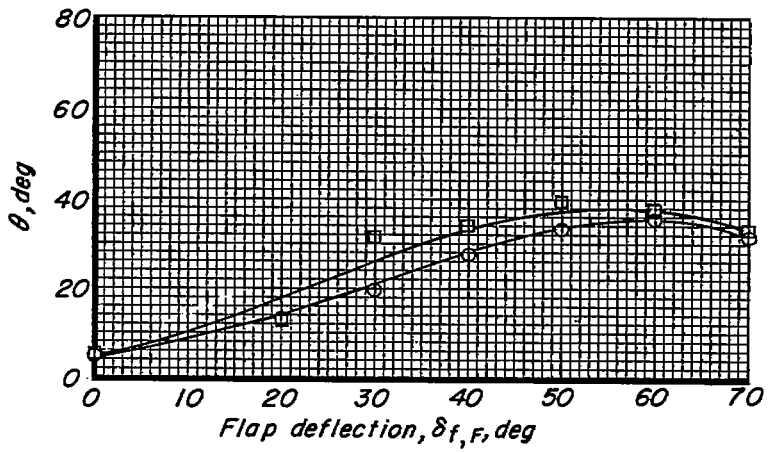

(d) Turning angle.

Figure 17.- Concluded.

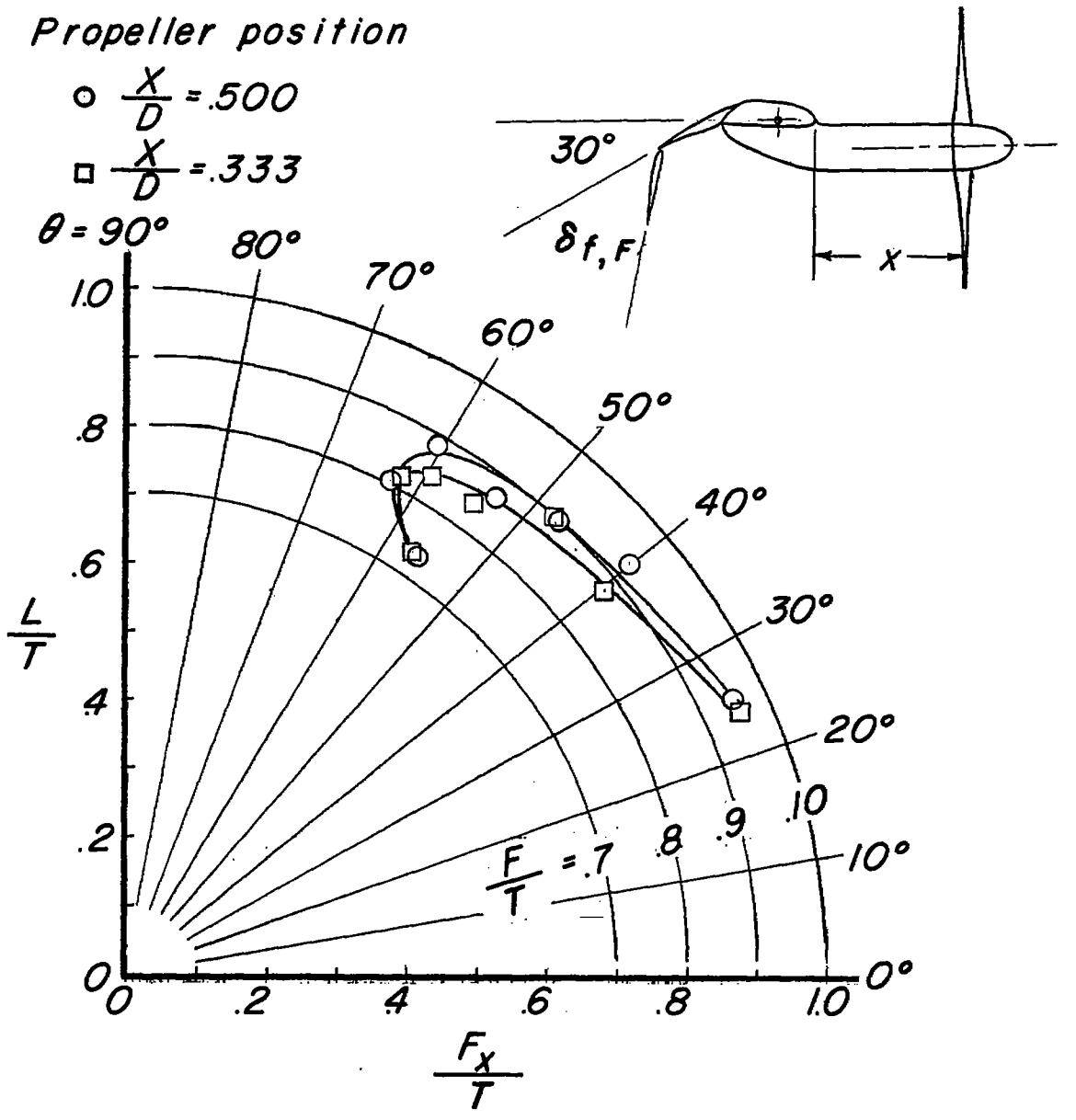

(a) Summary of turning effectiveness.

Figure 18.- Effect of chordwise displacement of propellers. $\frac{Y}{D}$ = -0.01; $\frac{Z}{D}$ = -0.104; $\delta_{f,s}$ = 30°; $\delta_{f,F}$, variable; full-span flaps.

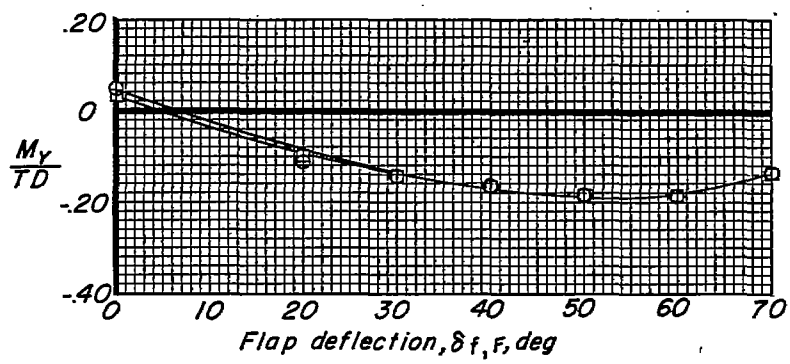

(b) Pitching moment.

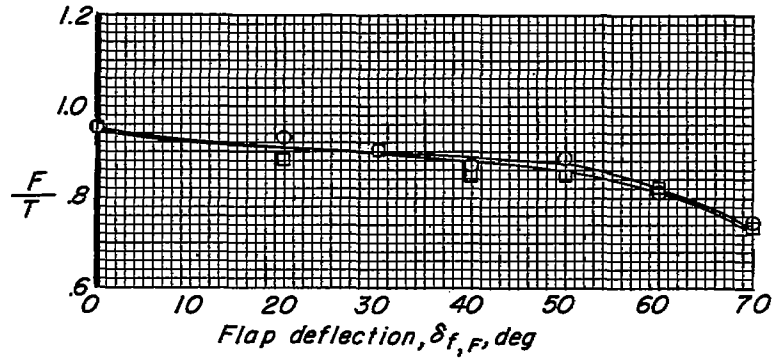

(c) Thrust-recovery factor.

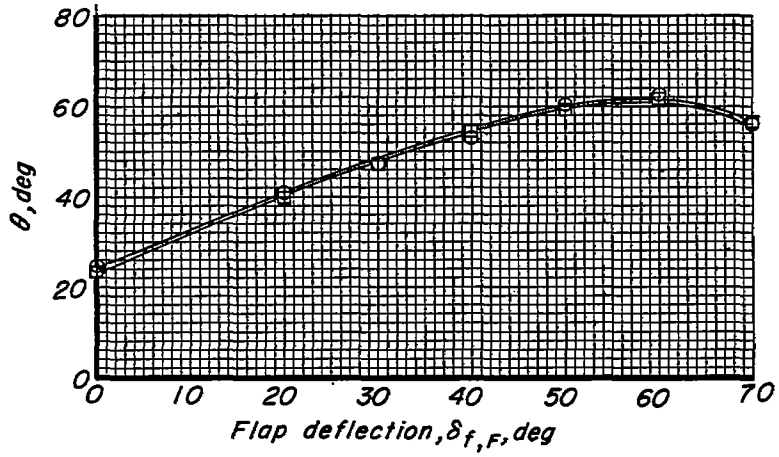

(d) Turning angle.

Figure 18.- Concluded.

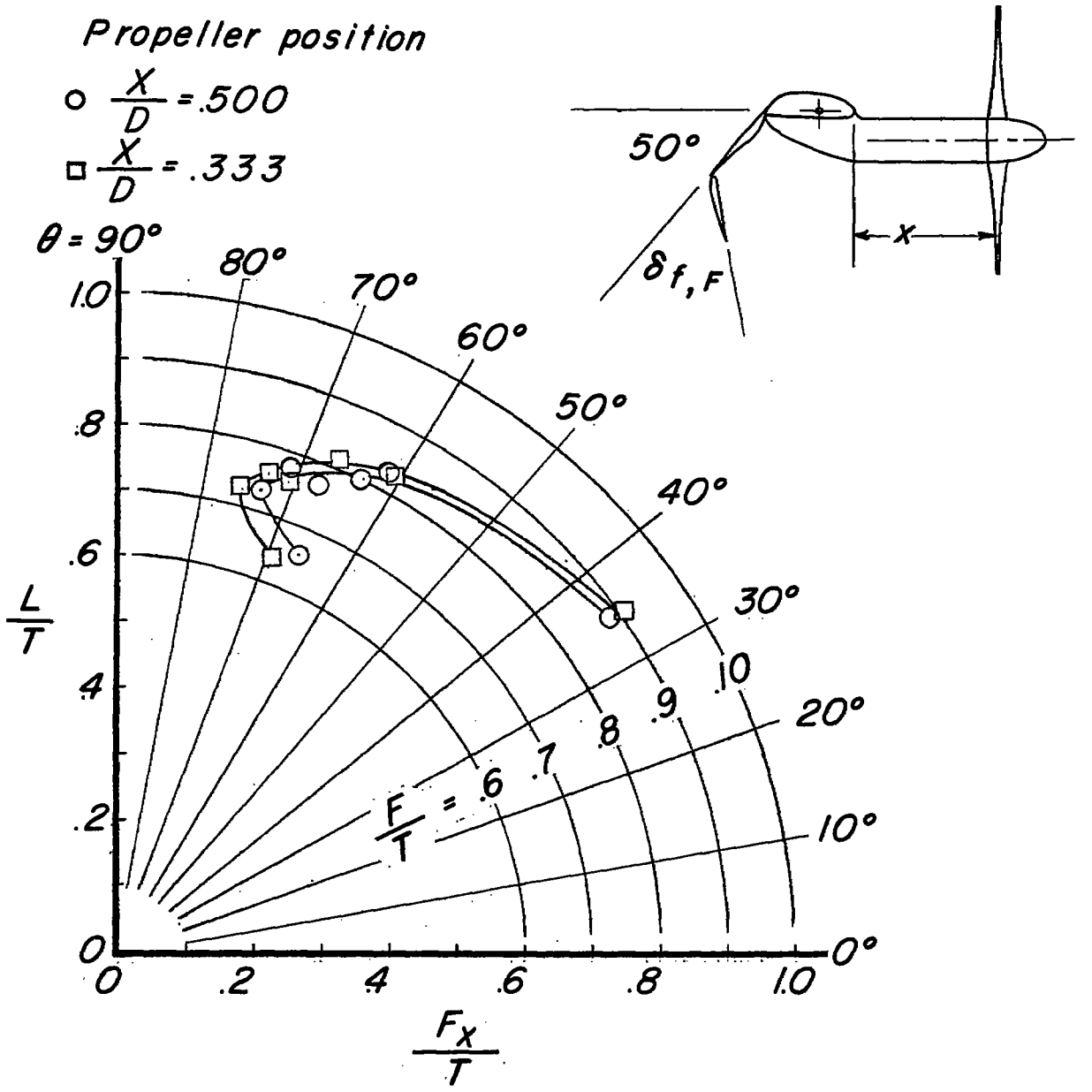

(a) Summary of turning effectiveness.

Figure 19.- Effect of chordwise displacement of propellers. $\frac{Y}{D} = -0.01$; $\frac{Z}{D} = -0.104$; $\delta_{f,s} = 50°$; $\delta_{f,F}$, variable; full-span flaps.

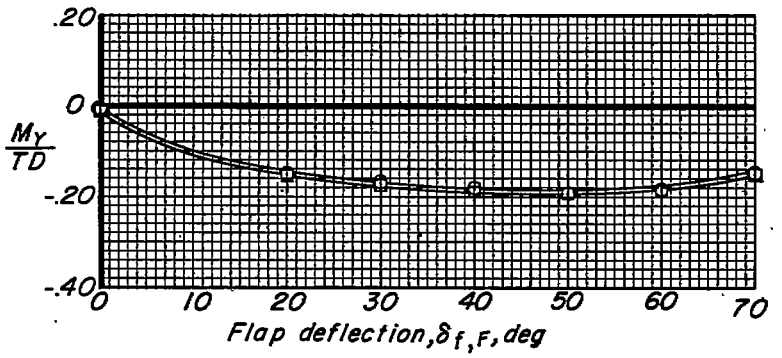

(b) Pitching moment.

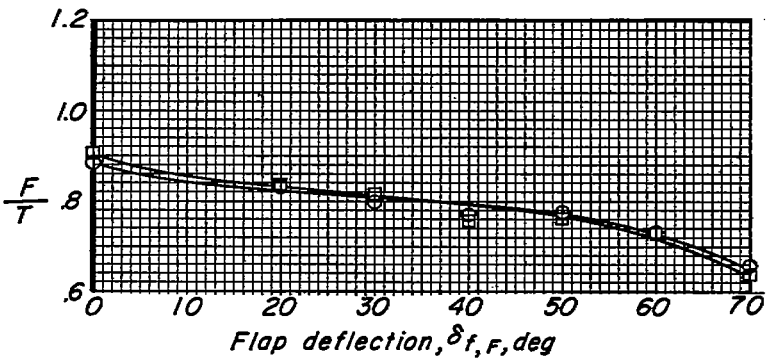

(c) Thrust-recovery factor.

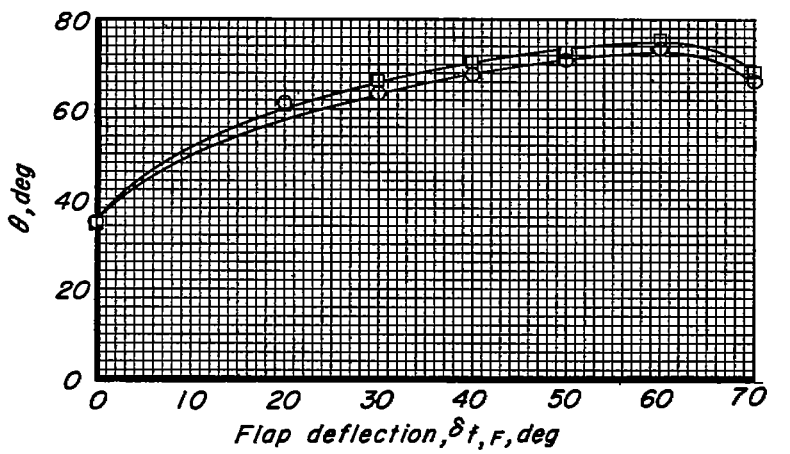

(d) Turning angle.

Figure 19.- Concluded.

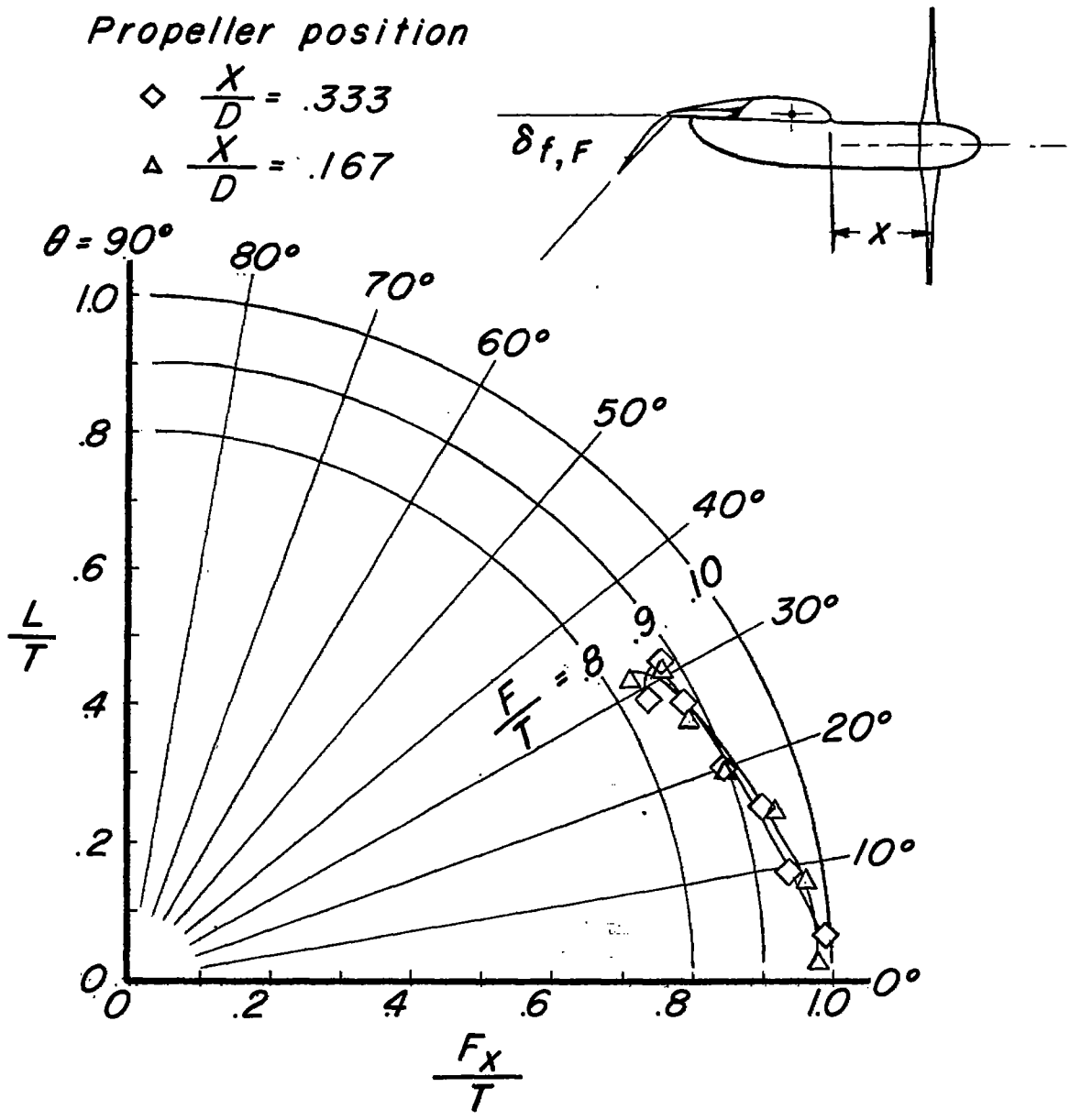

(a) Summary of turning effectiveness.

Figure 20.- Effect of chordwise displacement of propellers. $\frac{Y}{D} = -0.01$; $\frac{Z}{D} = -0.104$; $\delta_{f,s} = 0^\circ$; $\delta_{f,F}$, variable; segmented flaps.

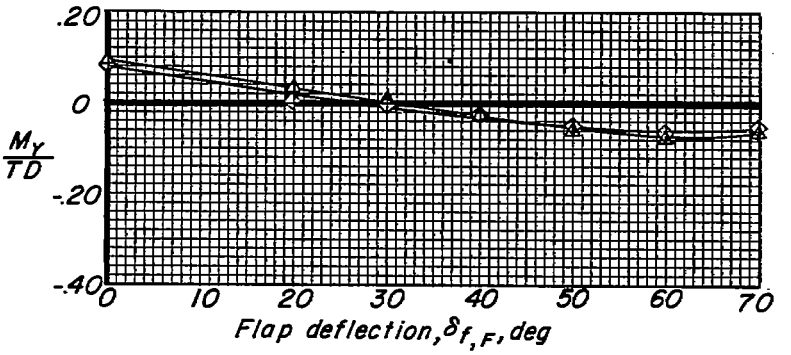

(b) Pitching moment.

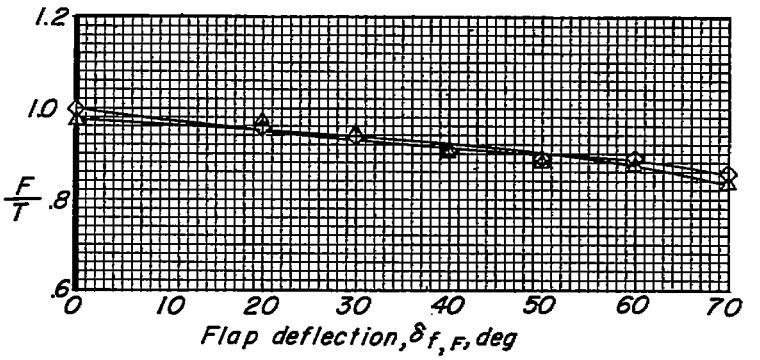

(c) Thrust-recovery factor.

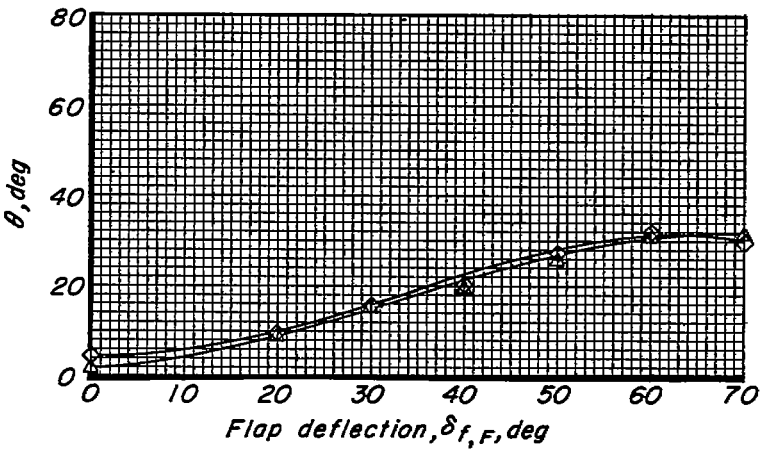

(d) Turning angle.

Figure 20.- Concluded.

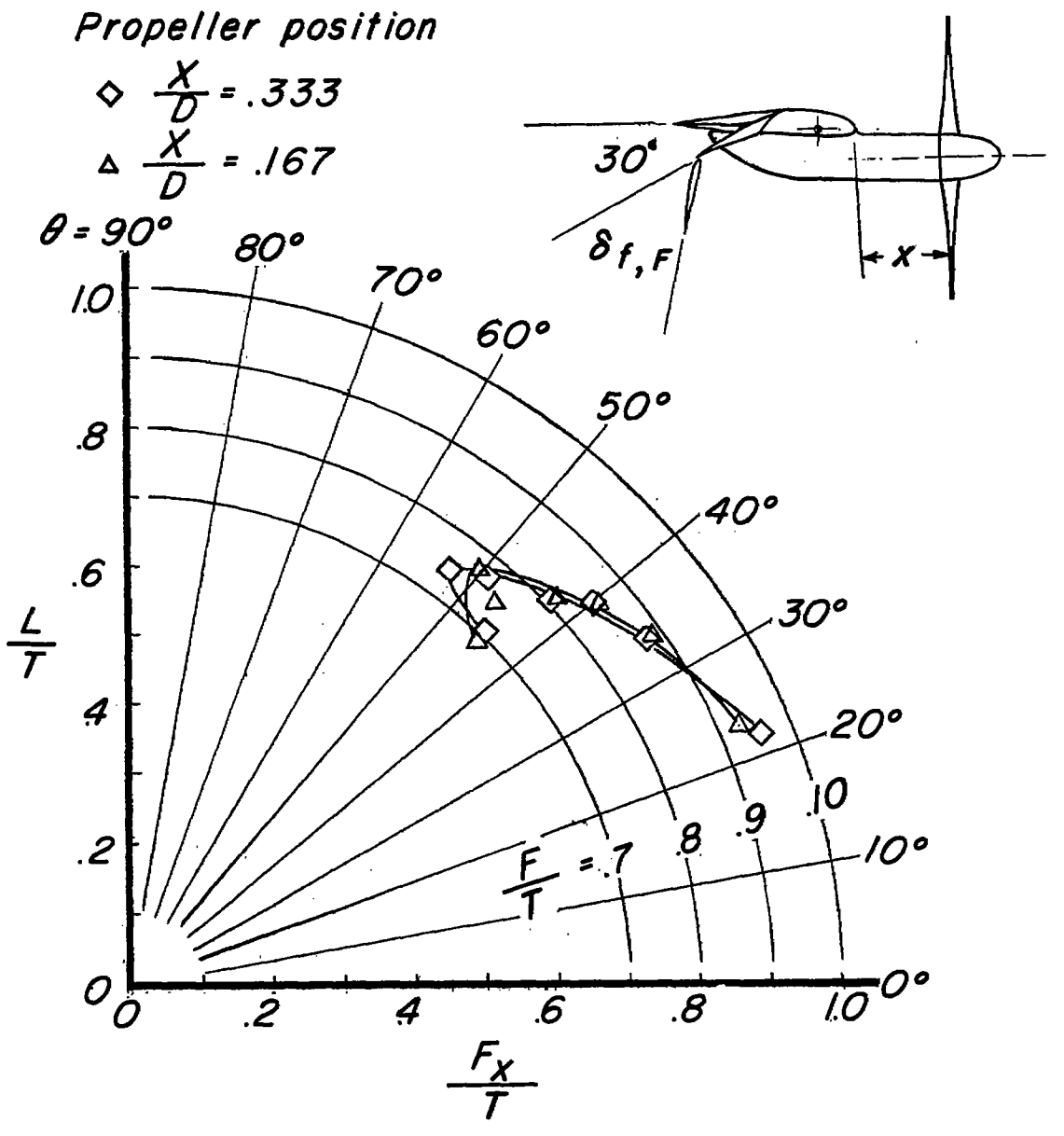

(a) Summary of turning effectiveness.

Figure 21.- Effect of chordwise displacement of propellers. $\frac{Y}{D} = -0.01$; $\frac{Z}{D} = -0.104$; $\delta_{f,s} = 30^\circ$; $\delta_{f,F}$, variable; segmented flaps.

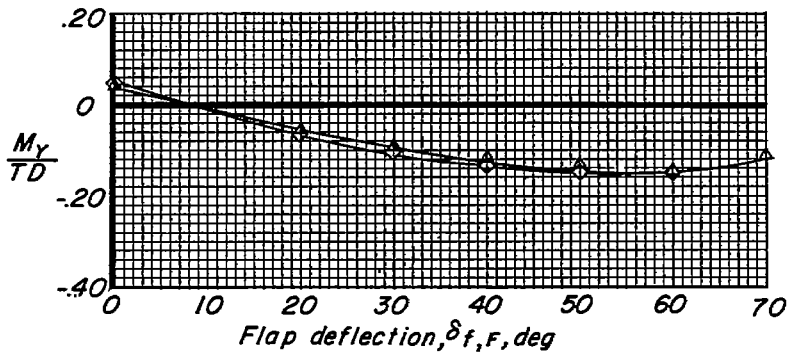

(b) Pitching moment.

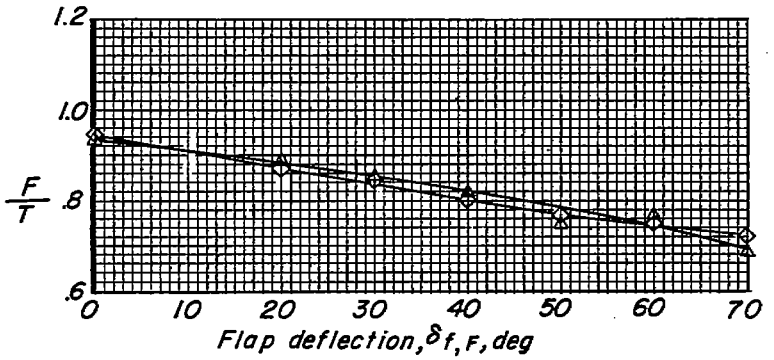

(c) Thrust-recovery factor.

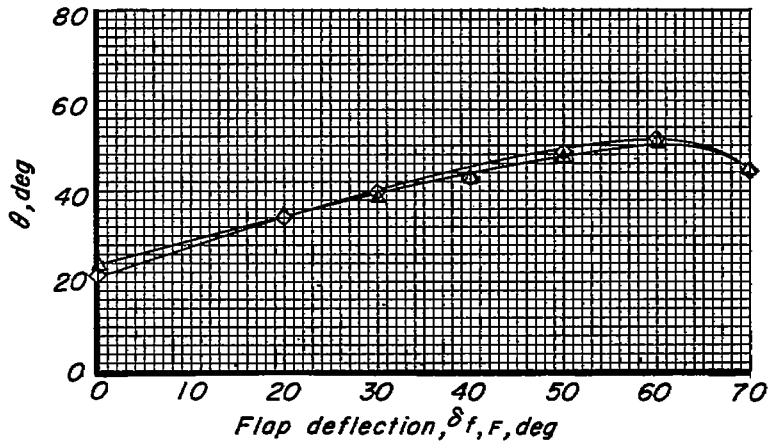

(d) Turning angle.

Figure 21.- Concluded.

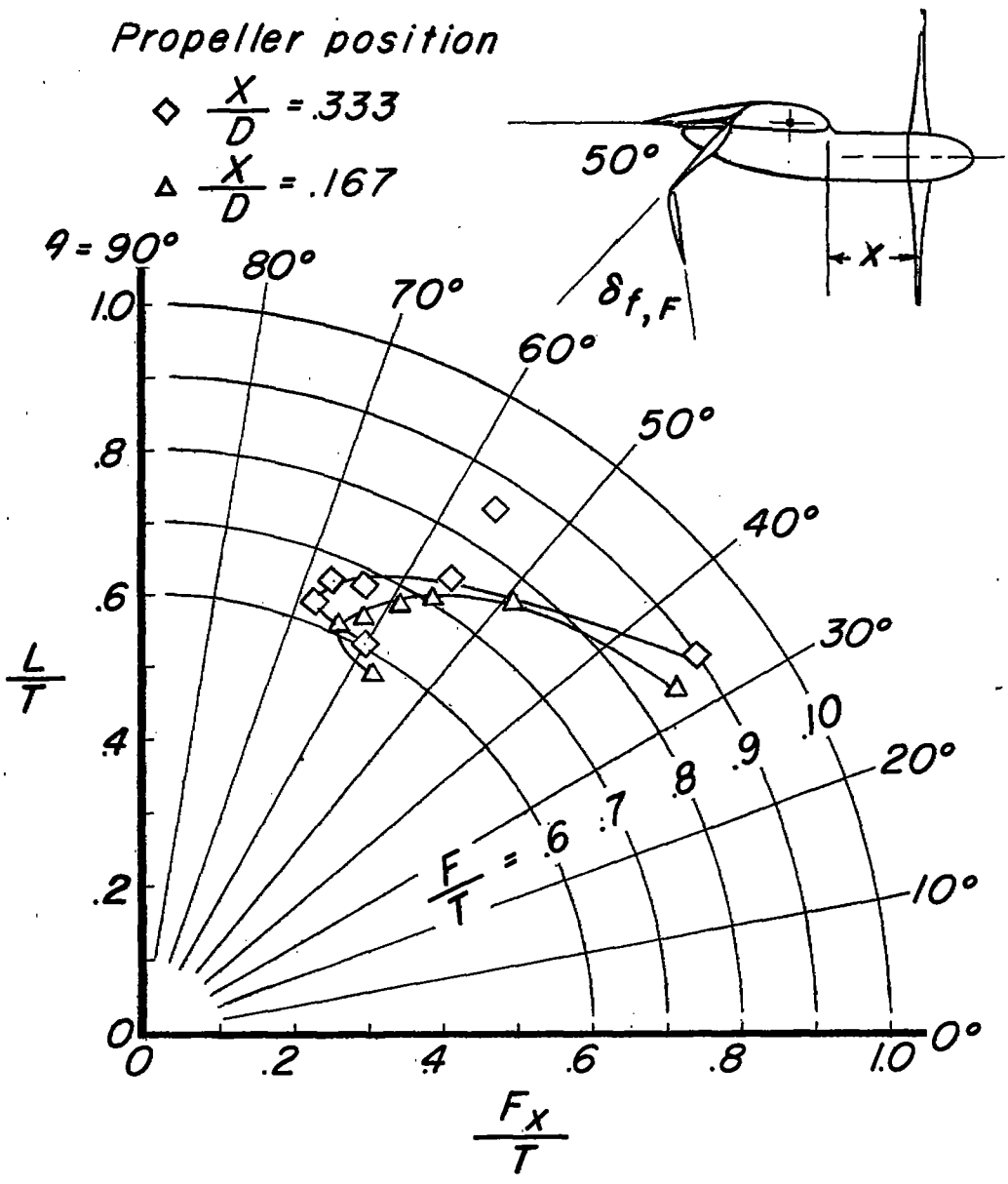

(a) Summary of turning effectiveness.

Figure 22.- Effect of chordwise displacement of propellers. $\frac{Y}{D} = -0.01$; $\frac{Z}{D} = -0.104$; $\delta_{f,s} = 50^{\circ}$; $\delta_{f,F}$, variable; segmented flaps.

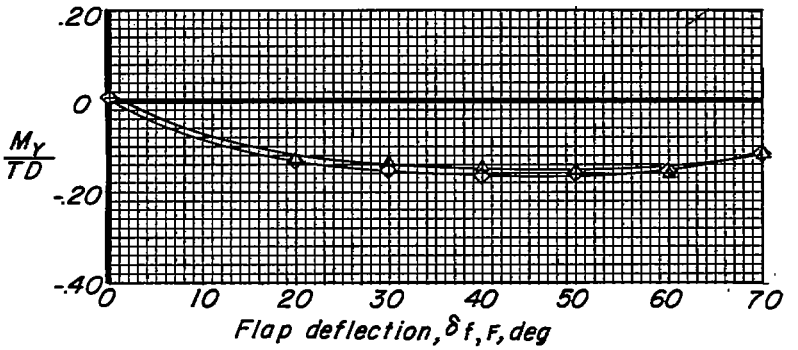

(b) Pitching moment.

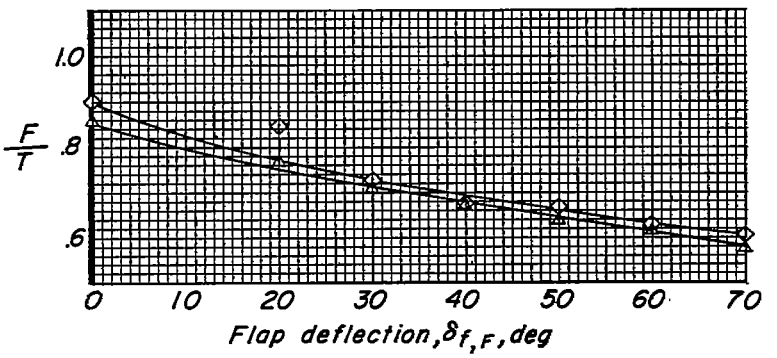

(c) Thrust-recovery factor.

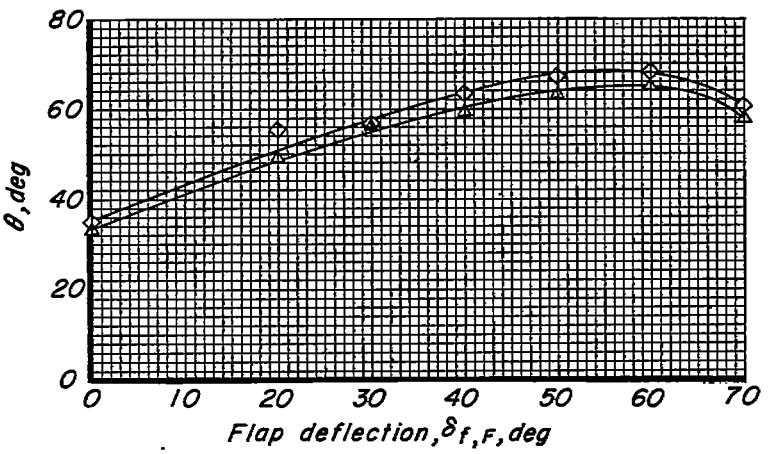

(d) Turning angle.

Figure 22.- Concluded.

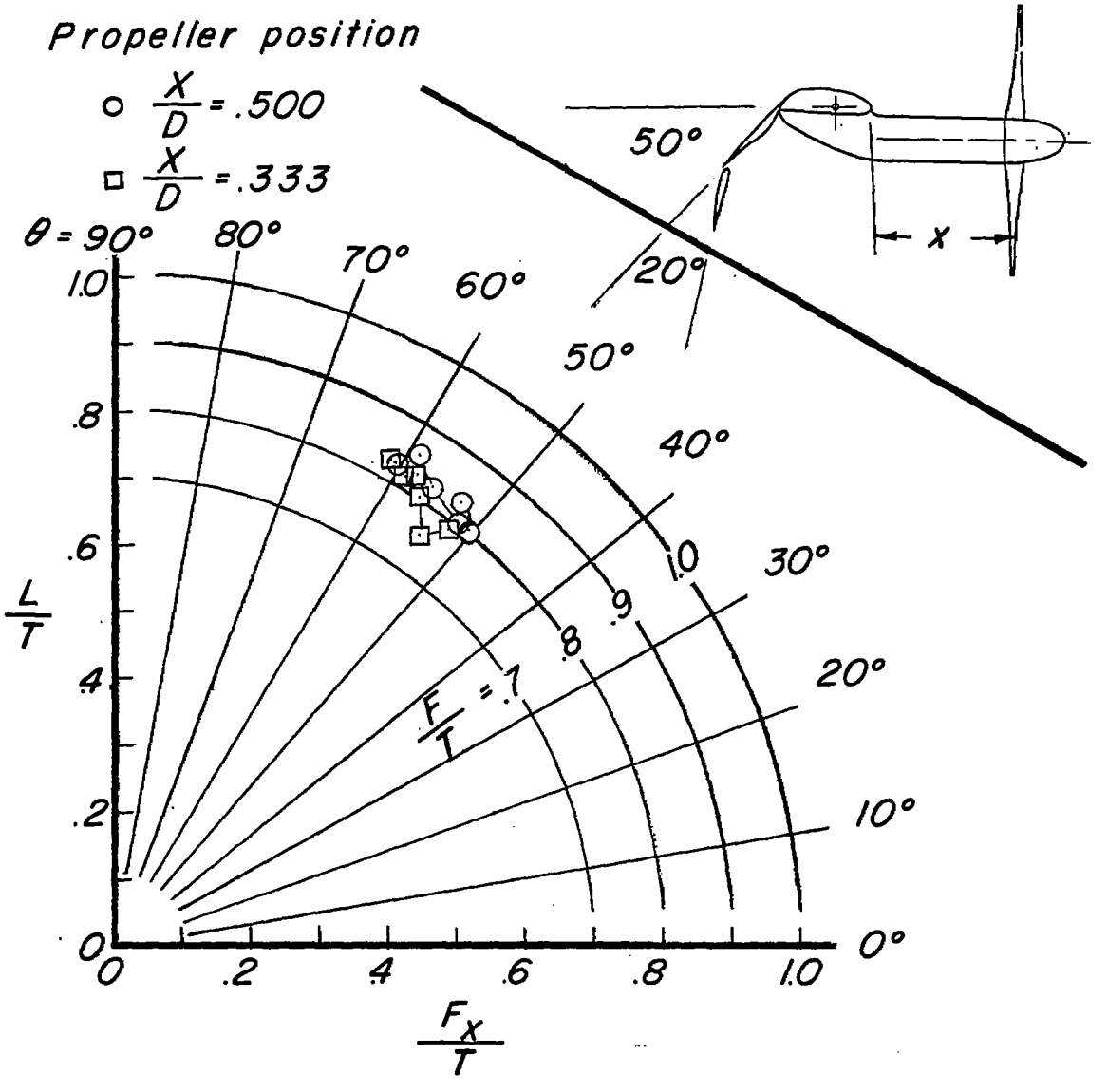

(a) Summary of turning effectiveness.

Figure 23.- Effect of chordwise displacement of propellers in the region of ground effect. $\frac{Y}{D}$ = -0.01; $\frac{Z}{D}$ = -0.104; $\delta_{f,s}$ = 50°; $\delta_{f,F}$ = 20°; α = 32°; full-span flaps; h/D, variable.

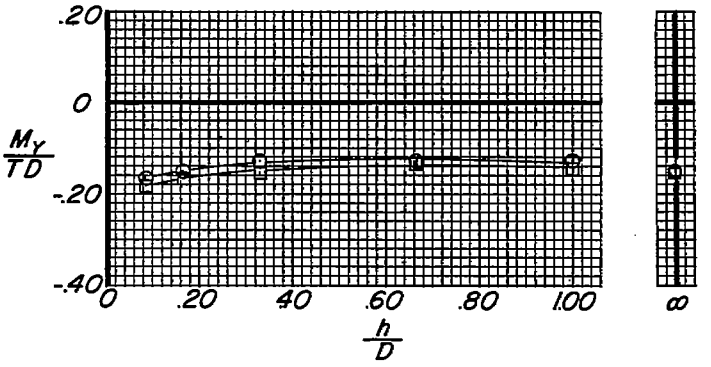

(b) Pitching moment.

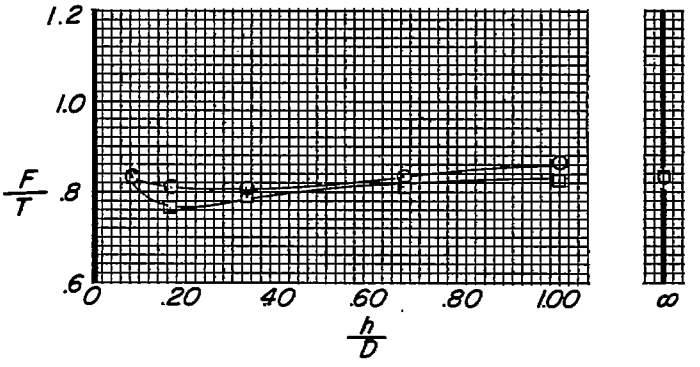

(c) Thrust-recovery factor.

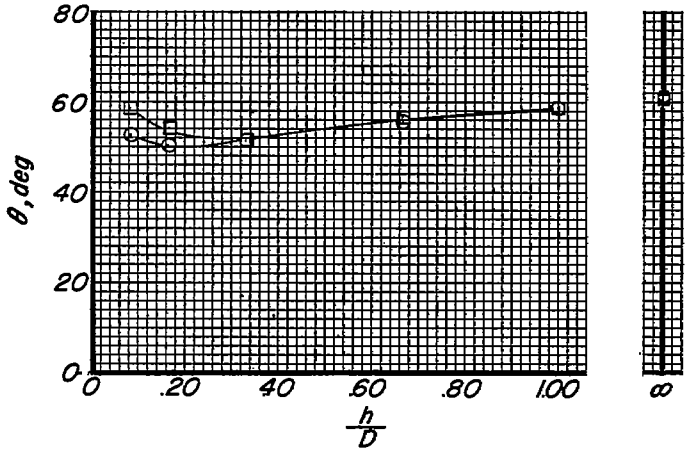

(d) Turning angle.

Figure 23.- Concluded.

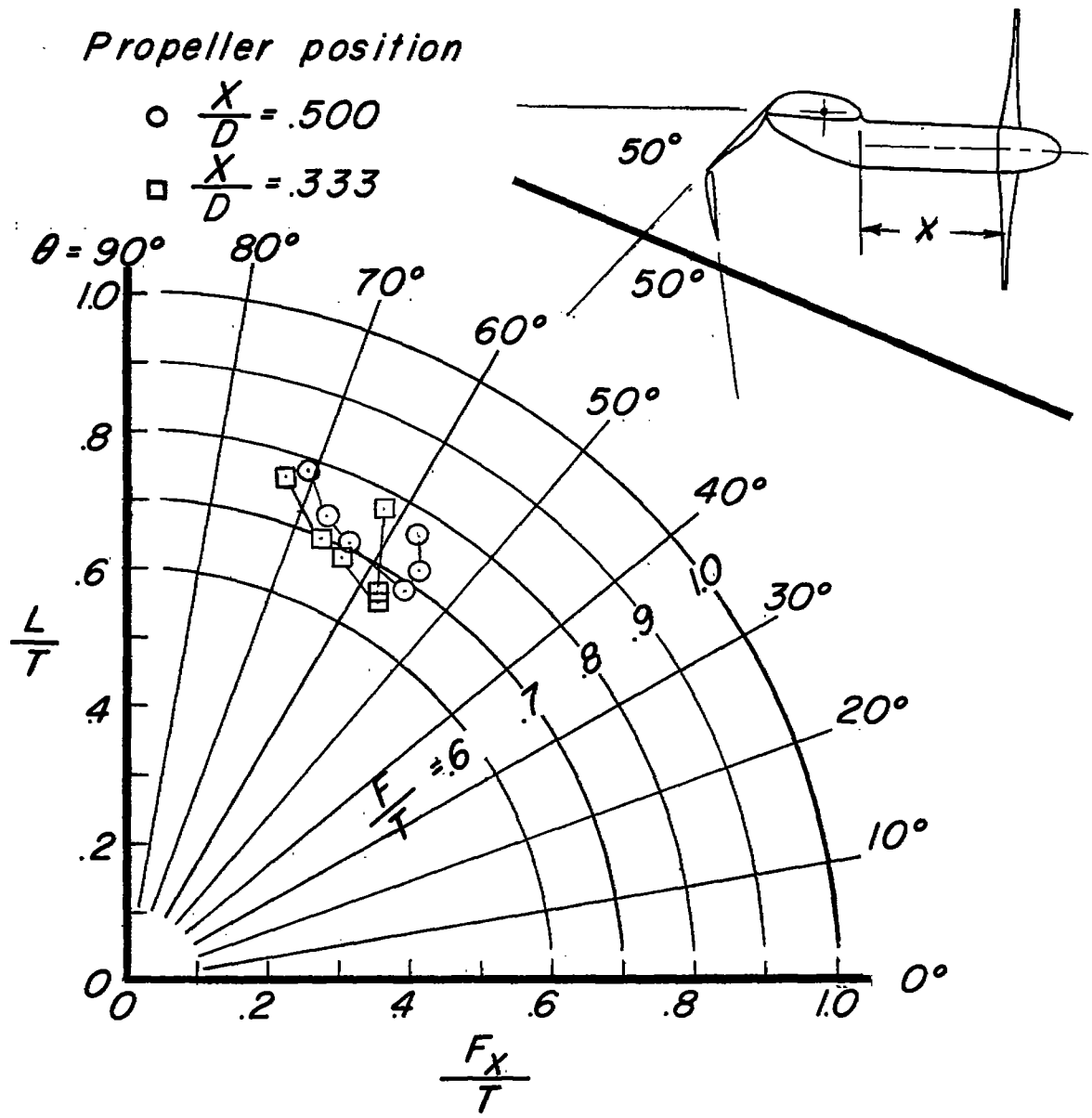

(a) Summary of turning effectiveness.

Figure 24.- Effect of longitudinal displacement of propellers in the region of ground effect. $\frac{Y}{D}$ = -0.01; $\frac{Z}{D}$ = -0.104; $\delta_{f,s}$ = 50°; $\delta_{f,F}$ = 50°; α = 20°; full-span flaps; h/D, variable.

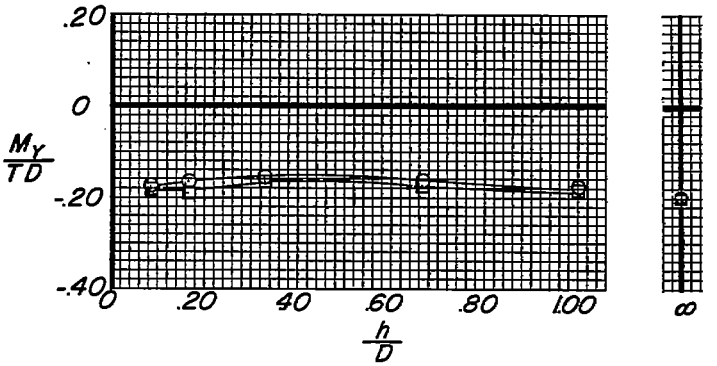

(b) Pitching moment.

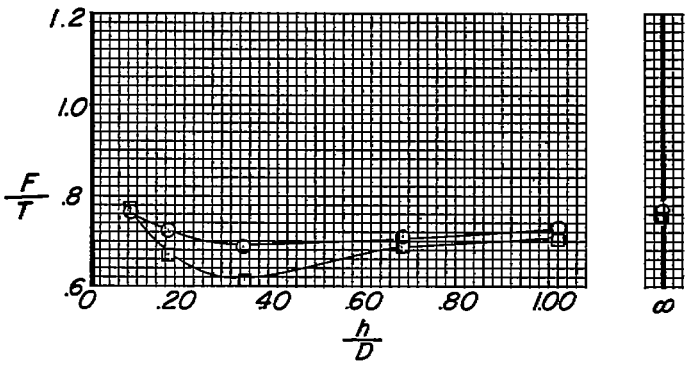

(c) Thrust-recovery factor.

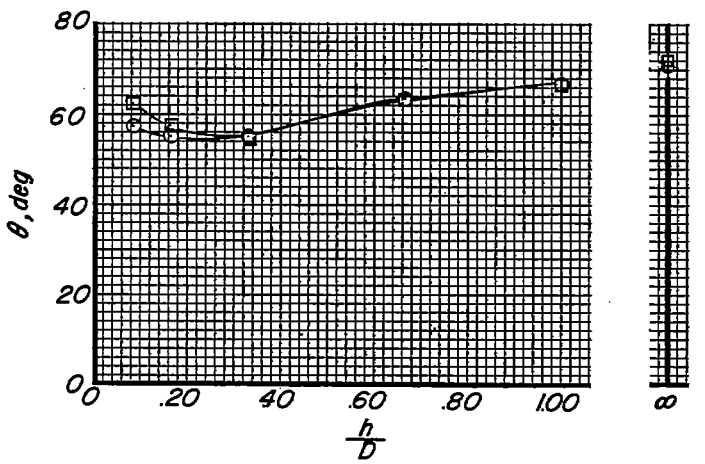

(d) Turning angle.

Figure 24.- Concluded.

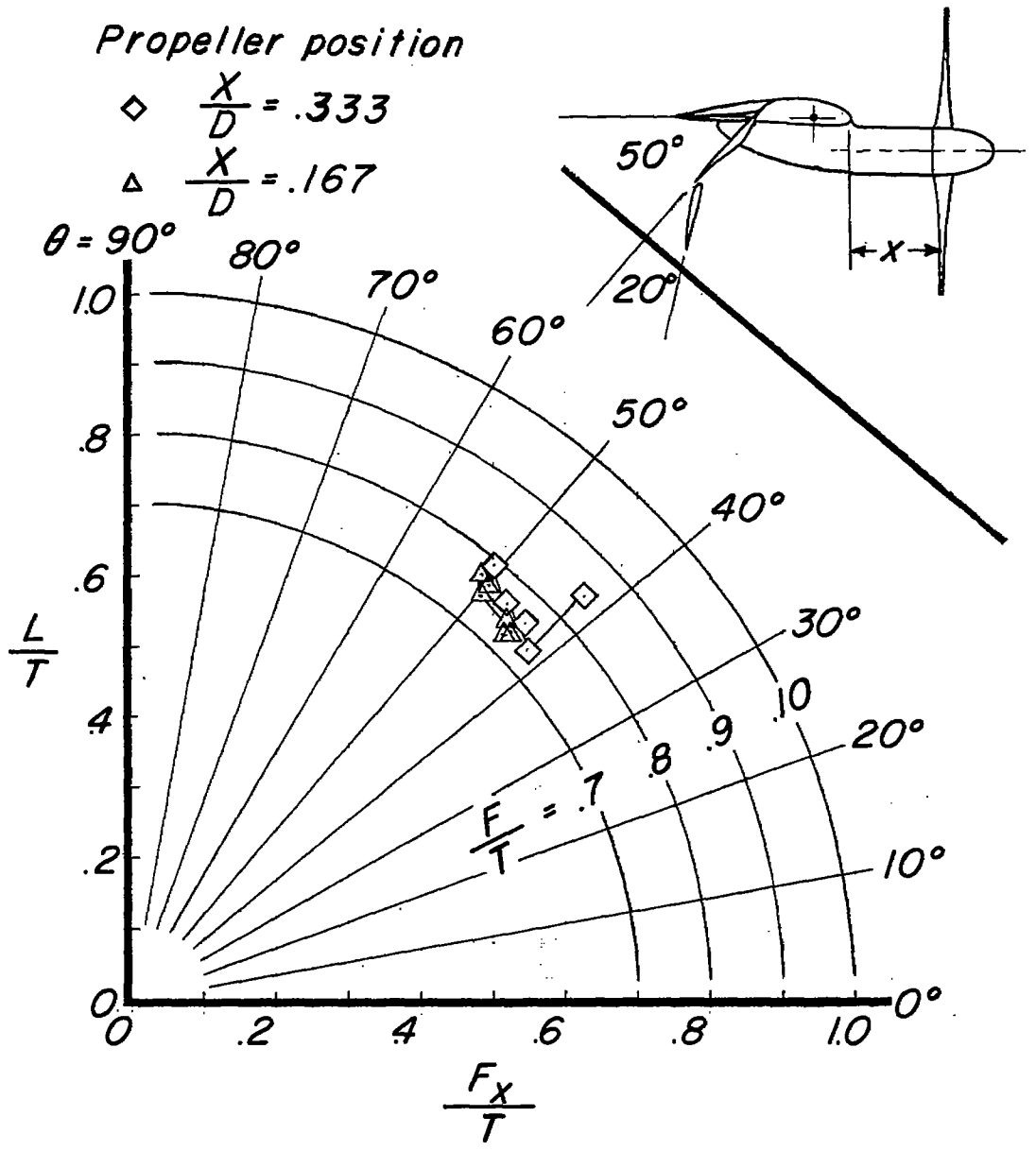

(a) Summary of turning effectiveness.

Figure 25.- Effect of chordwise displacement of propellers in the region of ground effect. $\frac{Y}{D} = -0.01$; $\frac{Z}{D} = -0.104$; $\delta_{f,s} = 50°$; $\delta_{f,F} = 20°$; $\alpha = 40°$; segmented flaps; h/D, variable.

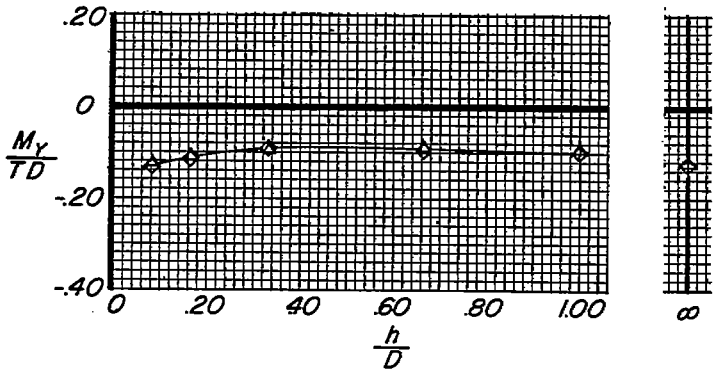

(b) Pitching moment.

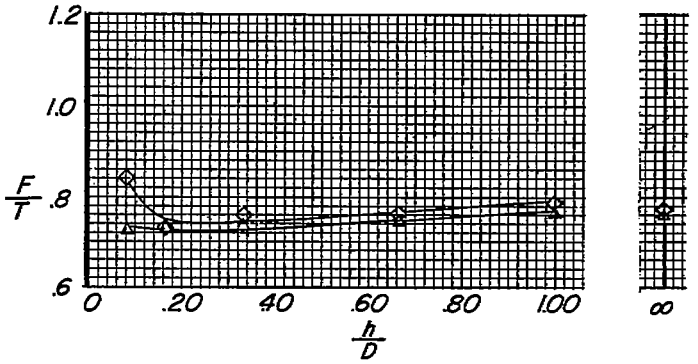

(c) Thrust-recovery factor.

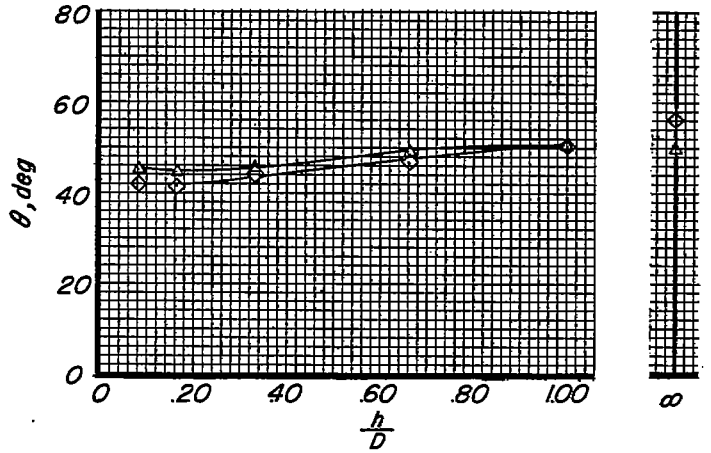

(d) Turning angle.

Figure 25.- Concluded.

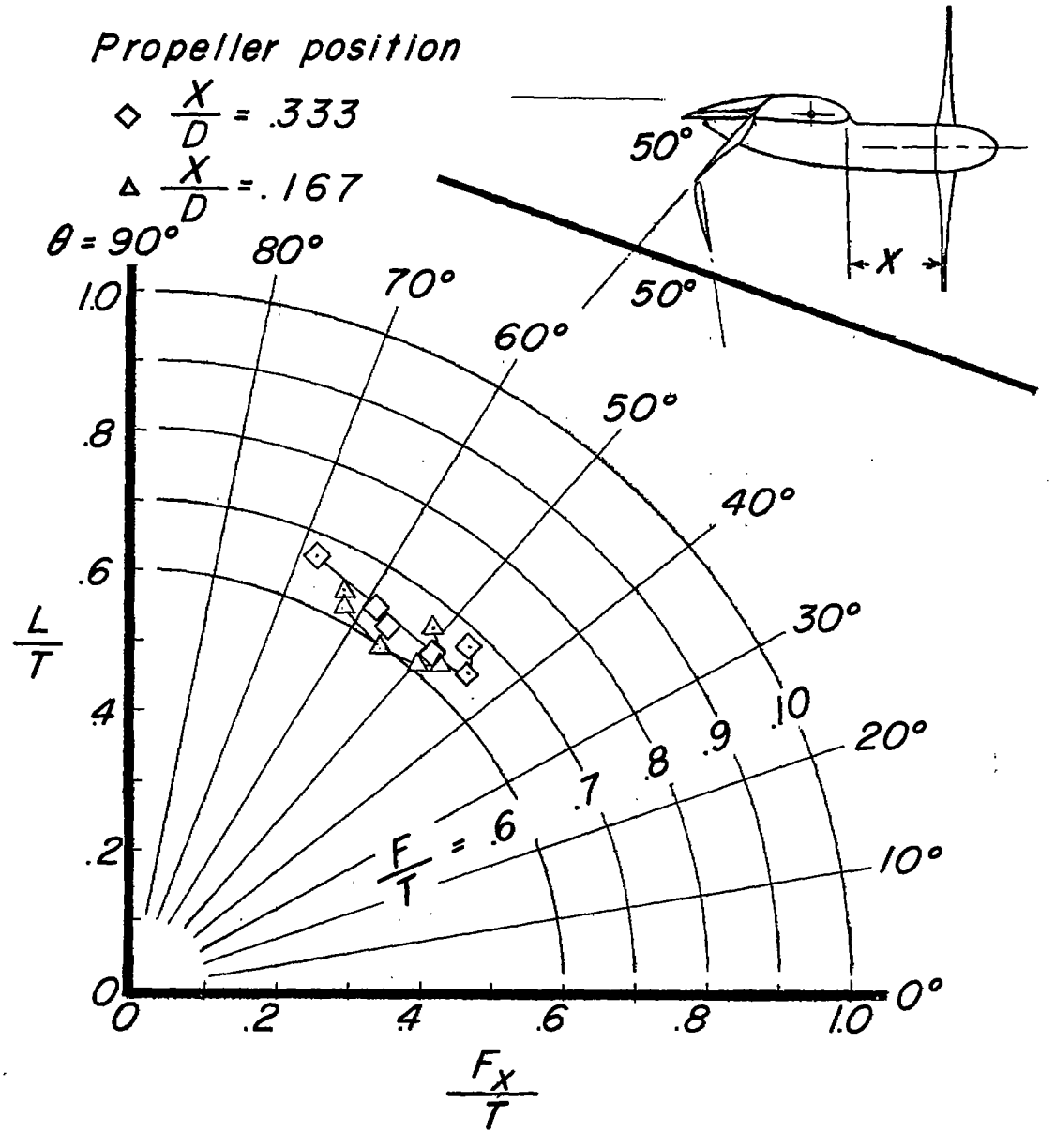

(a) Summary of turning effectiveness.

Figure 26.- Effect of chordwise displacement of propellers in the region of ground effect. $\frac{Y}{D} = -0.01$; $\frac{Z}{D} = -0.104$; $\delta_{f,s} = 50°$; $\delta_{f,F} = 50°$; $\alpha = 20°$; segmented flaps; h/D, variable.

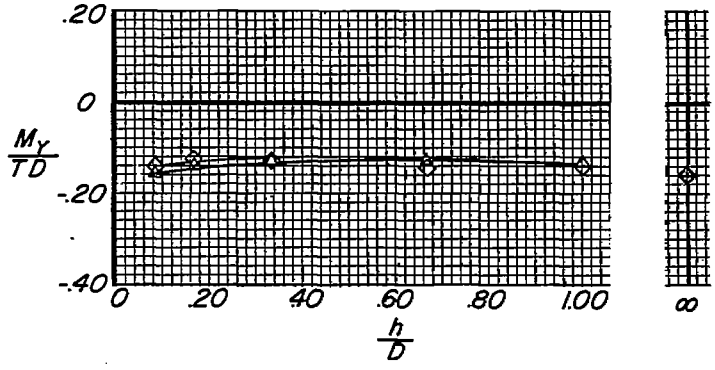

(b) Pitching moment.

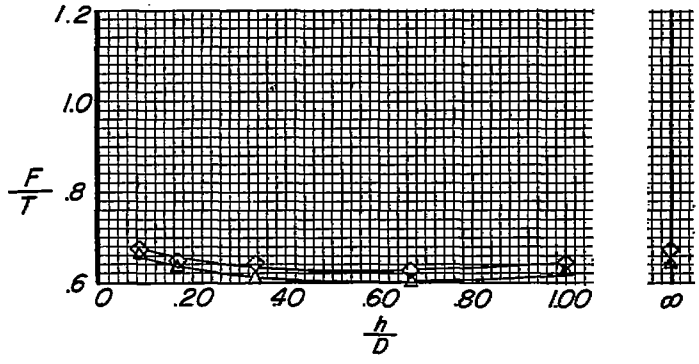

(c) Thrust-recovery factor.

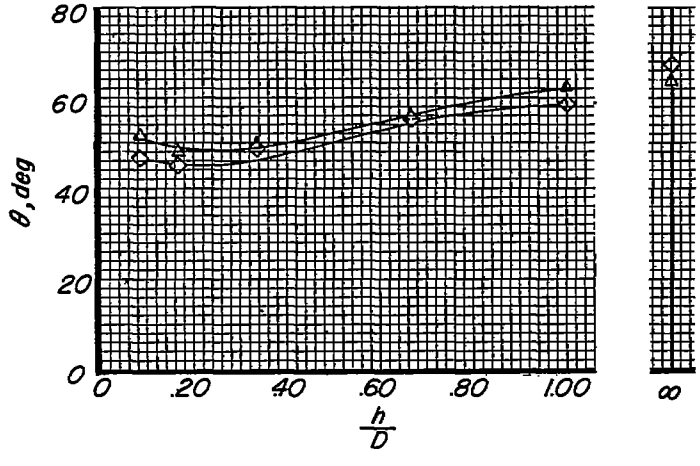

(d) Turning angle.

Figure 26.- Concluded.

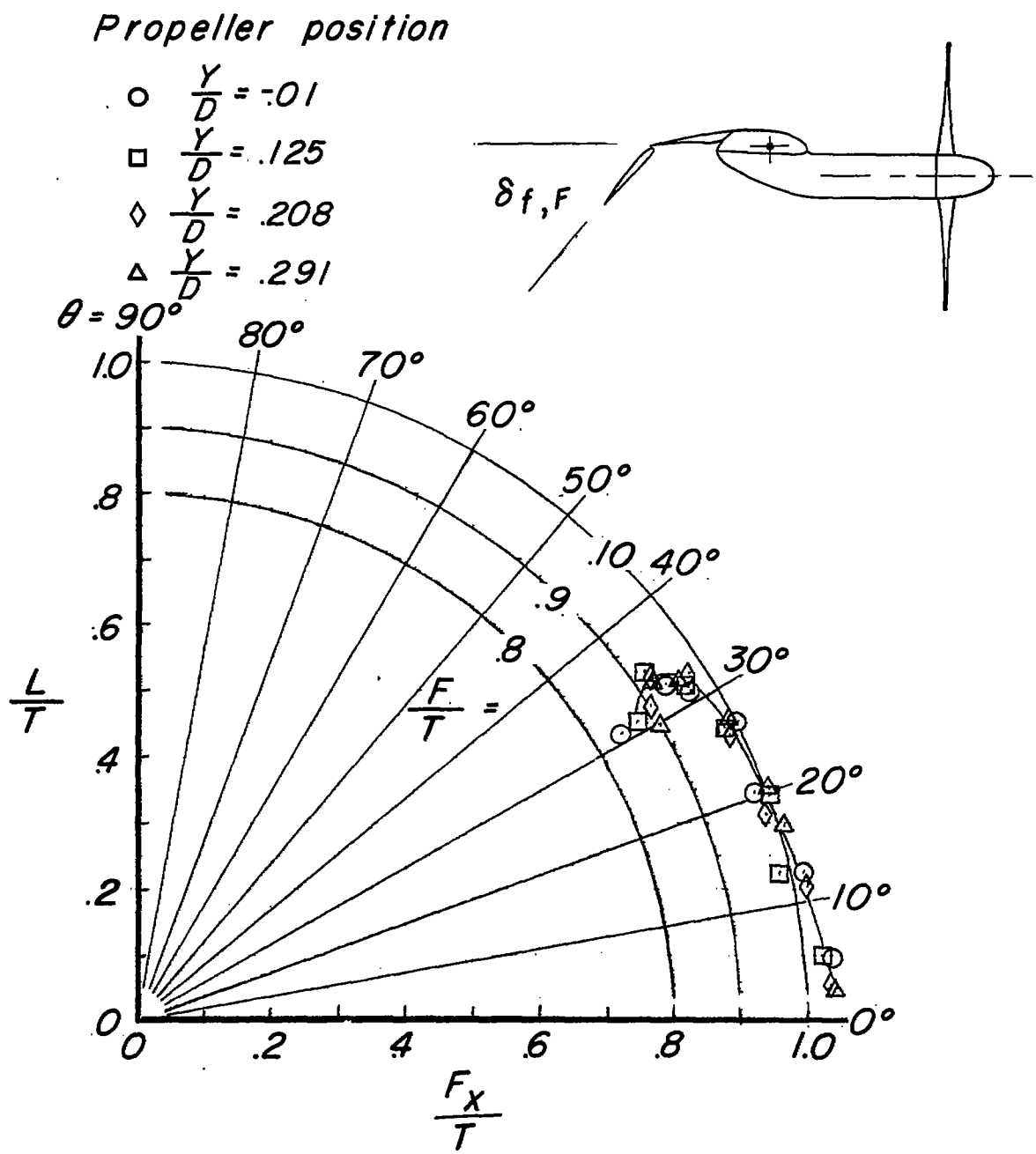

(a) Summary of turning effectiveness.

Figure 27.- Effect of propeller overlap. $\delta_{f,s} = 0^{\circ}$; $\delta_{f,F}$, variable; full-span flaps.

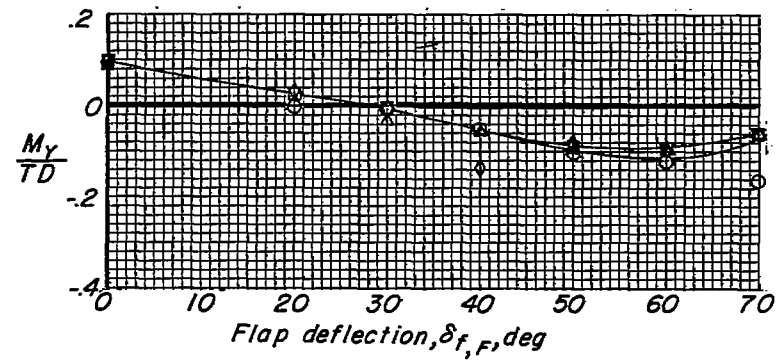

(b) Pitching moment.

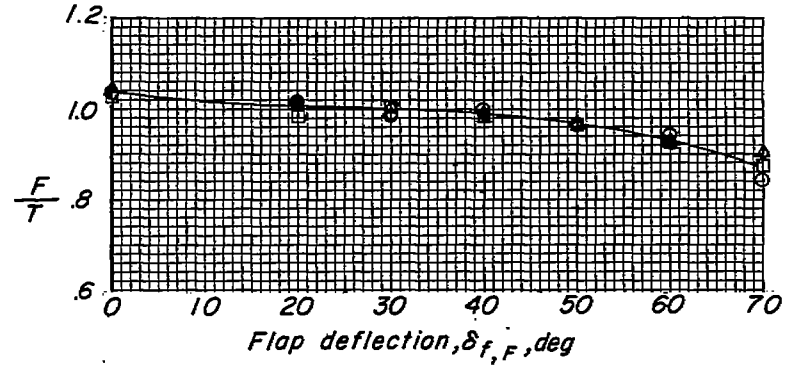

(c) Thrust-recovery factor.

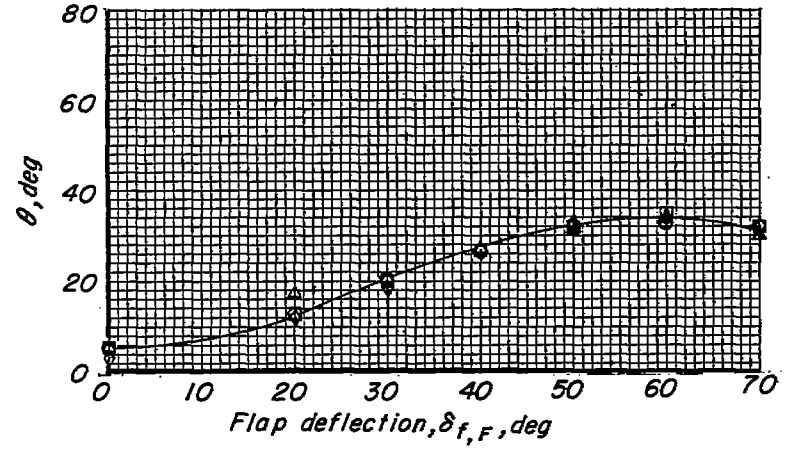

(d) Turning angle.

Figure 27.- Concluded.

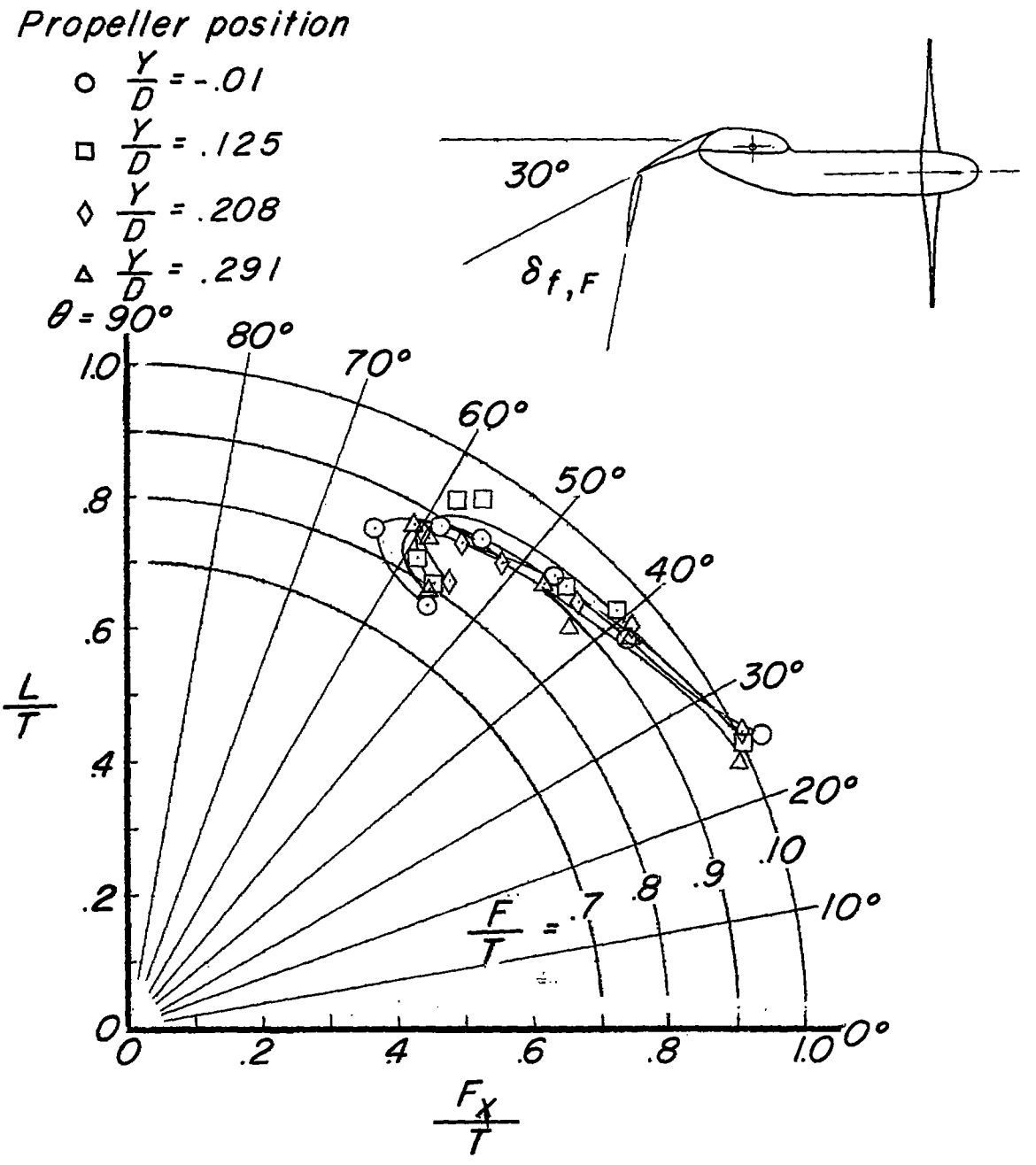

(a) Summary of turning effectiveness.

Figure 28.- Effect of propeller overlap. $\delta_{f,s} = 30^\circ$; $\delta_{f,F}$, variable; full-span flaps.

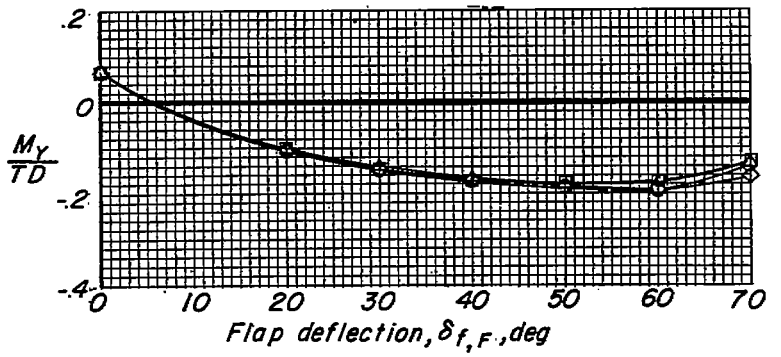

(b) Pitching moment.

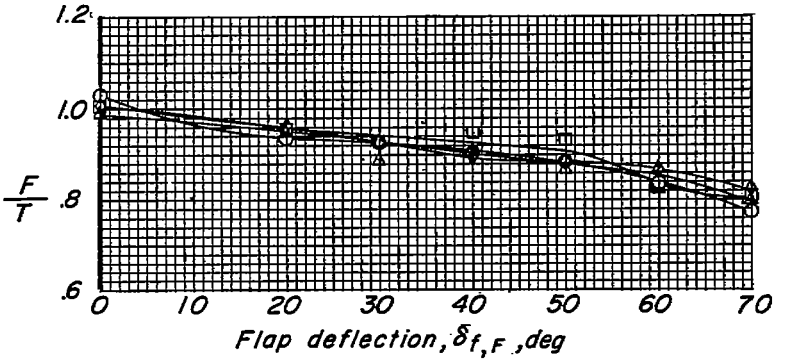

(c) Thrust-recovery factor.

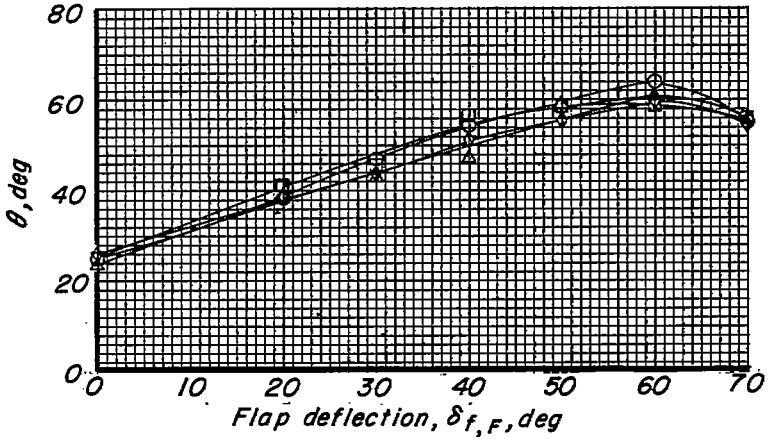

(d) Turning angle.

Figure 28.- Concluded.

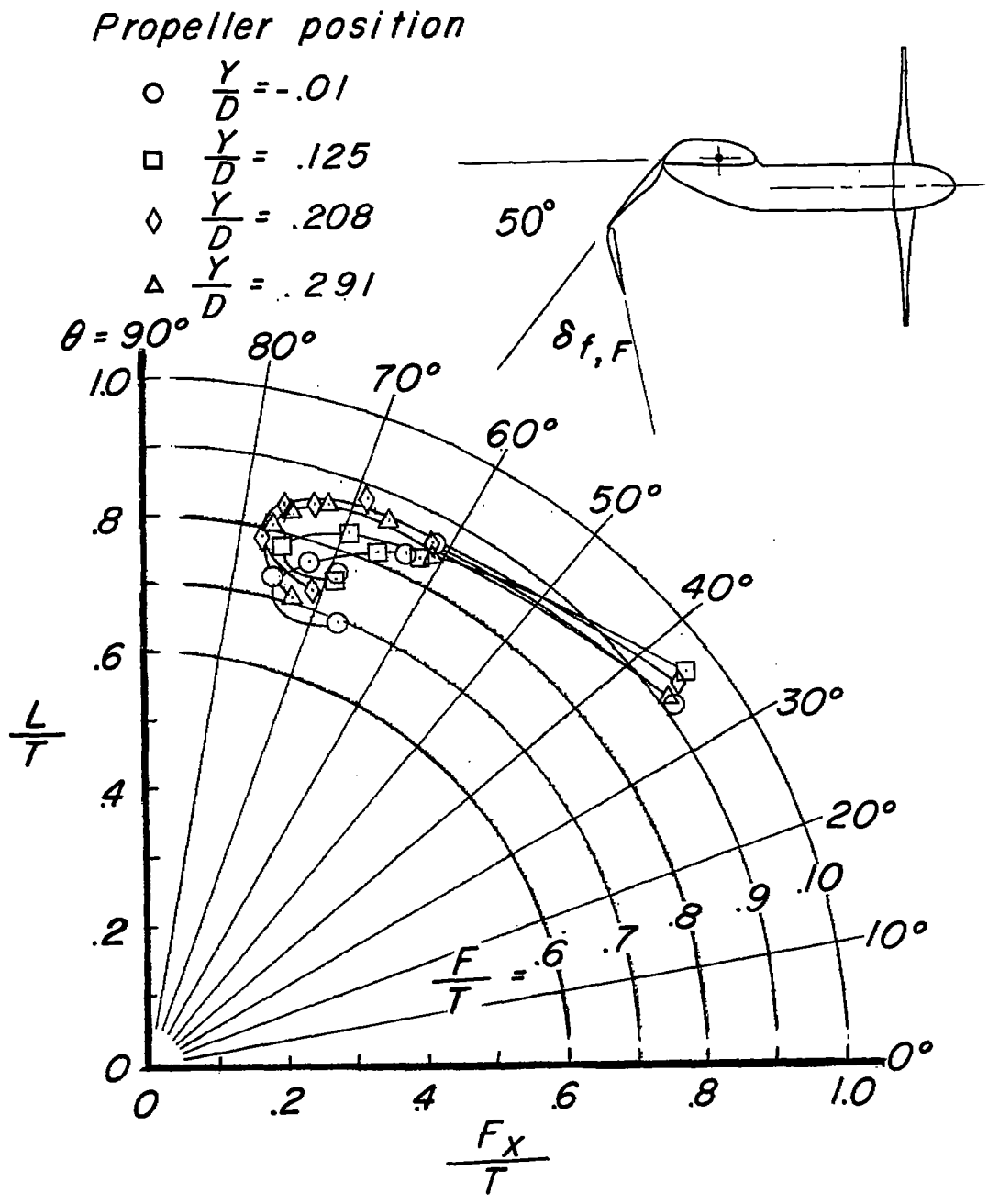

(a) Summary of turning effectiveness.

Figure 29.- Effect of propeller overlap. $\delta_{f,s} = 50°$; $\delta_{f,F}$, variable; full-span flaps.

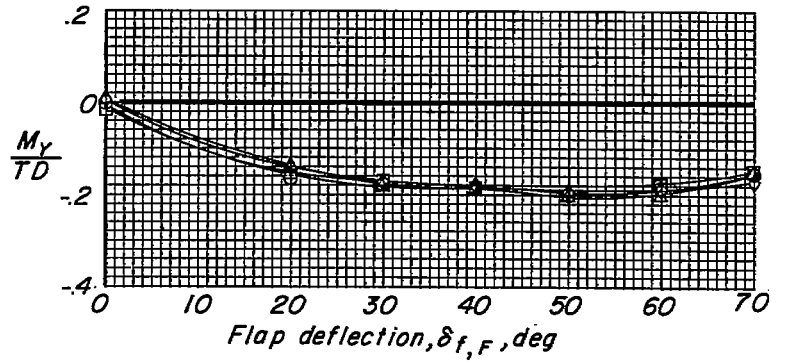

(b) Pitching moment.

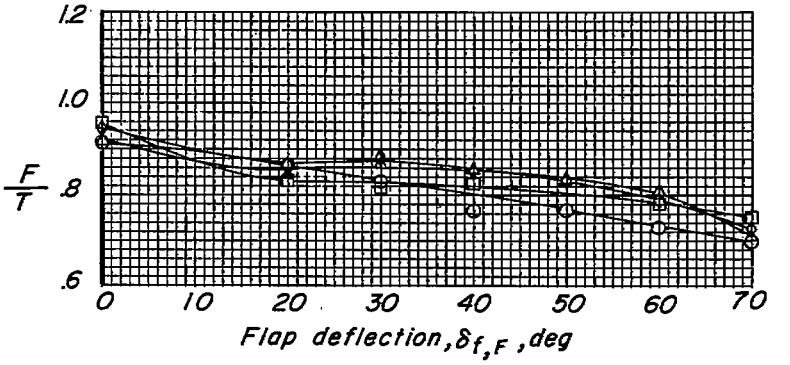

(c) Thrust-recovery factor.

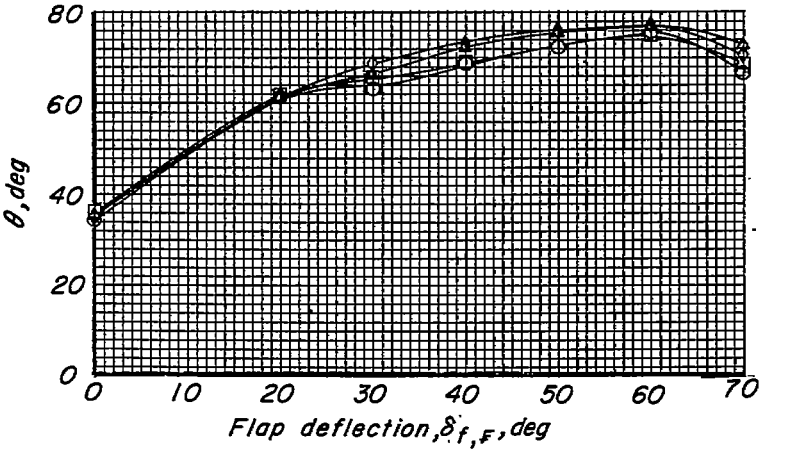

(d) Turning angle.

Figure 29.- Concluded.

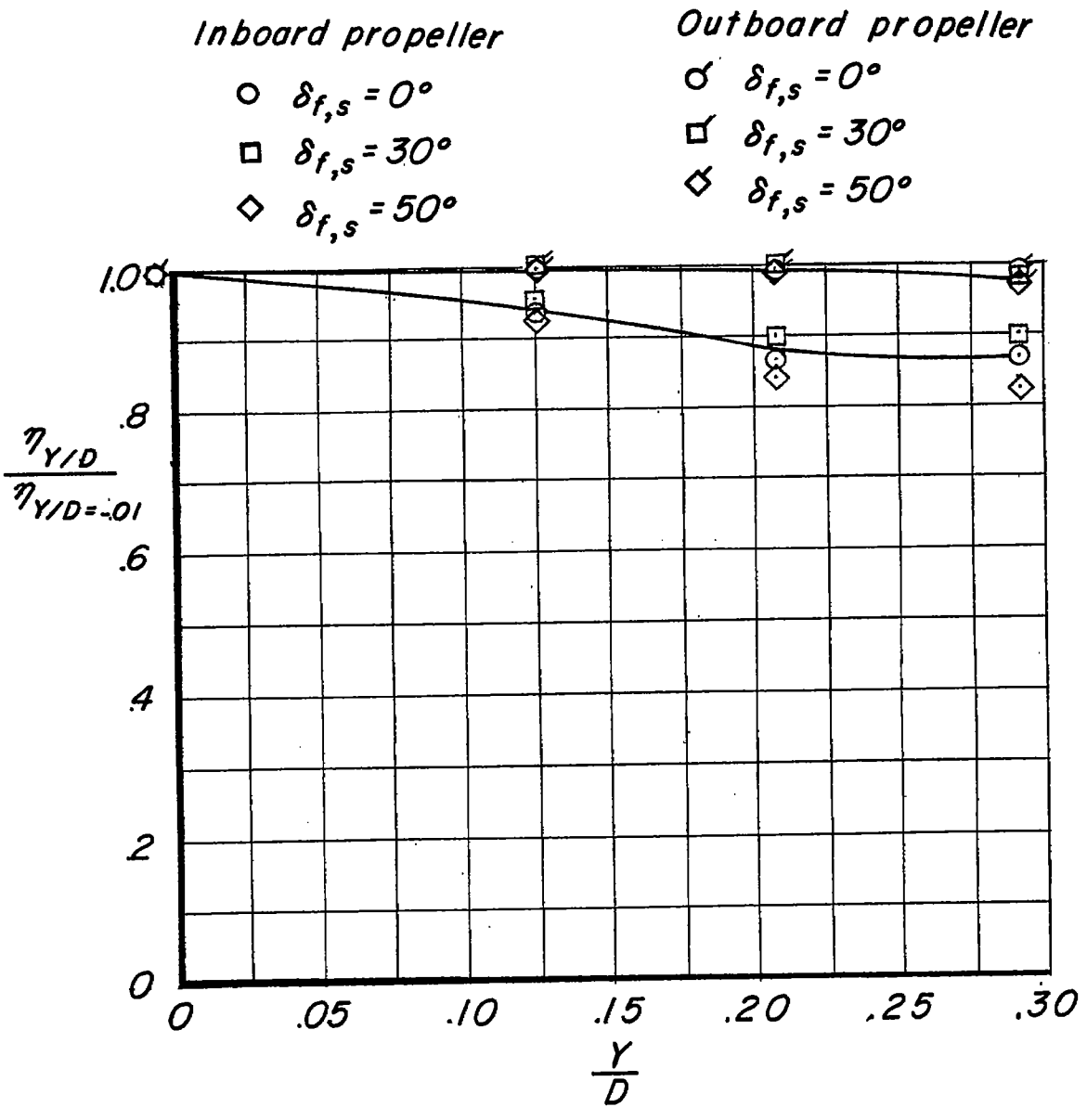

Figure 30.- Variation of average efficiency of propellers with overlap (averaged over $\delta_{f,F}$ range).

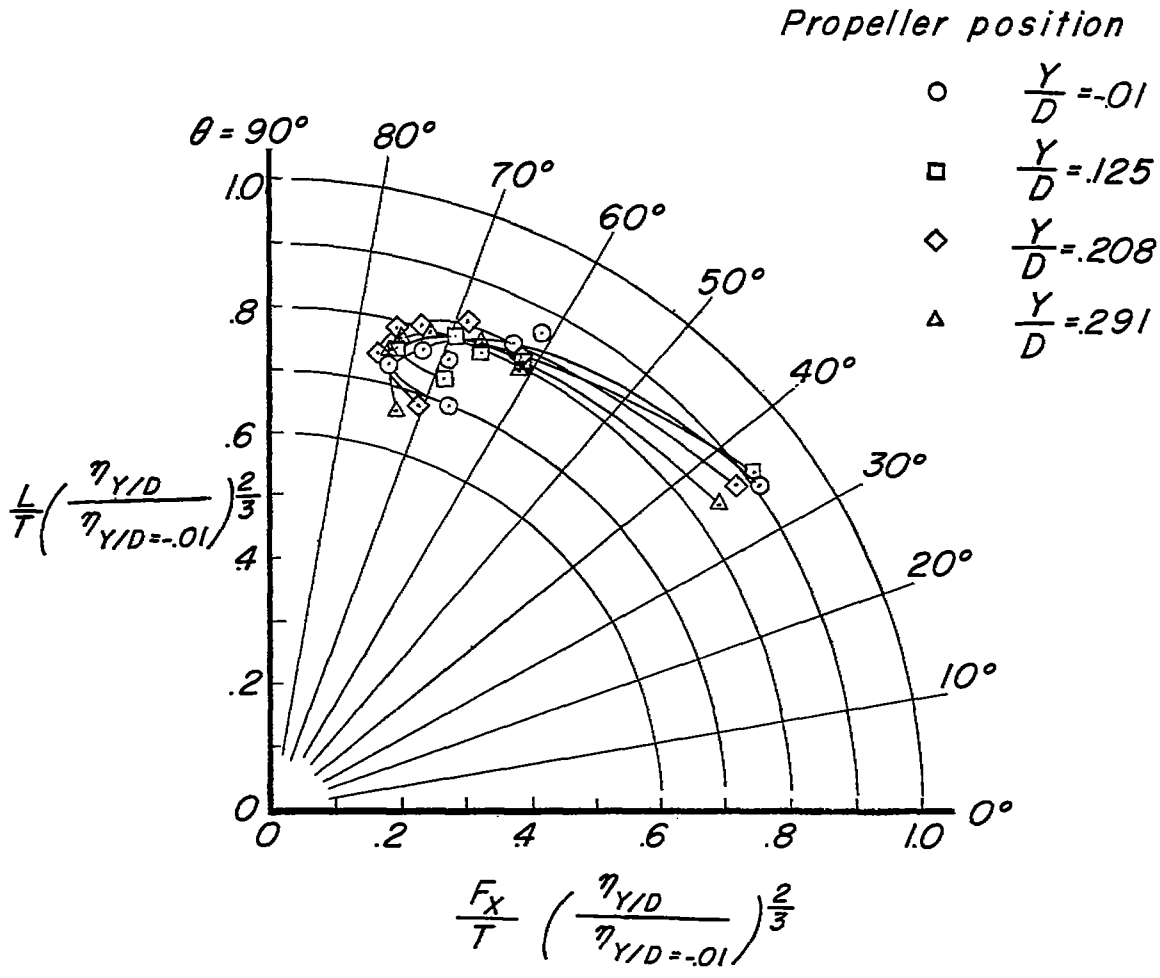

Figure 31.- Summary of turning effectiveness based on constant power. $\delta_{f,s} = 50^{\circ}$.

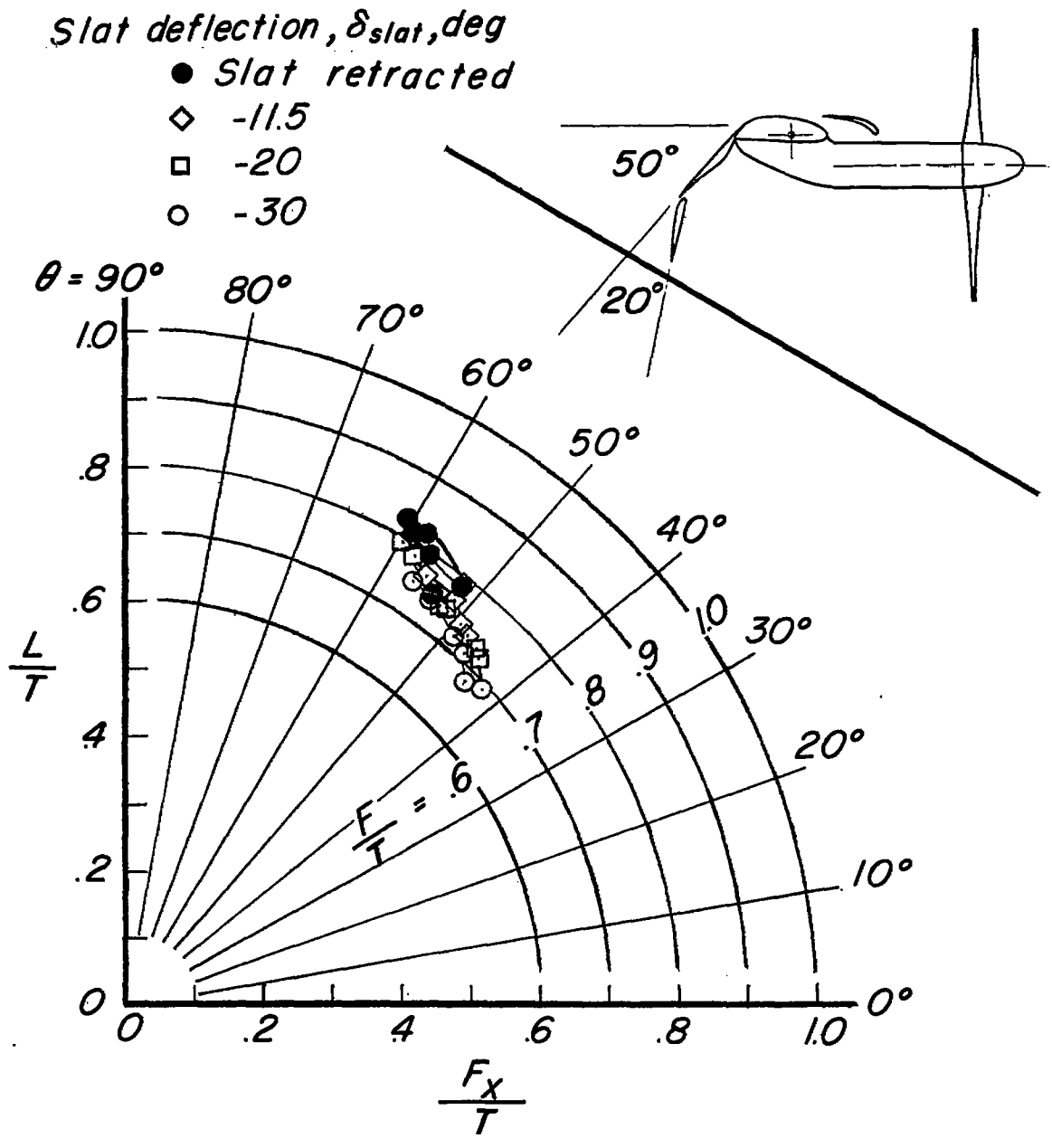

(a) Summary of turning effectiveness.

Figure 32.- Effect of slat deflection in low position. $\delta_{f,s} = 50°$; $\delta_{f,F} = 20°$; $\frac{X}{D} = 0.333$; $\frac{Z}{D} = -0.104$; $\alpha = 32°$; $\frac{h}{D}$, variable.

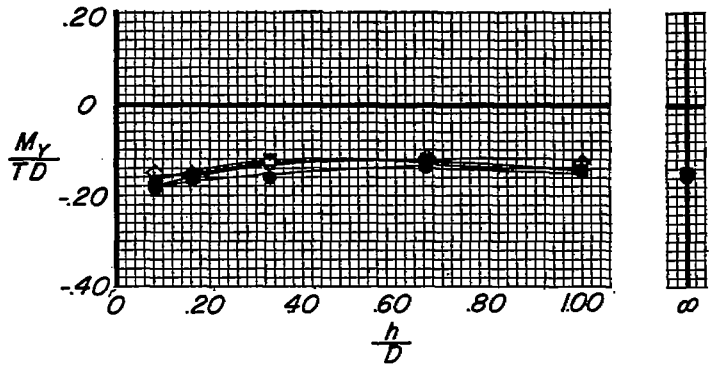

(b) Pitching moment.

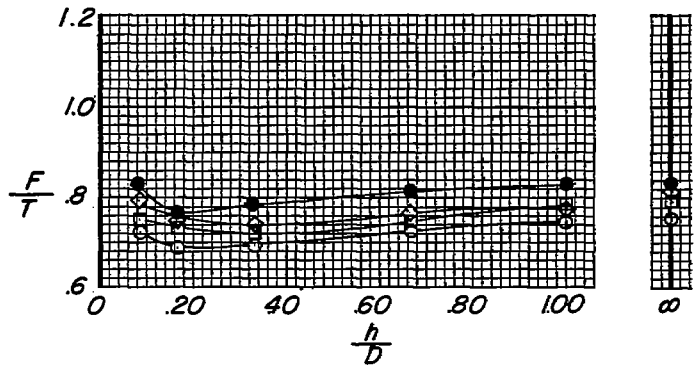

(c) Thrust-recovery factor.

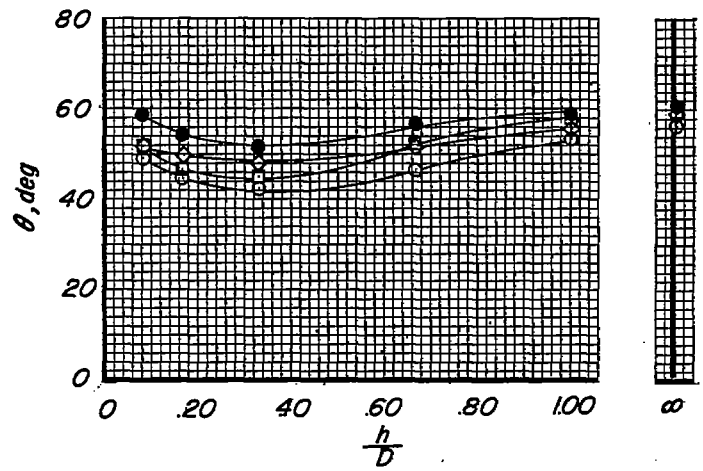

(d) Turning angle.

Figure 32.- Concluded.

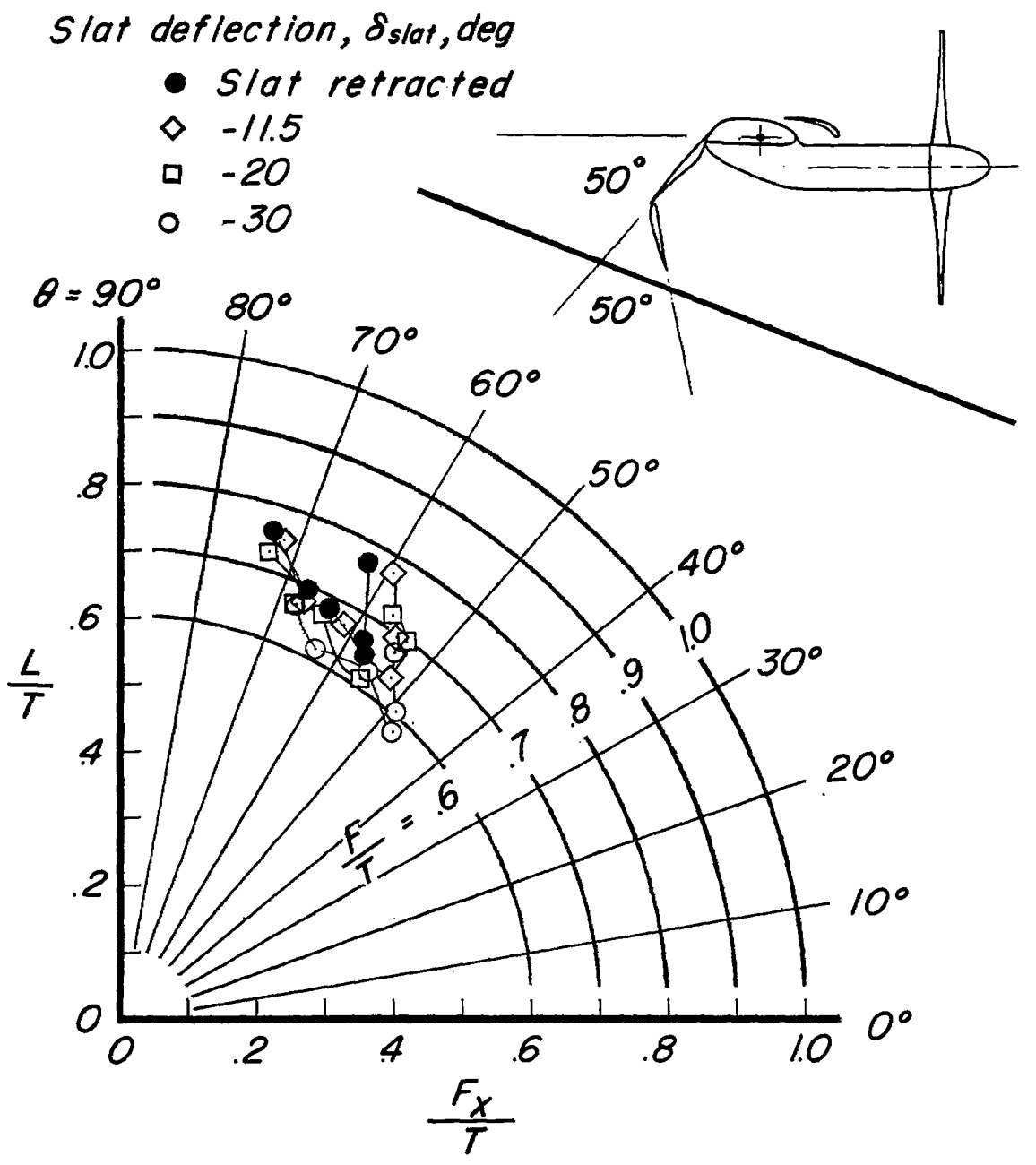

(a) Summary of turning effectiveness.

Figure 33.- Effect of slat deflection in low position. $\delta_{f,s} = 50°$; $\delta_{f,F} = 50°$; $\frac{X}{D} = 0.333$; $\frac{Z}{D} = -0.104$; $\alpha = 20°$; $\frac{h}{D}$, variable.

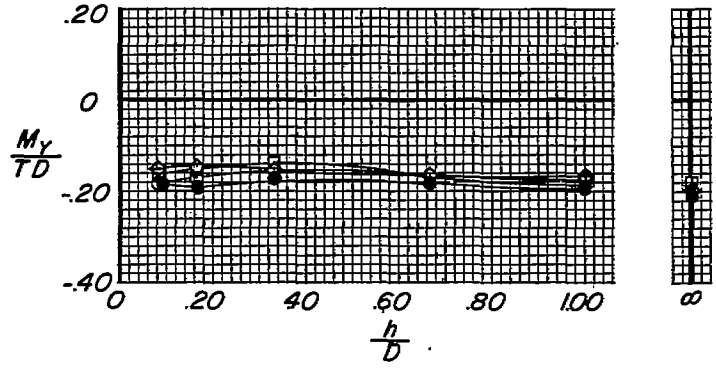

(b) Pitching moment.

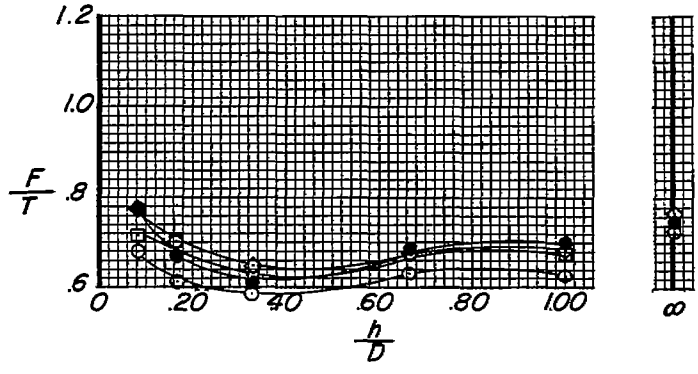

(c) Thrust-recovery factor.

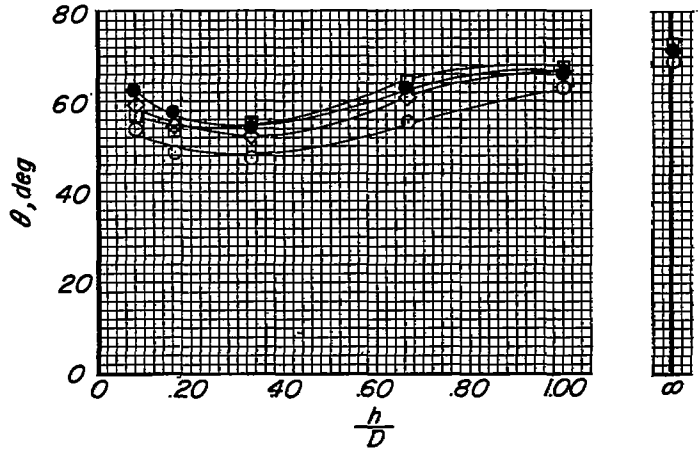

(d) Turning angle.

Figure 33.- Concluded.

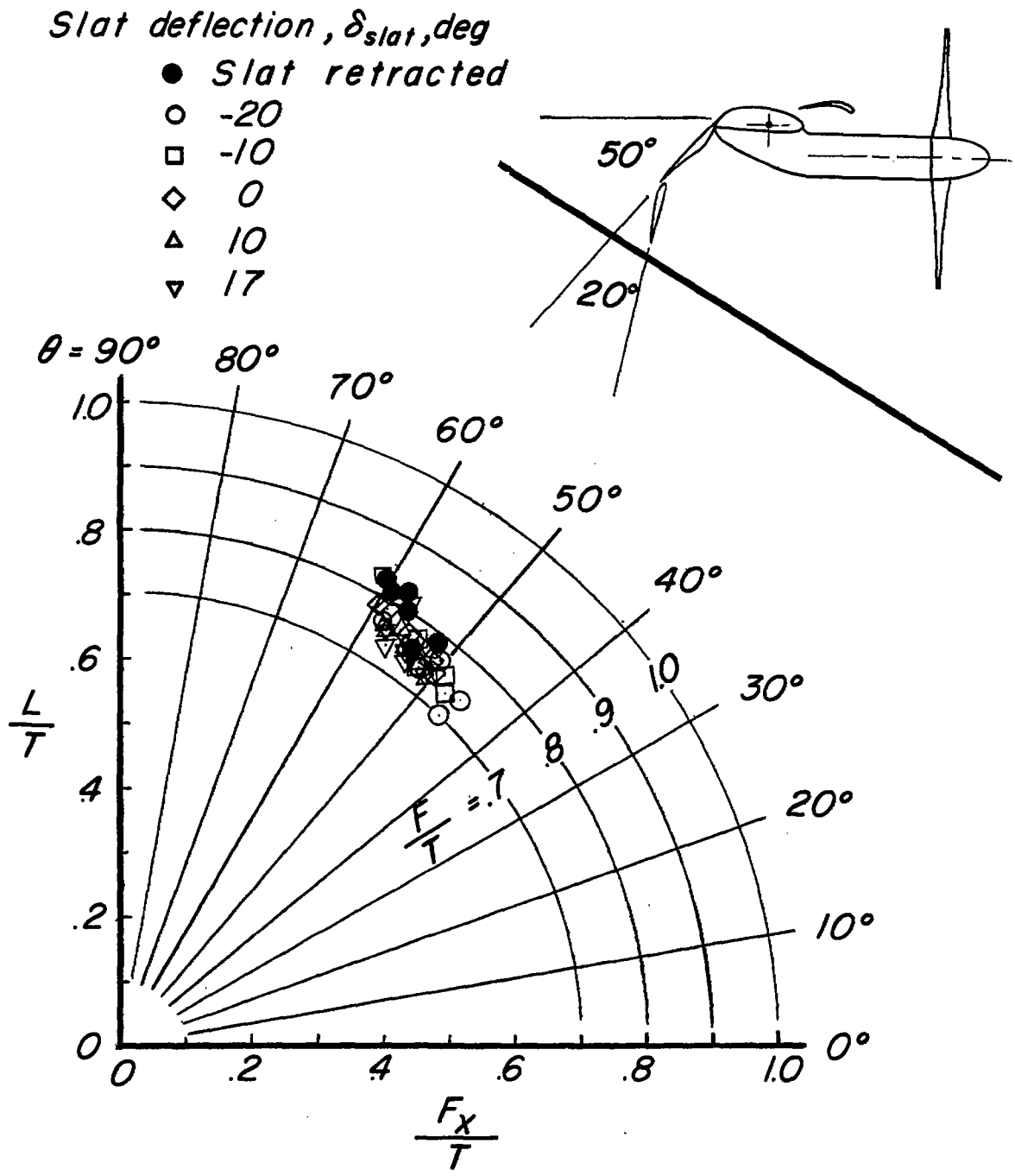

(a) Summary of turning effectiveness.

Figure 34.- Effect of slat deflection in middle position. $\delta_{f,s} = 50°$; $\delta_{f,F} = 20°$; $\frac{X}{D} = 0.333$; $\frac{Z}{D} = -0.104$; $\alpha = 32°$; $\frac{h}{D}$, variable.

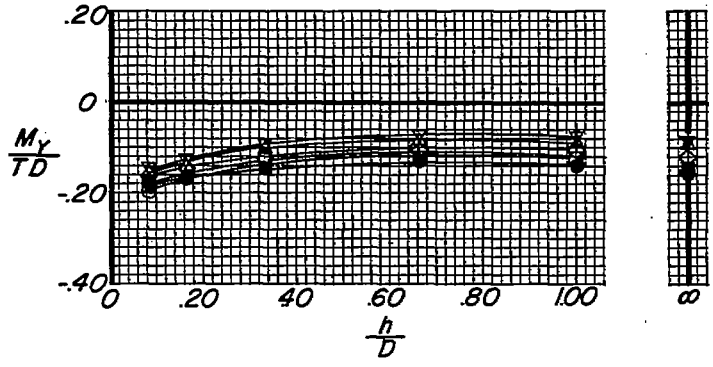

(b) Pitching moment.

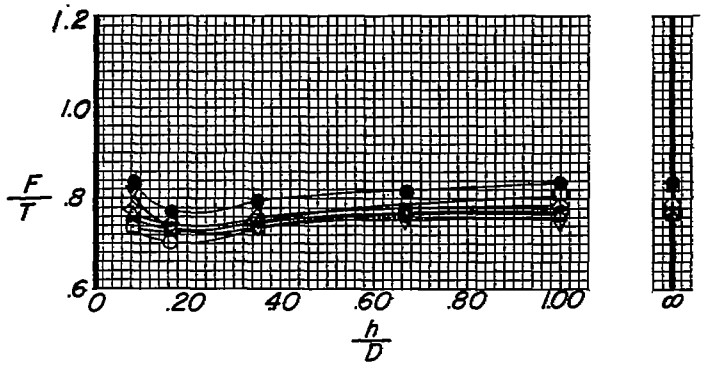

(c) Thrust-recovery factor.

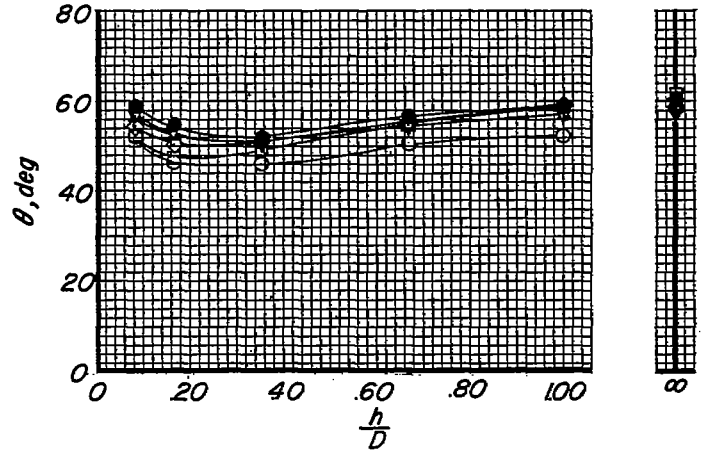

(d) Turning angle.

Figure 34.- Concluded.

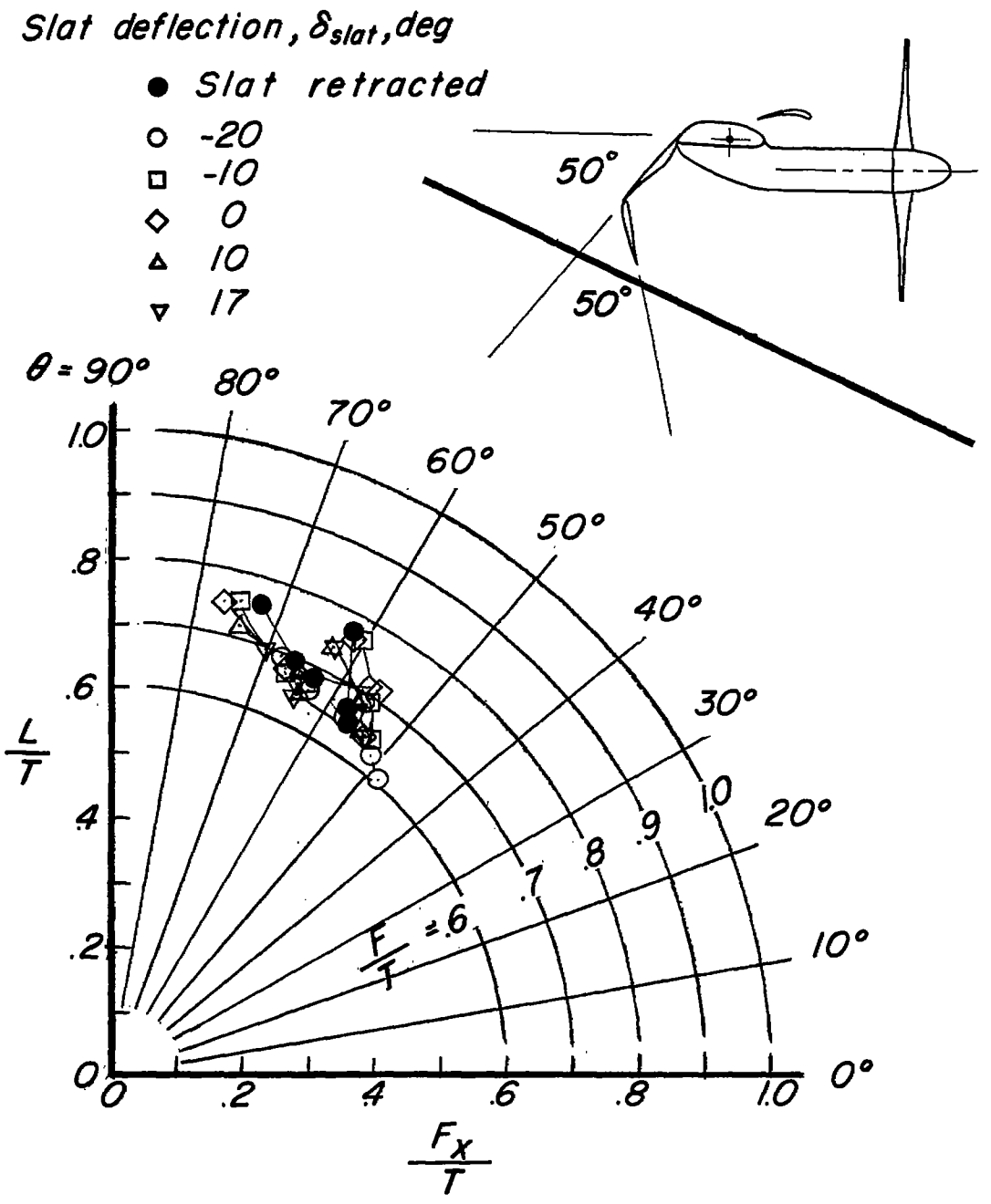

(a) Summary of turning effectiveness.

Figure 35.- Effect of slat deflection in middle position. $\delta_{f,s} = 50^{\circ}$; $\delta_{f,F} = 50^{\circ}$; $\frac{X}{D} = 0.333$; $\frac{Z}{D} = -0.104$; $\alpha = 20^{\circ}$; $\frac{h}{D}$, variable.

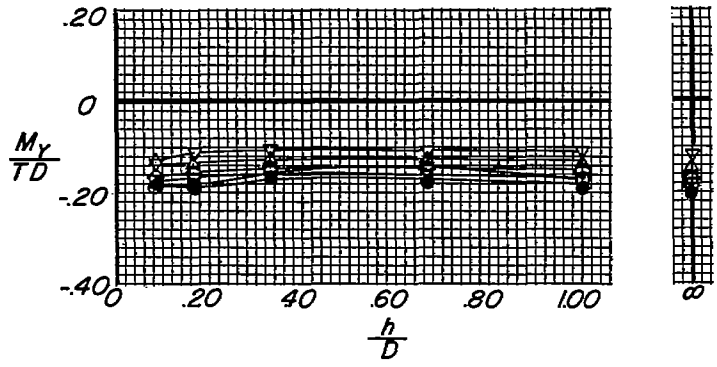

(b) Pitching moment.

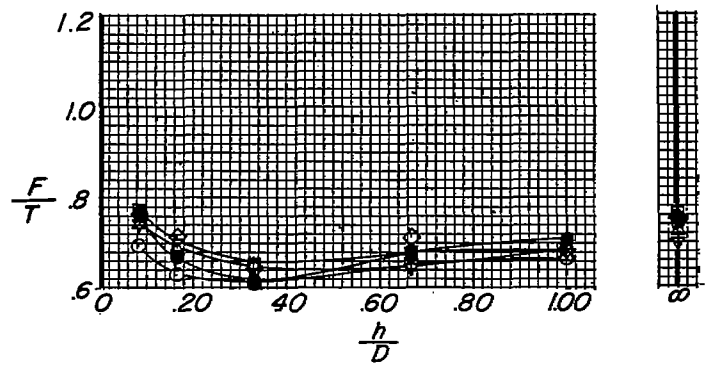

(c) Thrust-recovery factor.

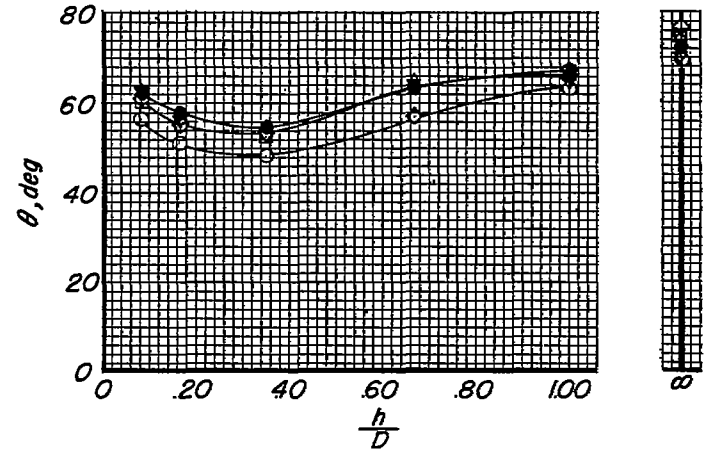

(d) Turning angle.

Figure 35.- Concluded.

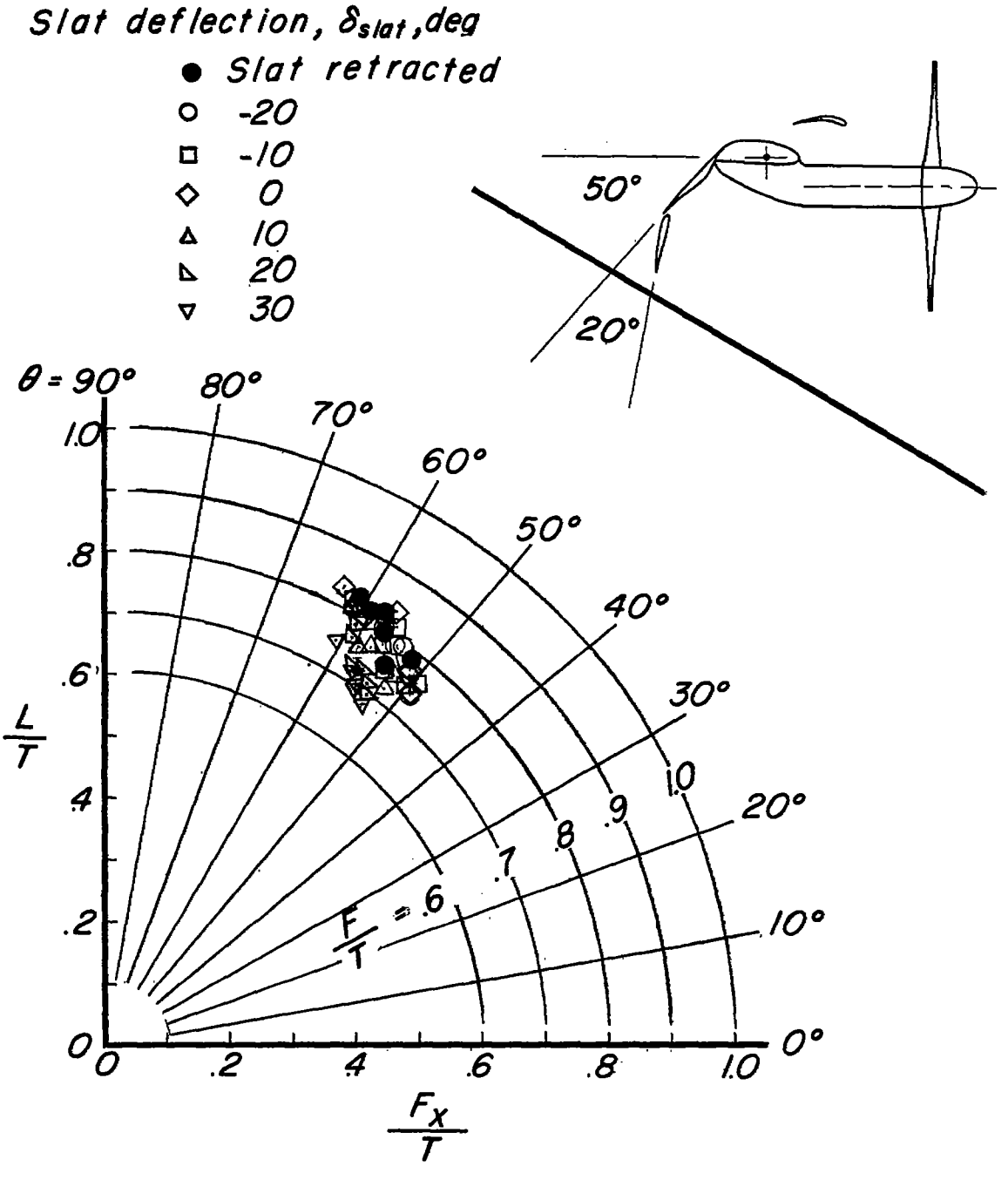

(a) Summary of turning effectiveness.

Figure 36.- Effect of slat deflection in high position. $\delta_{f,s} = 50°$; $\delta_{f,F} = 20°$; $\frac{X}{D} = 0.333$; $\frac{Z}{D} = -0.104$; $\alpha = 32°$; $\frac{h}{D}$, variable.

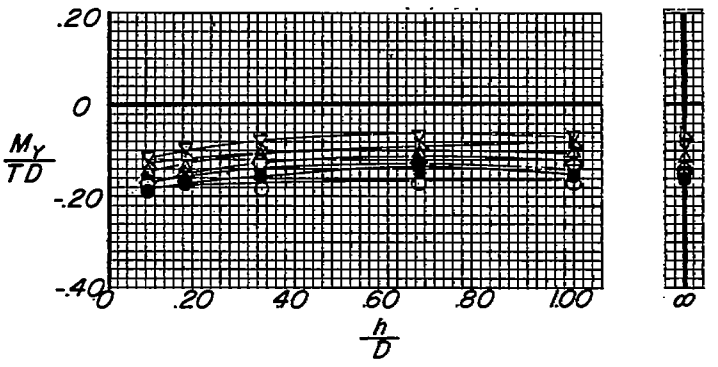

(b) Pitching moment.

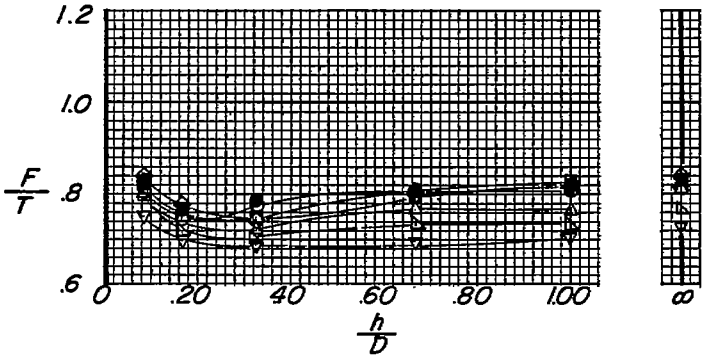

(c) Thrust-recovery factor.

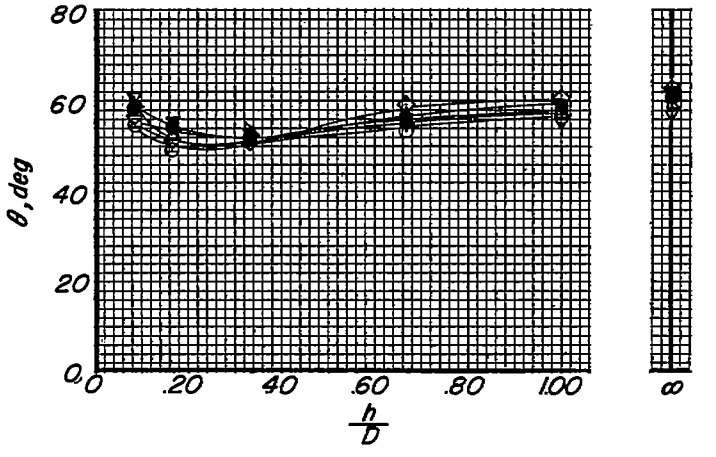

(d) Turning angle.

Figure 36.- Concluded.

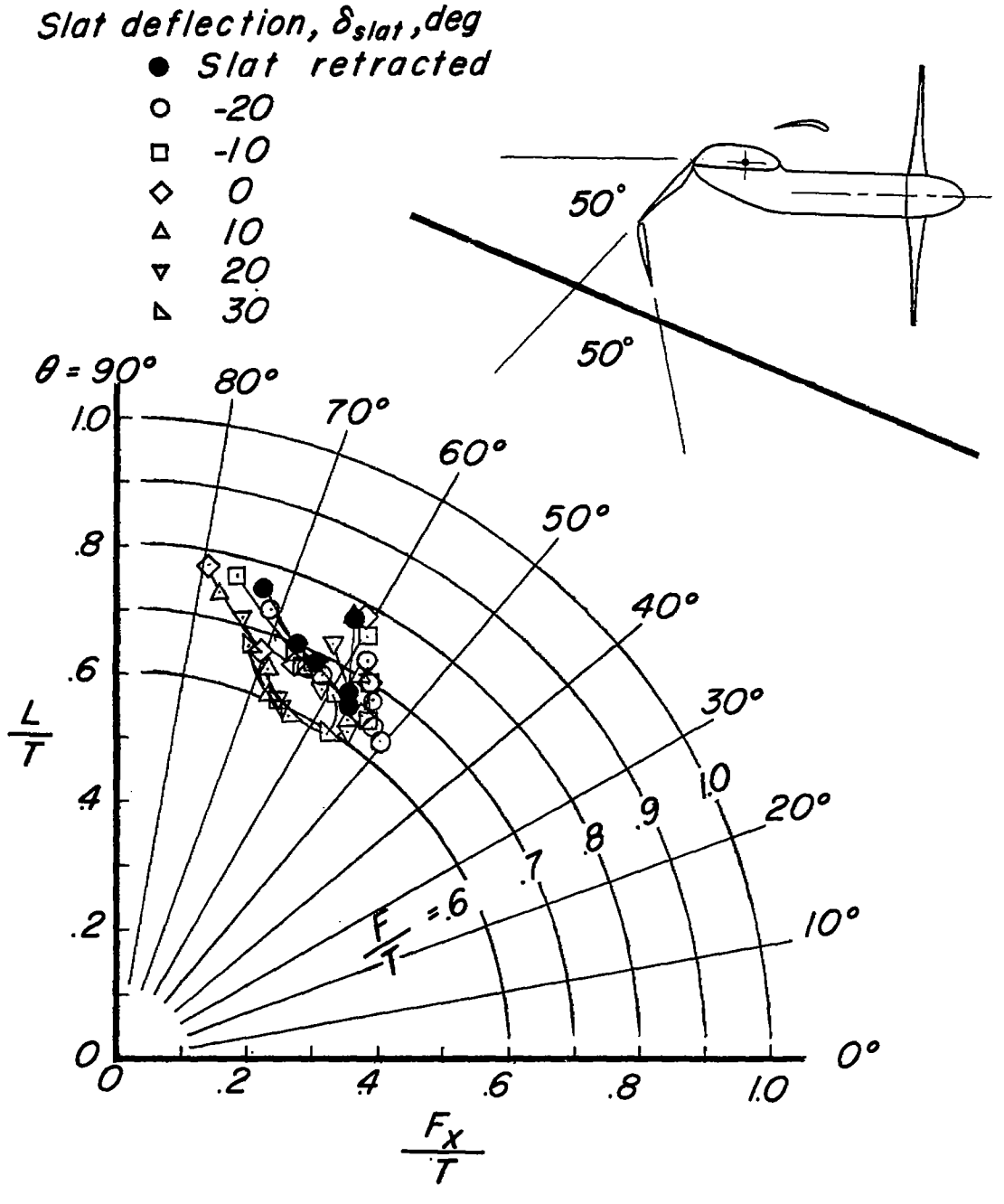

(a) Summary of turning effectiveness.

Figure 37.- Effect of slat deflection in high position. $\delta_{f,s} = 50°$; $\delta_{f,F} = 50°$; $\frac{X}{D} = 0.333$; $\frac{Z}{D} = -0.104$; $\alpha = 20°$; $\frac{h}{D}$, variable.

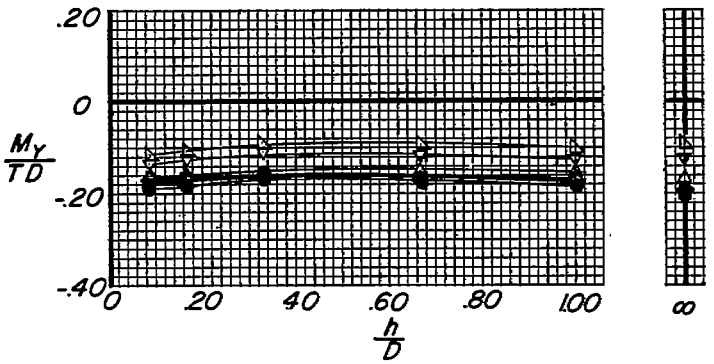

(b) Pitching moment.

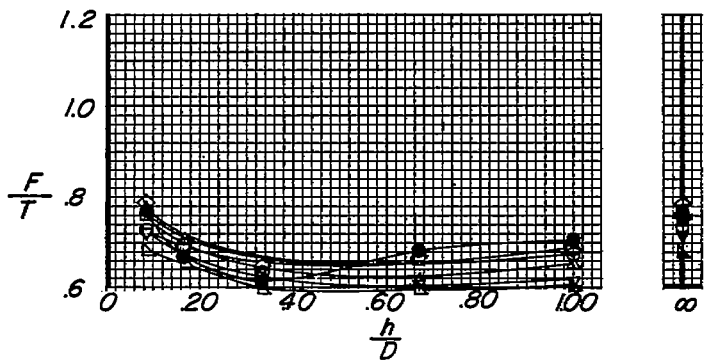

(c) Thrust-recovery factor.

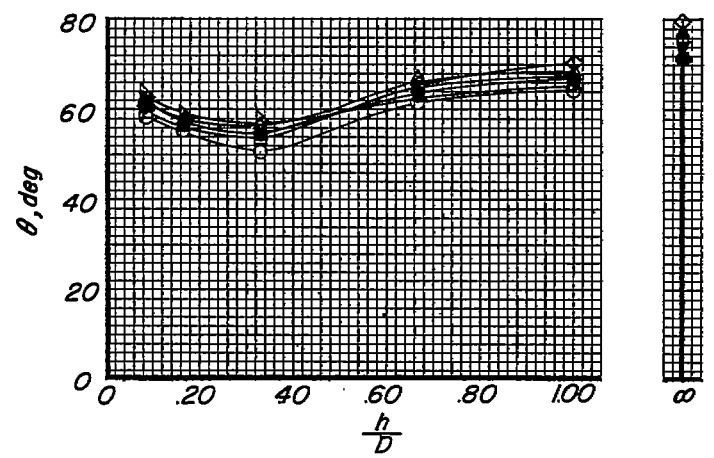

(d) Turning angle.

Figure 37.- Concluded.

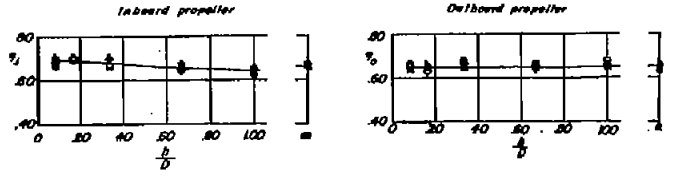

(a) Slat in high position. $\delta_{f,s} = 50^{\circ}$; $\delta_{f,F} = 50^{\circ}$.

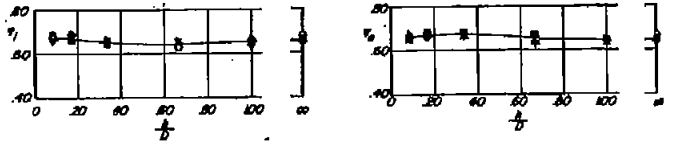

(b) Slat in high position. $\delta_{f,s} = 50^{\circ}$; $\delta_{f,F} = 20^{\circ}$.

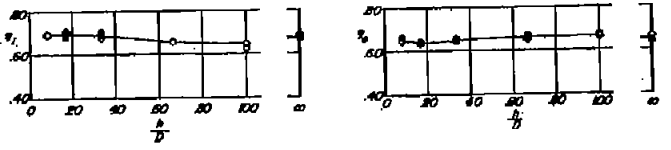

(c) Slat in low position. $\delta_{f,s} = 50^{\circ}$; $\delta_{f,F} = 50^{\circ}$.

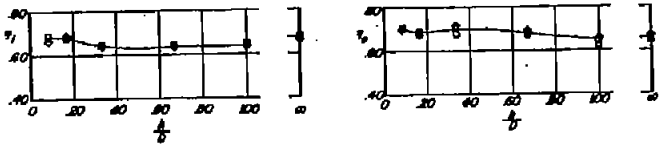

(d) Slat in low position. $\delta_{f,s} = 50^{\circ}$; $\delta_{f,F} = 20^{\circ}$.

Figure 38.- Effect of ground proximity on propeller static-thrust efficiency for two slat positions and flap configurations. $\frac{X}{D} = 0.333$; $\frac{Z}{D} = -0.104$.

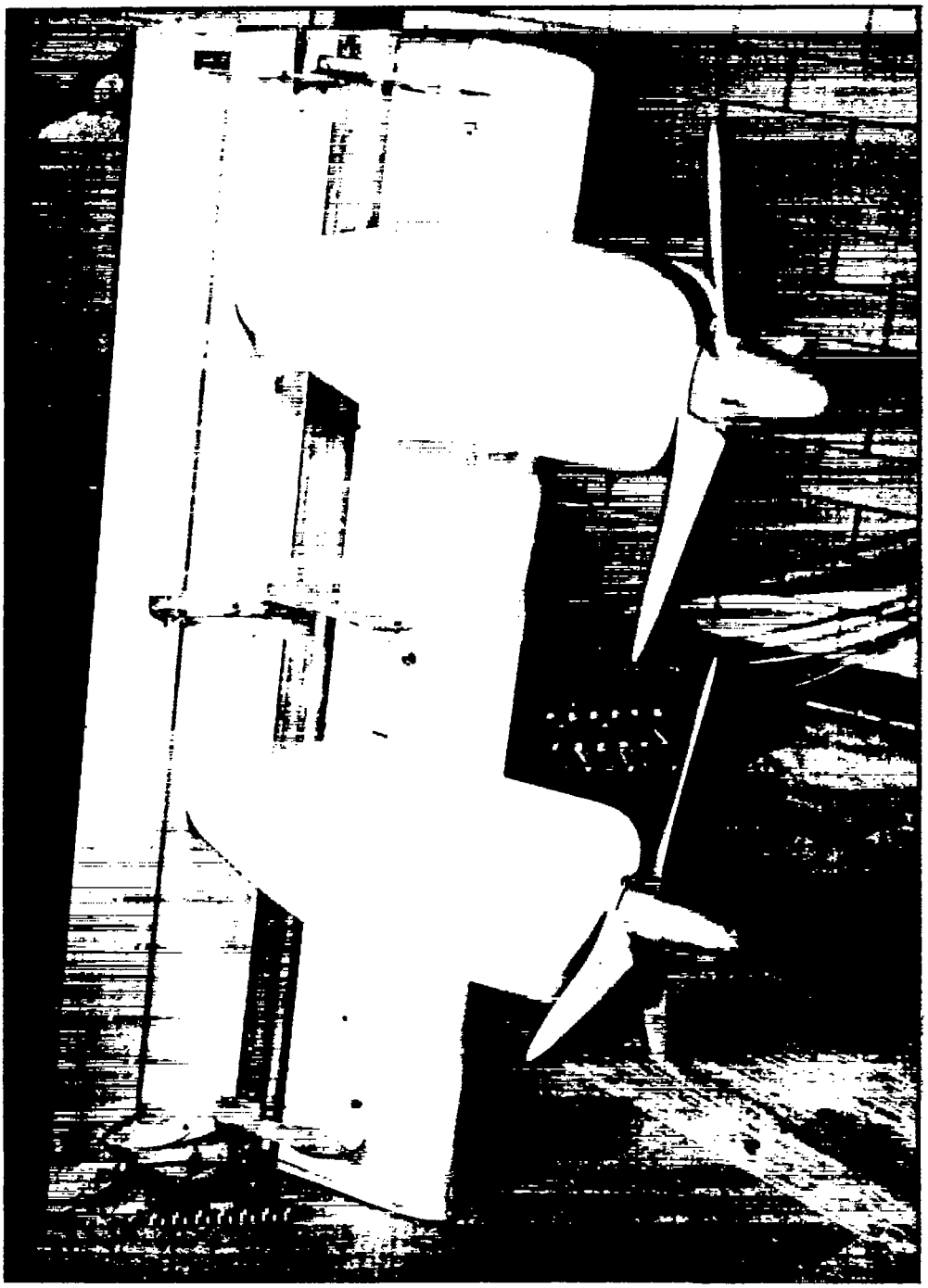

Figure 39.- Model with large nacelles. L-96617

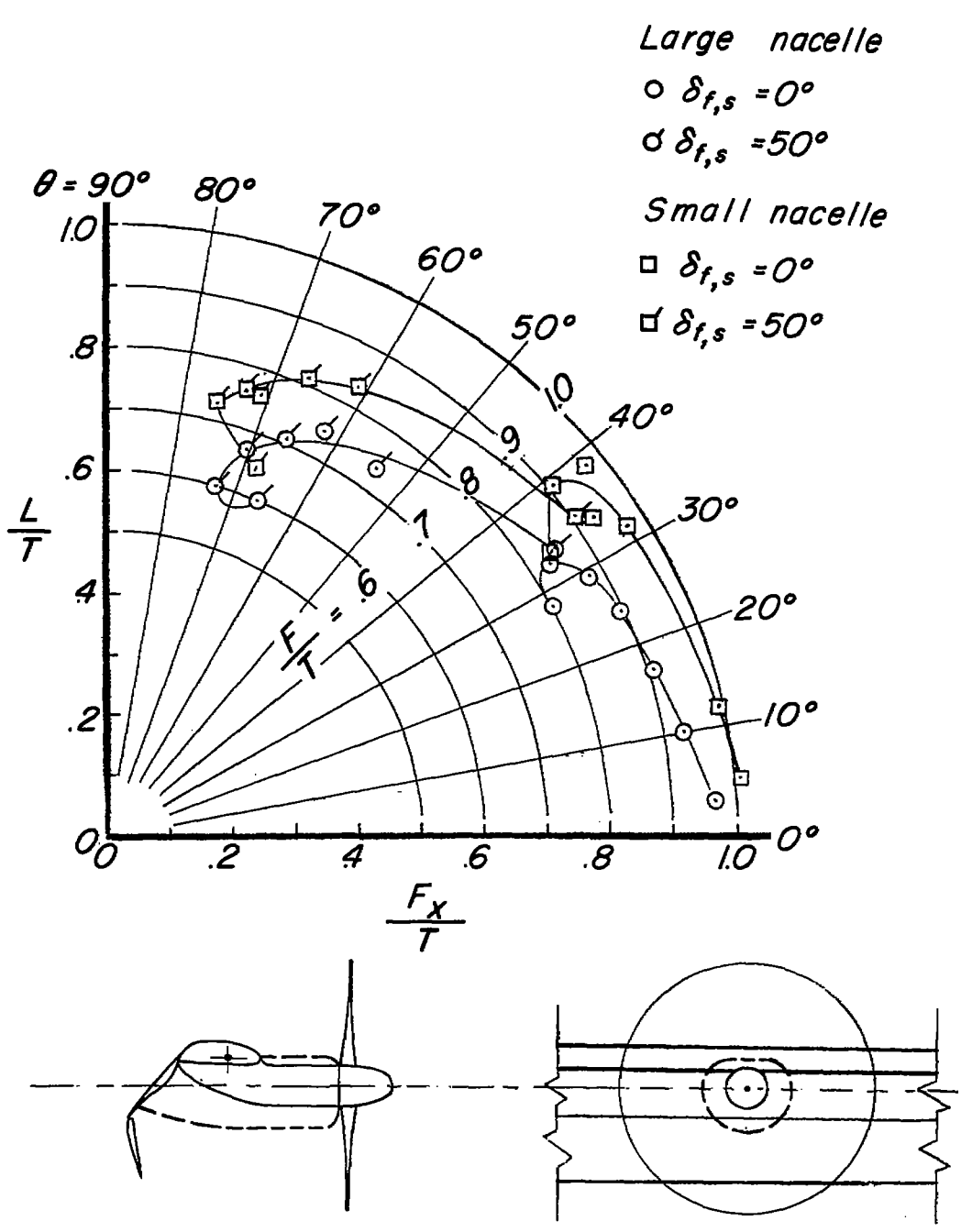

(a) Summary of turning effectiveness.

Figure 40.- The effect of nacelle size. $\frac{X}{D}$ = 0.333; $\frac{Z}{D}$ = -0.104; $\delta_{f,F}$, variable.

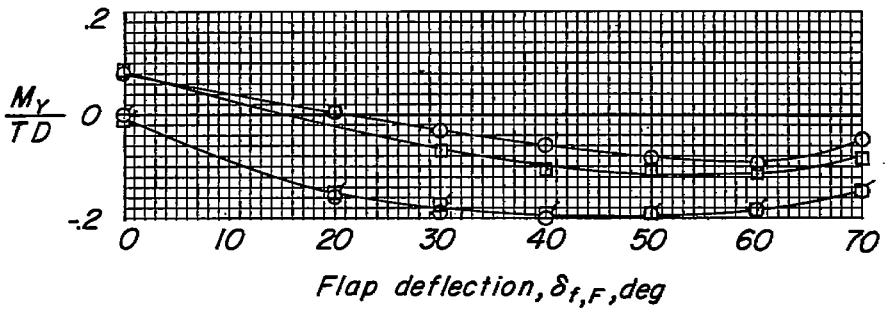

(b) Pitching moment.

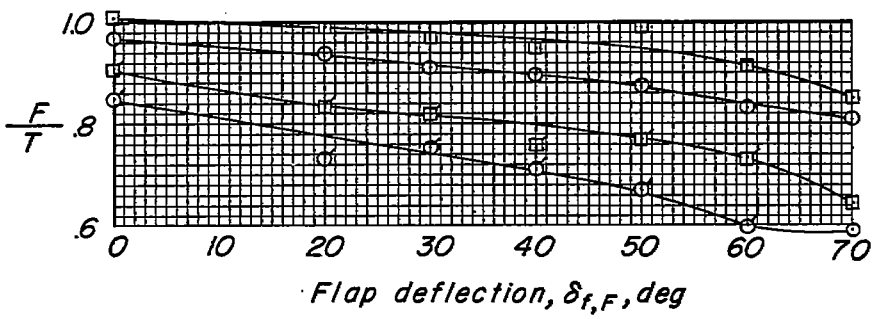

(c) Thrust-recovery factor.

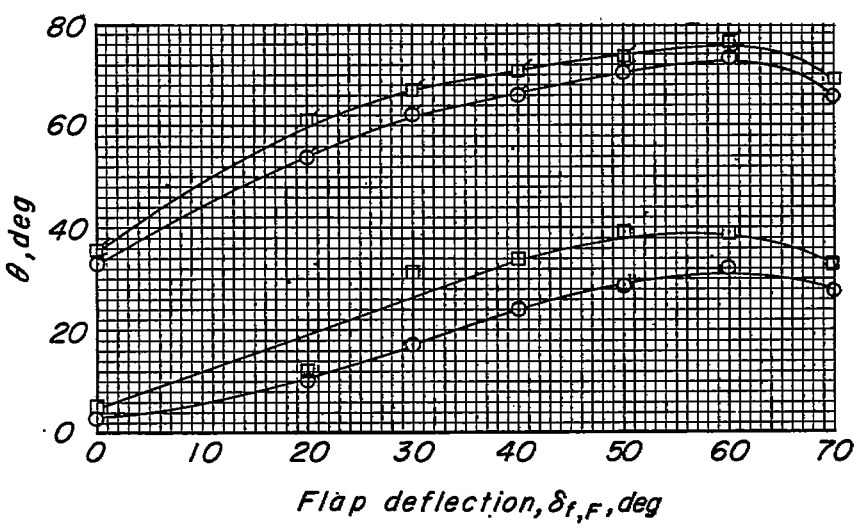

(d) Turning angle.

Figure 40.- Concluded.